ISSN 0711-6659

canadian acoustics
acoustique canadienne

Journal of the Canadian Acoustical Association - Revue de l'Association canadienne d'acoustique

MARCH 2023	MARS 2023
Volume 51 - - Number 1	Volume 51 - - Numéro 1

Editorial - Éditorial 3

Aeroacoustics - Aéroacoustique 5

Bio-Acoustics - Bio-acoustique 31

Underwater Acoustics - Acoustique sous-marine 39

Other Features - Autres rubriques 51

canadian acoustics

acoustique canadienne

Canadian Acoustical Association/Association Canadienne d'Acoustique P.B. 74068 Ottawa, Ontario, K1M 2H9

Association canadienne d'acoustique B.P. 74068 Ottawa, Ontario, K1M 2H9

Canadian Acoustics publishes refereed articles and news items on all aspects of acoustics and vibration. Articles reporting new research or applications, as well as review or tutorial papers and shorter technical notes are welcomed, in English or in French. Submissions should be sent only through the journal online submission system. Complete instructions to authors concerning the required "camera-ready" manuscript are provided within the journal online submission system.

L'**Acoustique Canadienne** publie des articles arbitrés et des informations sur tous les aspects de l'acoustique et des vibrations. Les informations portent sur la recherche, les ouvrages sous forme de revues, les nouvelles, l'emploi, les nouveaux produits, les activités, etc. Des articles concernant des résultats inédits ou des applications ainsi que les articles de synthèse ou d'initiation, en français ou en anglais, sont les bienvenus.

Canadian Acoustics is published four times a year - in March, June, September and December. This quarterly journal is free to individual members of the Canadian Acoustical Association (CAA) and institutional subscribers. **Canadian Acoustics** publishes refereed articles and news items on all aspects of acoustics and vibration. It also includes information on research, reviews, news, employment, new products, activities, discussions, etc. Papers reporting new results and applications, as well as review or tutorial papers and shorter research notes are welcomed, in English or in French. The Canadian Acoustical Association selected **Paypal** as its **preferred system** for the online payment of your subscription fees. Paypal supports a wide range of payment methods (Visa, Mastercard, Amex, Bank account, etc.) and does not requires you to have already an account with them. If you still want to proceed with a manual payment of your subscription fee, please Membership form and send it to the Executive Secretary of the Association (see address above). - - Dr. Roberto Racca - Canadian Acoustical Association/Association Canadienne d'Acoustique c/o JASCO Applied Sciences 2305–4464 Markham Street Victoria, BC V8Z 7X8 - - secretary@caa-aca.ca

Acoustique canadienne est publié quantre fois par an, en mars, juin, septembre et décembre. Cette revue trimestrielle est envoyée gratuitement aux membres individuels de l'Association canadienne d'acoustique (ACA) et aux abonnés institutionnels. L'**Acoustique canadienne** publie des articles arbitrés et des rubriques sur tous les aspects de l'acoustique et des vibrations. Ceci comprend la recherche, les recensions des travaux, les nouvelles, les offres d'emploi, les nouveaux produits, les activités, etc. Les articles concernant les résultats inédits ou les applications de l'acoustique ainsi que les articles de synthèse, les tutoriels et les exposées techniques, en français ou en anglais, sont les bienvenus. L'Association canadienne d'acoustique a sélectionné **Paypal** comme solution pratique pour le paiement en ligne de vos frais d'abonnement. Paypal prend en charge un large éventail de méthodes de paiement (Visa, Mastercard, Amex, compte bancaire, etc) et ne nécessite pas que vous ayez déjà un compte avec eux. Si vous désirez procéder à un paiement par chèque de votre abonnement, merci de remplir le formulaire d'inscription et de l'envoyer au secrétaire exécutif de l'association (voir adresse ci-dessus). - - Dr. Roberto Racca - Canadian Acoustical Association/Association Canadienne d'Acoustique c/o JASCO Applied Sciences 2305–4464 Markham Street Victoria, BC V8Z 7X8 - - secretary@caa-aca.ca

Contents - Table des matières

Editorial - Éditorial **3**

Aeroacoustics - Aéroacoustique **5**

The Association of Acoustic and Non-Acoustic Factors with Severe Aircraft Noise Annoyance - Results of the Survey of Noise Impacts on Canadian Communities
Julia Jovanovic, Colin Novak 5

Tonal Noise Prediction Of Serrated Trailing-Edge Airfoils
Yehia Salama, Basim Al Tlua, Joana Rocha 17

Bio-Acoustics - Bio-acoustique **31**

The effect of mouth opening levels on acoustic parameters of voice signal
leila Ghasisin, Fatemeh Abnavi, Mahtab Rasimahmoudi, Shirin Saberi 31

Underwater Acoustics - Acoustique sous-marine **39**

Soundscape Additions From Vessels Related To Transit Speed, Direction And Manoeuvres
Rianna Burnham, Brody Granger, Svein Vagle 39

Other Features - Autres rubriques **51**

Tribute to Ken Barron - Hommage à Ken Barron 51

AWC 2023 Montreal Conference Announcement and Call for Papers - Appel à communication - Semaine canadienne de l'acoustique AWC 2023 à Montréal 53

2023 CAA Prize Announcement - Annonce des Prix ACA 2023 57

CAA Announcements - Annonces de l'ACA 58


CONTROL NOISE
LOWER PROJECT COSTS
IMPROVE SPEECH PRIVACY
BOOST COMFORT & WELLNESS
QUICK ROI
INCREASE PRODUCTIVITY
FACILITY FLEXIBILITY
ENHANCE WORKPLACE CULTURE
SUPPORT FOCUS
LogiSon ACOUSTIC NETWORK
SOUND. THAT WORKS.™
Sound masking is more than a product. It's a service provided by professional technicians who know the effect isn't achieved from the moment they power the system, but by tuning the sound to an independently-proven curve. Designed right, tuned right—that's our motto. And the result is more consistent, comfortable and effective sound masking.
www.logison.com
© 2022 KR MOELLER ASSOCIATES LTD. LOGISON IS A REGISTERED TRADEMARK OF 777388 ONTARIO LIMITED. PHOTO BY VINCENT LIONS.

Editor’s note: Our association belongs to all of us
Éditorial: Notre association nous appartient à tous

Our association belongs to all of us

Dear reader, I would like to open this issue with a request. I have served in the role of Editor in Chief for some years now, and I have seen the many challenges of our association (and our world) over the last few years. This time has enforced in me the awareness of the importance of being a community of people that shares values, interested and experiences among peers.

Our association has a long history but it remains a little baby where we know each other well. Moving forward, we need to keep the intimacy of our association (and of this journal) but we would need to grow and become a bigger association.

There are many opportunities moving forward, from the next AWC that will be organized in the magnificent Montreal to the following 2024 yearly event, that we are planning with our ASA cousins in Ottawa from May 13- 17, 2024.

In brief, our plans are ambitious but we need the help of each of you. *Canadian Acoustics* is our place and the medium we have been always using to communicate each other, and present works, researches, and information. The pleasure to receive the hard copy of our journal, in the new layout and quality of printing we have now, plus the possibility to have our papers made available forever in an online open-access depository are extremely valuable, and represent one of the most valuable elements of our society.

For this reason, I would like to invite all of you to consider *Canadian Acoustics* more and more. A journal exists for the writers who contribute to it. Thanks to them we can enjoying reading their projects and papers, and thanks to their contribution we all discover what is happening in Canada within the world of acoustics. However, I know many readers have been silent or have not found the time recently to present their work to *Canadian Acoustics.*

This journal requires more than ever, more submissions, more technical notes, and more reviewers (the three aspects come together). I would encourage to reach me to volounteer and to consider JCAA as your home, that to keep high quality and quantity, needs to be nutried. Best!

Umberto Berardi - Editor in Chief.

Notre association nous appartient à tous

Cher lecteur, je voudrais ouvrir ce sujet avec une demande. J'occupe le poste de rédacteur en chef depuis quelques années maintenant, et j'ai vu les nombreux défis de notre association (et de notre monde) au cours des dernières années. Cette période a renforcé en moi la prise de conscience de l'importance d'être une communauté de personnes qui partagent des valeurs, des intérêts et des expériences entre pairs.

Notre association a une longue histoire mais elle reste un petit bébé où nous nous connaissons bien. Pour aller de l'avant, nous devons garder l'intimité de notre association (et de ce journal) mais nous aurions besoin de grandir et de devenir une plus grande association.

De nombreuses opportunités s'offrent à nous, du prochain AWC qui sera organisé dans la magnifique ville de Montréal, à l'événement annuel de 2024, que nous planifions avec nos cousins de l'ASA à Ottawa du 13 au 17 mai 2024.

En bref, nos projets sont ambitieux mais nous avons besoin de l'aide de chacun et chacune d'entre vous. L'*Acoustique Canadienne* est notre tribune ainsi que le moyen que nous avons toujours utilisé pour communiquer entre nous et présenter nos travaux, nos recherches et nos informations. Le plaisir de recevoir la version papier de notre journal, dans la nouvelle mise en page avec la qualité d'impression que nous avons maintenant, ainsi que la possibilité d'avoir nos articles disponibles pour toujours dans un espace d'accès libre en ligne sont extrêmement précieux, et représentent l'un des éléments les plus précieux de notre société.

C'est pourquoi j'aimerais vous inviter à prendre de plus en plus en considération la revue *Acoustique canadienne*. Une revue existe pour les auteurs qui y contribuent. Grâce à eux, nous pouvons prendre plaisir à lire leurs projets et leurs articles, et grâce à leur contribution, nous découvrons tous ce qui se passe au Canada dans le monde de l'acoustique. Cependant, je sais que de nombreux lecteurs sont restés muets ou n'ont pas trouvé le temps de présenter leurs travaux à Canadian Acoustics.

Cette revue a plus que jamais besoin d'un plus grand nombre de contributions, de notes techniques et d'évaluateurs (les trois aspects se rejoignent). Je vous encourage à me contacter pour me faire part de vos commentaires et à considérer JCAA comme votre foyer, lieu qui a besoin d'être alimenté pour maintenir une qualité et une quantité élevées. Je vous souhaite bonne chance !

Umberto Berardi – Rédacteur en chef


Improving our environments
with sound and vibration measurement solutions from Scantek.
DataKustik
53.0

The Association of Acoustic and Non-Acoustic Factors with Severe Air-Craft Noise Annoyance – Results of the Survey of Noise Impacts on Canadian Communities

Julia Jovanovic *[1], Colin Novak †[1]

[1]University of Windsor, Department of Mechanical, Automotive and Materials Engineering, Windsor, Canada

Résumé

De nombreux Canadiens sont affectés à divers degrés par des bruits dérangeants. Ceux qui vivent près des aéroports et des trajectoires de vol, sont exposés aux bruits des aéronefs qui peuvent causer de graves perturbations. Ses perturbations, sont l'effet le plus commun lors de l'exposition aux bruits aéronefs et elle constitue un paramètre clé dans les règlements et les directives provenant. Avec cela étant dit, il y a aussi des perturbations occasionnelles par des avions qui n'affecte pas les humains et cela est parce que leur niveau sonore n'est pas assez élevé pour devenir une nuisance. Une compréhension approfondie de la nuisance sonore et de tous ses facteurs acoustiques et non-acoustiques qui peuvent y contribuer est essentielle à sa gestion. Le Survey of Noise Impacts on Canadian Communities 2021 (SONICC 2021) est un questionnaire distribué dans les régions où se trouve un aéroport international, tel que Pearson à Toronto, qui visent à identifier les facteurs sonores, acoustiques et non-acoustiques, qui leur perturbaient le plus. Bien que l'analyse présentée dans ce document note que la prévalence de l'exposition aux bruits augmente les dérangements, les niveaux sonores seuls n'étaient pas le meilleur indicateur de la probabilité qu'une personne soit perturbé. La prise en compte de facteurs situationnels, personnels et attitudinaux tels que la perception d'un changement de bruit, l'accoutumance, le sentiment d'injustice et la sensibilité au bruit a considérablement amélioré la capacité à prédire la gêne qui est plus sévère. Cet article présente les résultats de l'étude SONICC 2021 et suggère comment ces résultats peuvent contribuer à une approche plus globale de la prédiction et de l'atténuation de la gene.

Mots clefs: Bruit des aéronefs, gêne induite par le bruit, facteurs non-acoustiques, enquête sur la gêne, prédiction de la gene

Abstract

Many Canadians are affected to various extends by environmental noise. Those living near airports and flight paths are exposed to aircraft noise that can cause severe disturbance and annoyance amongst the population. Annoyance is the most common effect of aircraft noise exposure, and as such, is a key metric in regulations and guidelines. However, it is anecdotally understood that annoyance from aircraft noise cannot be attributed to a measured noise level alone and that there are other contributing factors. Thorough understanding of noise annoyance and all possible acoustic and non-acoustic contributors is critical to its management. The Survey of Noise Impacts on Canadian Communities 2021 (SONICC 2021) was a questionnaire distributed around Toronto Pearson International Airport, which sought to identify both acoustic and non-acoustic factors associated with severe noise annoyance. While the analysis in this paper noted that prevalence of severe annoyance increased with higher noise exposure, noise levels alone were not the best predictor of a respondent's likelihood of being highly annoyed. Consideration of situational, personal, and attitudinal factors such as perceived change in noise, habituation, feeling of unfairness, and noise sensitivity significantly improved the ability to predict severe annoyance. This paper shares the results of SONICC 2021 and suggests how these findings can inform a more holistic approach to annoyance prediction and mitigation.

Keywords: Aircraft noise, noise-induced annoyance, non-acoustic factors, annoyance survey, annoyance prediction

1 Introduction

Aircraft noise can impact many communities surrounding an airport, especially when the airport is near or within an urban environment, as is the case for Toronto Person International Airport. Prolonged exposure to high and even moderate levels of aircraft noise has been speculated to have numerous psychological and physiological effects. Cardiovascular disease, cognitive impairment, sleep disturbance and annoyance are considered the critical health outcomes of environmental noise exposure by the World Health Organization, although further research is necessary to support these findings (WHO) [1].

Annoyance is the most well-corroborated and common effect of environmental noise and is understood as a feeling of displeasure, disturbance, or irritation that is caused by an unwanted sound [2]. It is recognized as a health effect endpoint of long-term environmental noise exposure as well as a modifying factor contributing to other health effect endpoints such as hypertension. [3]

Aircraft noise annoyance is the principal metric used to gauge the impacts of aircraft noise on communities. It is also used as the basis for regulations and guidelines aimed at protecting people from the effects of excessive noise exposure [4, 5]. To help quantify the relationship between annoyance

* jovano11@uwindsor.ca

† novak1@uwindsor.ca

and noise exposure, dose-response functions have been developed and updated since the 1970's. These functions correlate cumulative noise exposure levels to the percentage of the population that is highly annoyed (%HA) by the exposure. The International Commission on Biological Effects of Noise considers %HA to be the main indicator of community annoyance [6].

Dose-response functions are used to inform both annoyance prediction and mitigation. While clearly a relationship exists between the level of noise and annoyance, much variance is seen in the data [7]. The variance in dose-response functions cannot be explained by acoustic factors alone. Studies have consistently identified the influence of non-acoustic factors on annoyance. Personal, situational, and attitudinal variables have been found to be contributors to annoyance. [8-11] A better understanding of the non-acoustic components will enhance annoyance prediction and better inform effective mitigation measures.

The Survey of Noise Impacts on Canadian Communities (SONICC) assessed a number of non-acoustic and acoustic variables and their association to severe annoyance. In this work, an annoyance prediction model with noise exposure as the sole predictor of severe annoyance is compared to an alternate model having both acoustic and non-acoustic variables as the predictors. Further, the results of SONICC 2021 are discussed in an effort to develop a more holistic understanding of the mindsets of HA and NON-HA respondents.

2 Method

2.1 Data collection

SONICC was distributed in the spring of 2021 to the communities around Toronto Pearson International Airport. 8,000 addresses were randomly selected in areas having various aircraft noise exposure levels, as identified by the modelled aircraft noise contours shown in Figure 1. An equal number of surveys were intended for distribution in five zones, although the zones with the highest noise exposure had few or no residential addresses. The surveys that were intended for these zones were equally distributed amongst the remaining zones. The distribution and response rates from each zone are outlined in Table 1. Respondents to the survey were given an option to reply by mail (using enclosed return envelope), online or via device using a QR code. From
the returned responses, those that did not provide an address to facilitate the study's noise calculations were eliminated from the analysis as it would not be possible to determine their noise contour range of exposure. The remaining 720 responses were further filtered to eliminate those that did not respond to the ISO noise annoyance questions. Altogether, 693 surveys were included in the analysis that was used in this paper.

Figure 1: SONICC survey distribution zones based on PPD NEF. contours.

2.2 Questionnaire

SONICC 2021 was comprised of three sections that examined various demographic, situational, personal, and attitudinal factors identified in the literature as possible contributors to severe annoyance. *Part A – Neighbourhood and Home Related Quality of Life* included questions about the respondent's self-reported exposure to aircraft noise, their assessment of how aircraft noise has changed over the past year, their expectations for how aircraft noise will change over the coming years, the length of residency in their current home, their ability to habituate to the noise, their expectations of noise exposure when first moving to the neighbourhood, and the approximate value of their home. *Part B – Demographics* contained questions about age, gender, education, and approximate household income. *Part C – Noise Source and Impacts* assessed the levels of long-term annoyance using two questions from ISO/TS 15666:2003(E) [12] given as follows:

Table 1. SONICC distribution zones, return rates, HA distribution

Zone	Zone description	# of surveys	% of total distribution	# of surveys returned	Rate of return	# of HA respondents	% HA
1	NEF 40+	0	0%	0	0%	0	0%
2	NEF 35-40	1	0%	0	0%	0	0%
3	NEF 30-35	1,202	15%	77 (RR 6.4%)	11%	20	26%
4	NEF 25-30	3,398	42%	332 (RR 9.8%)	46%	66	20%
5	15 km – NEF 25	3,399	42%	309 (RR 9.1%)	43%	17	6%

(5 – Point Annoyance Question)
Thinking about the last (12 months or so), when you are here at home, how much does noise from aircraft bother, disturb or annoy you?

_Not at all
_Slightly
_Moderately
_Very
_Extremely

(11- Point Annoyance Question)
Thinking about the last (12 months or so), what number from 0 to 10 best shows how much you are bothered, disturbed, or annoyed by aircraft noise? [12]

Respondents were also asked to identify, from a list of seven examples, the noise sources that affect them while at home. The noise sources included neighbourhood (i.e., lawn mowers), entertainment (i.e., music, fireworks), traffic (i.e., automobile), railroad, construction, aircraft, and product (i.e., AC, dishwasher, fridge). Respondents were asked to select all that apply. A multi-noise score (1-7) was assigned to each respondent based on the number of noise sources selected. In addition, other personal and attitudinal factors were examined such as misfeasance with authorities; a score given based on an average of responses to three questions about the belief that there is a lack of communication, action, and accountability by authorities. A feeling of unfairness score was calculated based on the responses to two questions relating to the belief that there is a lack of compensation for tolerating the noise and the belief that there is an unfair distribution of noise. An attitude towards airport authorities score was an average calculated based on the responses to the following questions:

My local airport (1 - Strongly disagree to 5 - Strongly agree):

- Is an organization I trust
- Is well managed
- Is profit driven
- Is efficient
- Is transparent/open
- Is engaged in the community
- Is environmentally responsible
- Is socially responsible
- Handles emergency situations well
- Manages noise well

The answers to these questions were normalized to a 1 - 5 scale, 1 being a negative attitude towards authorities and 5 being a positive attitude towards authorities, prior to averaging. Thus, a question that is 'positively' worded such as 'is an organization I trust', the 1-5 scale remains as the respondent answered, while a question that is negatively worded such as 'is profit driven', the 1-5 scale is reversed from the respondent's answer (i.e., 1 becomes a 5, 2 becomes a 4 and 3 remains the same). Any unanswered questions were omitted from the calculation of the average score.

A respondent's attitude towards the noise and the noise source was also given a score based on the average response to the following questions (1 - Strongly agree to 5 - Strongly disagree):

- Air travel is fun and useful
- Aircraft noise affects my physical health
- Aircraft noise affects my mental health
- Having an airport in the area is good for the economy (jobs, tourism etc.)
- Air travel causes air pollution
- Night flights are an essential part of airport operations
- Air travel is dangerous
- Cargo flights are essential for timely delivery of goods
- Aircraft noise makes my home less valuable
- It is convenient to have an airport in the area
- Air travel contributed to the spread of COVID 19

The answers to these questions were normalized in the same manner described above, prior to averaging. A low score relates to a negative attitude towards the noise and source and a high score relates to a positive attitude. A further question assessed the respondent's noise sensitivity (1 – not at all sensitive to 5 – extremely sensitive to noise). Lastly, the respondent's coping capacity was determined based on the dichotomous answer to the question 'When I am bothered by noise, I feel helpless / cannot escape the noise '(1 – True/lack of coping capacity, 2 – False/presence of coping capacity). Additional questions were included in SONICC that were not used as variables in the prediction models, but rather to further the understanding of the impacts and perceptions of aircraft noise in affected communities.

2.3 Noise exposure modelling

The noise exposure at each response location was modelled using AEDT 3C. The noise exposure was modelled using the DNL (day-night level) metric, which is an averaged noise level over a 24-hour period with a 10 dBA penalty added for nighttime noise (23:00-7:00). Although Canada uses the Noise Exposure Forecast (NEF) metric for predictions of aircraft noise impacts, the DNL metric is more comparable to the international literature. The aircraft noise exposure was modelled for the 95th percentile day or peak planning day (PPD) traffic volumes, according to the methodology mandated by Transport Canada, for the 12-month period prior to the distribution of the survey [5].

2.4 Statistical analysis

Two statistical analyses were performed on the data, an independent t-test and a logistic regression. To begin, an independent t-test was performed for each variable identified in the survey in order to assess if the means of the highly annoyed (HA, annoyance score above 72) and non-highly annoyed (NON-HA, annoyance score below 72) groups of respondents are statistically different. By performing the independent t-test first, it was possible to identify all the variables of interest which demonstrate clear differences of sentiments between HA and NON-HA respondents. The results of this analysis are given in Tables 2-5.

In the next part of the statistical analysis, two logistic regression models were tested. Model 1 had the level of noise exposure as the only variable to predict one's likelihood of being HA. Model 2, in addition to noise exposure, included several non-acoustic predictor variables. The variables identified as statistically significant from the independent t-test were first evaluated for collinearity using collinearity statistics from a linear regression model. From the original eleven variables, two were removed due to collinearity: self-reported noise exposure (possibly collinear with modelled noise exposure level) and misfeasance with authorities (possibly collinear with attitude towards airport authorities). The nine remaining variables were used as inputs in a binary logistic model. The results of the logistic regression are outlined in Table 6.

3 Results / Discussion

The overall response rate for SONICC 2021 was 9.31%. Some responses were excluded from the analysis due to incompleteness of critical questions, leaving 693 valid responses. From these, 21% reported being highly annoyed by aircraft noise over the last 12 months; the remaining 79% were NON-HA.

3.1 Acoustic and non-acoustic variables - Results of independent sample t-test

Table 2 outlines the distribution of HA and NON-HA respondents by noise exposure interval. The highest number of respondents are from areas which are exposed to noise above DNL 55 dBA. This is not unexpected because communities affected by higher levels of noise are more likely to be engaged in the topic of aircraft noise, and therefore more likely to participate in the survey. More than half (54%) of the HA respondents come from areas exposed to DNL 60 dBA or more, while only 25% of NON-HA come from those exposure levels. 88% of HA are exposed to noise above DNL 55 dBA. The data in Table 2 shows that the mean noise exposure for HA and NON-HA is statistically different, thus noise level is a potential acoustic factor that can help in the prediction of severe annoyance.

Table 2: Noise exposure by annoyance - SONICC survey.

	HA		Non-HA		p-value	Total
	n	%	n	%		n
Aircraft Noise (DNL)					**<0.001**	
<35 dBA	1	1%	82	14%	--	83
35-39 dBA	3	2%	75	13%	--	78
40-44 dBA	3	2%	36	6%	--	39
45-49 dBA	2	2%	52	9%	--	54
50-54 dBA	6	5%	78	14%	--	84
55-59 dBA	41	34%	104	18%	--	145
>60dBA	66	54%	144	25%	--	210

*n is the number of surveys, p-value is the significance level, values below 0.001 are statistically significant.

Table 3 summarizes the results of the independent t-test for Section A of SONICC. Six variables were tested for statistically significant differences of means between the HA and NON-HA respondents. The results demonstrate whether HA respondents are more likely to respond differently to a question than NON-HA respondents. Questions that have statistically different responses between the two groups are identified as variables that can possibly contribute to the prediction of noise annoyance and are selected as inputs for the logistic regression performed in the second stage of the analysis.

Self-reported noise exposure was found to be a statistically significant variable. 63% of all respondents reported being exposed to aircraft noise continuously or always. This is not unexpected due to the targeted distribution of the survey to areas that are known to be affected by aircraft noise. This percentage increases to 98% of HA respondents reporting being exposed to aircraft noise continuously or always. Some consideration was given to a possible response bias, where HA respondents could be reporting an amplified level of exposure. This was rebutted by a mapping of the respondent locations who answered ‘continuously’ or ‘always’ to the self-reported noise exposure question. This mapping confirmed that most of ‘continuously’ or ‘always’ respondents were indeed located in areas that were likely subjected to significant noise exposure on a regular basis. Thus, self-reported noise exposure is a variable that can be used in an annoyance prediction model, particularly when there is a lack of access to noise data (modelled or measured).

Perceived change in noise was also found to be statistically significant. 25% of HA respondents reported that there was a significant increase in noise in the past 12 months compared to only 2% of NON-HA. This result was unexpected given that the ‘last 12 months’ (approximately May 2020 to May 2021) that were being assessed experienced significant reductions of aircraft traffic due to COVID 19 travel restrictions which were first implemented in March 2020. On closer examination, reduced traffic volumes at Toronto Pearson allowed for some condensed flight paths that concentrated traffic over a narrower corridor which may have created a perception of increased volume for some people, but conversely would also reduce the exposure for others. This finding highlights the possibility of increased prevalence of severe annoyance with narrowing flight paths such as Required Navigation Performance (RNP) routes, which are proposed to be implemented for all airports in the European Union in the coming years [13].

Additionally, 41% of the HA respondents acknowledged that noise has either somewhat or significantly decreased over the last 12 months, yet they remain HA. This is a disconcerting finding for authorities who invest significant efforts to reduce cumulative exposure by 1-2 dBA in hopes of reducing community annoyance. Perceived change in noise can potentially be an acoustic (if confirmed by objective assessment) or non-acoustic factor that can contribute to annoyance prediction.

HA respondents’ expectations for future noise were also found to be statistically different compared to those of NON-HA. 80% of HA respondents expected that noise will somewhat or significantly increase over the coming years, while only 58% of NON-HA shared this sentiment. Thus, expectation for future noise is identified as a non-acoustic factor that

Table 3: Results of SONICC 2021 Section A-Neighbourhood and Home Related Quality of Life

		HA		NON-HA		p-value	TOTAL
		n	%	n	%		n
Self-reported noise exposure						**<0.001**	
blank	No answer	0	0%	9	1%	--	9
1	Continuously	55	45%	61	11%	--	116
2	Always	65	53%	254	45%	--	319
3	Sometimes	2	2%	205	36%	--	207
4	Never	0	0%	42	7%	--	42
Perceived change in noise over the past 12 mo.						**<0.001**	
blank	No answer	3	2%	20	4%	--	23
blank	No aircraft noise exposure	0	0%	28	5%	--	28
1	Significantly increased	31	25%	10	2%	--	41
2	Somewhat increased	11	9%	26	5%	--	37
3	Stayed the same	23	19%	102	18%	--	125
4	Somewhat decreased	33	27%	153	27%	--	186
5	Significantly decreased	17	14%	203	36%	--	220
blank	Don't know	4	3%	29	5%	--	33
Future expectations for noise						**<0.001**	
blank	No answer	4	3%	14	2%	--	18
1	Significantly increase	78	64%	191	33%	--	269
2	Somewhat increase	20	16%	145	25%	--	165
3	Stay the same	4	3%	100	18%	--	104
4	Somewhat decrease	1	1%	22	4%	--	23
5	Significantly decrease	6	5%	8	1%	--	14
blank	Don't know	9	7%	91	16%	--	100
Past expectations for how affected one expected to be by aircraft noise upon moving to their home						0.012	
blank	No answer	2	2%	10	2%	--	12
1	Unaffected / not affected	30	25%	220	39%	--	250
2	Less affected	31	25%	78	14%	--	109
3	Somewhat affected	46	38%	247	43%	--	293
4	Greatly affected	13	11%	16	3%	--	29
Length of residency						0.999	
blank	No answer	1	1%	6	1%	--	7
1	Less than 1 year	0	0%	6	1%	--	6
2	1-2 years	2	2%	9	2%	--	11
3	3-4 years	8	7%	20	4%	--	28
4	5 years or longer	111	91%	530	93%	--	641
Habituation to noise						**<0.001**	
blank	No answer	5	4%	16	3%	--	21
0	No	89	73%	178	31%	--	267
1	Yes	25	20%	212	37%		237
blank	Not bothered by noise	3	2%	165	29%	--	168

can contribute to annoyance prediction.

A question was included in the survey to assess a respondent's expectations for aircraft noise exposure prior to moving into their current home. This question did not show a statistically significant difference in responses between HA and NON-HA, mainly because the majority of both groups did not expect to be as affected by aircraft noise prior to moving to their home. This exposes a problem with access to valid information / guidelines. Health Canada in their most recent guidance on aircraft noise, recommend that an individual planning to move to a neighbourhood near an airport, should consult the noise contour map for the area and follow guidelines outlined in a Transport Canada document entitled TP 1247E Part IV Aircraft Noise [5, 14]. This guideline offers outdated and misleadingly concise predictions as to the expected community reaction to different aircraft noise levels. A better understanding of acoustic and non-acoustic factors affecting severe annoyance would allow for more informed guidance for those contemplating a move to an aircraft noise affected area. This in turn could help mitigate the levels of severe annoyance in communities surrounding the airport.

The 'length of residency' was not found to be a statistically significant variable as most respondents reported having lived in their current home for 5 years or more. On the other hand, habituation to noise was found to be statistically significant. 73% of HA respondents reported not being able to get used to the noise, while only 31% of NON-HA reported the same, making it a possible non-acoustic contributor to annoyance.

Table 4 shows the results of the demographic variables examined in Section B of SONICC. None of the demographic factors including home value, age, gender, education, and household income showed a statistically significant difference between HA and NON-HA respondents. This is important because it is often hypothesized that demographic factors have an impact on annoyance, despite this being consistently disproven [9, 15].

Table 5 evaluates numerous situational, attitudinal, and personal factors from Section C of SONICC. The first variable is a multi-noise source score. Respondents were asked which noise sources impacted them while at home. The hypothesis being tested was that HA respondents would report being affected by more noise sources than NON-HA. This was not the case and there was no statistically significant difference between the two groups.

All attitudinal factors, misfeasance with authorities, feeling of unfairness, attitude towards airport authorities, and attitudes towards the noise and noise source, were found to be statistically significant. The HA group had a significantly higher misfeasance with authorities and feeling of unfairness average scores in comparison to NON-HA respondents. HA also had significantly more negative attitudes towards authorities and the noise/source.

Personal factors like sensitivity to noise and coping capacity were also found to be statistically significant. 54% of HA reported being very or extremely sensitive to noise, while only 19% of NON-HA reported the same. 75% of HA respondents lacked coping capacity and reported feeling helpless and unable to escape the noise in comparison to 26% of NON-HA. Situational, attitudinal, and personal factors are all non-acoustic variables, yet they formed the bulk of inputs in the logistic regression model for the prediction of severe annoyance, demonstrating the significant implications of excluding non-acoustic factors from the prediction and mitigation of annoyance.

As stated earlier, the independent t-test was performed first and the logistic regression second. This was because a logistic regression significantly lowered the size of the study sample. Due to the nature of the survey (mailed, not in-person interview) many respondents did not answer every question. Only those that answered the survey in its entirety were analyzed in the logistic regression, effectively reducing the sample size from 693 to 285. A logistic regression can sometimes render critical variables as statistically insignificant due to a small sample size, and inversely trivial variables can be identified as statistically significant in large sample sizes [16].

3.2 Noise annoyance prediction model – Results of logistic regression

Based on the results of the independent t-test, nine variables (1 acoustic and 8 non-acoustic) were tested in two binary logistic models. The first model had only noise exposure level (DNL) as a predictor variable. This model, although statistically significant, was not a good predictor of severe annoyance. It did not predict a single HA respondent. The second model significantly improved prediction by predicting nearly 68% of the HA cases. This model identified five variables that can predict better than chance someone's likelihood of being HA. Aircraft noise level (DNL), perceived change in noise, habituation to noise, feeling of unfairness, and self-reported noise sensitivity were found to be statistically significant in this model. Amongst these variables, noise sensitivity and feeling of unfairness, both non-acoustic variables, had the highest association to severe annoyance. The OR values of each variable in both models are listed in Table 6 and can be seen in Figure 2.

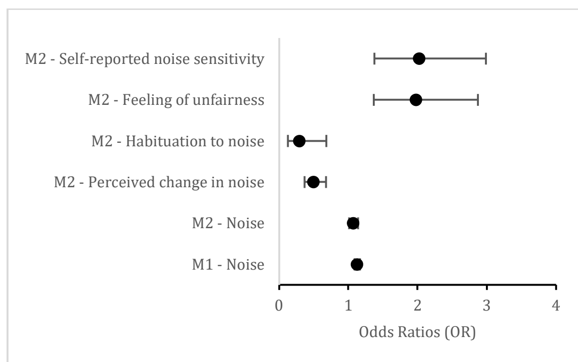

Figure 2: Model 1 and Model 2 variables and odd ratios

The analysis in Table 6 highlights the role of non-acoustic factors in annoyance predication. The only two acoustic variables that were found to be statistically significant predictors of annoyance; the modelled aircraft noise level and the perceived change in noise (self-reported and not verified), have the lowest odds ratio (OR) from the statistically significant variables, considering that an OR of 1 means no association between exposure and outcome. Even when the noise level is plugged into the model at intervals of 4 dBA, the OR ratio only increases to 1.48. Conversely, non-acoustic factors such as habituation to noise, feeling of unfairness, and noise sensitivity, were all found to be statistically significant variables with higher association to the outcome of severe annoyance than the acoustic factors tested. Thus, non-acoustic variables are as, if not more important in the study, prediction, and perhaps even mitigation of noise annoyance than acoustic ones.

Table 4: Results of Section B Demographics of SONICC survey.

		HA		NON-HA		p-value	TOTAL
		n	%	n	%		n
Self-reported home value						0.084	
blank	No answer	26	21%	101	18%	--	127
1	Under 200 000	2	2%	5	1%	--	7
2	200 001 - 4000 000	2	2%	11	2%	--	13
3	400 001 - 600 000	3	2%	33	6%	--	36
4	600 001 - 800 000	11	9%	76	13%	--	87
5	800 001 - 1 M	27	22%	129	23%	--	156
6	1M +	42	34%	151	26%	--	193
blank	Don't know	9	7%	65	11%	--	74
Age						0.468	
blank	No answer	8	7%	33	6%	--	41
1	Under 18	0	0%	1	0%	--	1
2	18-19	0	0%	1	0%	--	1
3	20-24	0	0%	3	1%	--	3
4	25-34	1	1%	11	2%	--	12
5	35-44	13	11%	44	8%	--	57
6	45-54	15	12%	74	13%	--	89
7	55-64	35	29%	134	23%	--	169
8	65-74	30	25%	144	25%	--	174
9	75+	20	16%	126	22%	--	146
Gender						0.898	
blank	No answer	26	21%	77	13%	--	103
1	Female	44	36%	229	40%	--	273
2	Male	52	43%	263	46%	--	315
blank	Other	0	0%	2	0%	--	2
Education						0.384	
blank	No answer	22	18%	52	9%	--	74
1	Master/Doctorate	20	16%	74	13%	--	94
2	Post-secondary	56	46%	314	55%	--	370
3	High school	21	17%	118	21%	--	139
4	Elementary	3	2%	13	2%	--	16
Household income						0.551	
blank	No answer	56	46%	186	33%	--	242
1	Under 20,000	2	2%	15	3%	--	17
2	20,000-46,605	11	9%	67	12%	--	78
3	46,606-93,208	20	16%	139	24%	--	159
4	93,209-144,489	20	16%	90	16%	--	110
5	144,490-205,842	9	7%	48	8%	--	57
6	205,843 +	4	3%	26	5%	--	30

3.3 Additional survey questions and findings

Some additional questions were included in SONICC that provided insight into the nature of the noise disturbance, its impacts, and the affected populations. When asked about the level of disturbance / annoyance from various noise sources including neighbourhood activities, entertainment, traffic, railroad, construction, aircraft, and product, both HA and NON-HA ranked aircraft noise as the most annoying, followed by traffic and neighbourhood (HA)/entertainment (NON-HA). HA respondents' average level of annoyance

Table 5: Results of Section C Noise Source and Impacts of SONICC survey.

		HA		NON-HA		p-value	TOTAL
		n	%	n	%		n
Multi-noise source score (neighbourhood, entertainment, traffic, railroad, construction, aircraft, product)						0.240	
blank	No answer	1	1%	20	4%	--	21
1	Affected by 1 source	23	19%	143	25%	--	166
2		45	37%	141	25%	--	186
3		28	23%	110	19%	--	138
4		14	11%	81	14%	--	95
5		9	7%	42	7%	--	51
6		2	2%	17	3%	--	19
7	Affected by all 7 sources	0	0%	17	3%		17
Misfeasance with authorities		Avg Score		Avg Score		**<0.001**	Avg Score
1	No misfeasance					--	
to		4.06		2.52		--	2.88
5	High misfeasance					--	
Feeling of unfairness		Avg Score		Avg Score		**<0.001**	Avg Score
1	No feeling of unfairness						
to		4.39		2.66			3.08
5	High feeling of unfairness						
Attitude towards airport authorities		Avg Score		Avg Score		**<0.001**	Avg Score
1	Negative attitude						
to		2.18		3.05			2.9
5	Positive attitude						
Attitude towards noise and source		Avg Score		Avg Score		**<0.001**	Avg Score
1	Negative attitude						
to		2.48		3.34			3.14
5	Positive attitude						
Self-reported noise sensitivity						**<0.001**	
blank	No answer	0	0%	3	1%		3
1	Not at all	1	1%	90	16%		91
2		11	9%	109	19%		120
3	Somewhat	47	39%	263	46%		310
4		28	23%	68	12%		96
5	Extremely	35	29%	38	7%		73
Coping capacity (feeling helpless)						**<0.001**	
blank	No answer	10	8%	85	15%		95
1	Lack of coping capacity	92	75%	148	26%		240
2	Presence of coping capacity	20	16%	278	49%		298
blank	Not bothered by noise	0	0%	60	11%		60

from each noise source mentioned above was higher than NON-HA, possibly pointing to an inherent noise sensitivity in HA respondents that was also supported by the responses to the self-reported noise sensitivity question.

To understand if there is a statistical difference between aircraft noise HA vs NON-HA respondents' sentiments towards other noise sources, respondents' annoyance ratings for all seven noise sources were tested with an independent sample t-test. Response differences were only statistically significant for traffic noise. Those highly annoyed by aircraft noise were more likely to also be severely annoyed by traffic noise compared to those that were non-highly annoyed by

Table 6 : Significance, Odds Ratios (OR) and 95 % Confidence Intervals (CI) for HA in relation to noise exposure (DNL) and non-acoustic factors. Note : Model is statistically significant where $p<0.001$; Variables are statistically significant where $p<0.05$.

	Model 1 (n=693)		Model 2 (n=285)	
Model significance	<0.001		<0.001	
	p-value	OR (95% CI)	p-value	OR (95% CI)
Aircraft noise level (DNL) (OR per dBA)	**<0.05**	**1.129** (1.091-1.169)	**<0.05**	**1.073** (1.012-1.138)
Perceived change in noise	--	--	**<0.05**	**0.499** (0.369-0.675)
Future expectations for noise	--	--	0.303	1.252 (0.816-1.921)
Habituation to noise	--	--	**<0.05**	**0.295** (0.128-0.683)
Feeling of unfairness	--	--	**<0.05**	**1.981** (1.367-2.869)
Attitudes towards airport authorities	--	--	0.257	1.257 (0.846-1.866)
Attitudes towards noise and source	--	--	0.137	0.583 (0.286-1.187)
Self-reported noise sensitivity	--	--	**<0.05**	**2.027** (1.376-2.987)
Coping capacity (feeling helpless)	--	--	0.058	0.431 (0.181-1.029)

aircraft noise. This finding can be used in the prediction of annoyance for residents contemplating a move to an aircraft noise impacted community. As traffic noise affects many more people daily, more individuals can recollect this experience. Those who report being highly annoyed by traffic noise will likely be severely annoyed by aircraft noise as well. Traffic noise annoyance can therefore become a proxy metric for aircraft noise annoyance to help an individual determine the likelihood that they will be severely annoyed in an aircraft-noise-affected neighbourhood.

Respondents were also asked to indicate their levels of annoyance prior to COVID 19 travel restrictions, as this would evoke a recollection of higher air traffic volumes. It was determined that 44% of those that indicated being HA prior to COVID 19 restrictions were now reporting being NON-HA, likely due to the significant reduction in traffic. From the 465 that were NON-HA prior to COVID 19 restrictions, 15 identified becoming HA in the past year. It is hypothesized that these newly HA respondents might have become so due to condensed flight paths or as a result of a higher presence at home due to the pandemic lockdown.

In the questions that were used to compute a misfeasance with source authorities score, the biggest concern for both HA and NON-HA was the unfair distribution of noise. This sentiment has also been consistently expressed by community members around the airport. While many authorities believe that narrowing flightpaths through required navigation performance (RNP) will result in reduced noise impacts, this measure can increase the feeling of unfair distribution of noise, and therefore evoke higher levels of severe annoyance, albeit in a smaller portion of the population. This is not to say that PBN is not an effective measure to reduce aviation's environmental impacts, however it should be expected that severe annoyance will increase for some which will require-active management.

In the question that was used to devise an attitude towards the noise and source score, the most notable findings were that HA respondents were much more likely to believe that aircraft noise affects their mental health (83%) versus NON-HA (31%); that aircraft noise affects their physical health (75%) versus NON-HA (27%); that aircraft noise makes their homes less valuable (83%) versus NON-HA (41%). Studies by health and real-estate authorities could be performed to address these concerns, and in way of that possibly mitigate severe annoyance. Across all questions about attitudes towards the noise and source, HA tended to have a more negative stance than NON-HA. Even the belief that 'air travel contributed to the spread of COVID 19' was more strongly professed by HA (79%) than NON-HA (56%). The direction of causality for these attitudes is unknown.

Regarding the question that sought to evaluate the attributes of the noise/source that were most annoying to the respondent, both HA and NON-HA ranked noise level (how loud the aircraft is) as the most disturbing factor, followed by the number of aircraft then the time of the flights for HA and the time of flights followed by the number of aircraft for NON-HA.

When asked about the activities affected by aircraft noise, both HA and NON-HA ranked conversations and outdoor activities as most affected, followed by sleeping patterns. This points to the possibility of relatively low aircraft noise events (around and slightly above the level of speech), being obtrusive or disruptive and possibly evoking high levels of annoyance. This finding might also encourage a broader vocabulary for communicating noise conditions. The use of relational metrics such as the number above (NA) a given noise level (for example interference of speech at 3 meters apart) might improve the understanding of acoustic impacts in a given area. For instance, if someone was told that an address was subject to an average noise exposure level of DNL 55 dBA, this description might not be understood. Conversely, if they were told that while outdoors in the evening, they might expect their conversation to be impaired or disrupted 6 times within an hour on average, this will likely be more relatable.

When asked about the actions taken in response to the disturbance, most HA respondents identified closing windows and doors, feeling helpless / not being able to escape the noise, avoiding the outdoors, and considering moving to a quieter neighbourhood respectively. NON-HA report closing doors and windows, moving to a quieter space, and avoiding the outdoors respectively. The largest discrepancy in answers between HA and NON-HA was reflected in the feeling of helplessness/not being able to escape the noise (HA – 82%, NON-HA – 35%), and the consideration of moving to a quieter neighbourhood (HA – 68%, NON-HA – 24%). The feeling of helplessness has previously been observed in other studies that link exposure to aircraft noise to mental health challenges like depression [17]. This finding can inform possible annoyance mitigation strategies that aim to enhance a community's coping capacity through measures such as voluntary home purchasing, relocation programs, an effective noise complaint process and collaborative decision-making that will help individuals feel empowered and able to affect change.

Another question examined the times that aircraft noise was most disturbing / annoying. Respondents identified being most annoyed in the summer, followed by spring, fall and winter. As for the time of day, most annoying were nights followed by evening, days, and mornings. Respondents also reported being more annoyed on the weekends than weekdays. This can possibly inform aircraft noise metrics and/or how authorities schedule things like runway maintenance, operations etc.

Lastly, when asked about complaint behaviour 83% of HA and 93% of NON-HA reported never having submitted a noise complaint. These are important statistics as they highlight the common misconception that equates complaints to severe annoyance and vice versa.

3.4 Study notes

This study was done in the spring of 2021, amidst COVID 19 travel restrictions. During this period, many residents possibly had a greater 'at home' presence. These exceptional conditions could have uniquely impacted the results of the SONICC survey, although this condition may persist as more companies are offering the work from home option to their employees. In addition, the survey was executed around a single airport. A larger cross-sectional Canadian survey upon the return of pre-pandemic traffic is warranted which might result in the identification of additional acoustic and non-acoustic contributors to severe annoyance.

4 Conclusion

The analysis in this paper highlights the contribution of non-acoustic factors to the study of aircraft noise annoyance. While the presence of noise was found to be a clear qualifier for noise-induced annoyance, personal, situational, and attitudinal variables identified in SONICC were also associated with severe annoyance. Non-acoustic variables such as habituation to noise, feeling of unfairness, and noise sensitivity, were all found to be more predictive of severe annoyance than noise exposure levels. Due to the subjective nature of such non-acoustic variables, they are rarely integrated into policy, guidelines, or discussions with stakeholders. This leads to the erroneous belief that noise perception and annoyance can be predicted with categorical, overgeneralized dose-response type scales. While this type of guidance may be necessary for land-use planning purposes, it should not be viewed in isolation, nor should it be the go-to method for potential residents to assess how much annoyance they will experience in a particular aircraft affected area.

Authorities, law makers, community members and other stakeholders alike can benefit from understanding public sentiment about noise and all factors that play a role in noise annoyance. This type of knowledge may inform everything from airport operations and planning (i.e., time of day and flight path distribution), mitigation efforts (i.e., increasing coping capacity for affected communities), community outreach (i.e., providing more holistic information and guidance as to the effects of various acoustic and non-acoustic factors on annoyance) and even policy (i.e., including clauses about all levels of aircraft noise exposure in real-estate transactions). Disregarding the contributions of non-acoustic factors in severe annoyance may leave authorities with few mitigation options, other than striving for marginal reductions in noise exposure which are often not reflected in community perception and annoyance outcomes. Alternatively, managing noise exposure as well as non-acoustic factors allows for a multi-pronged approach for mitigating the effects of aircraft noise on communities.

Remerciements/Acknowledgments

The current research is sponsored by MITACS and supported by the University of Windsor and the Greater Toronto Airports Authority.

References

[1] Environmental Noise Guidelines for the European Region, 2018. https://www.euro.who.int/en/publications/abstracts/environmental-noise-guidelines-for-the-european-region-2018 (accessed 1.14.22).

[2] D. Ouis. Annoyance from Road Traffic Noise: A Review. J. Environ. Psychol. 21, 101–120, 2001. https://doi.org/10.1006/jevp.2000.0187

[3] T. Münzel, M. Sørensen, T. Gori, F.P. Schmidt, X. Rao, F.R. Brook, L.C. Chen, R.C. Brook, S. Rajagopalan. Environmental Stressors and Cardio-Metabolic Disease: Part II-Mechanistic Insights. Eur. Heart J. 38, 557–564, 2017. https://doi.org/10.1093/eurheartj/ehw294

[4] S. Fidell. Assessment of the effectiveness of aircraft noise regulation. Noise Health 1, 17, 1999.

[5] Transport Canada. TP 1247 E - Land Use in the Vacinity of Aerodromes, 2013.

[6] M. Basner, C. Clark, A. Hansell, J.I. Hileman, S. Janssen, K. Shepherd, V. Sparrow. Aviation Noise Impacts: State of the Science. Noise Health 19, 41–50, 2017. https://doi.org/10.4103/nah.NAH_104_16

[7] S. Fidell, V. Mestre, P. Schomer, B. Berry, T. Gjestland, M. Vallet, T. Reid. A first-principles model for estimating the prevalence of annoyance with aircraft noise exposure. J. Acoust. Soc. Am. 130, 791–806, 2011. https://doi.org/10.1121/1.3605673

[8] S. Bartels, F. Márki, U. Müller. The influence of acoustical and non-acoustical factors on short-term annoyance due to aircraft noise in the field — The COSMA study. Sci. Total Environ. 538, 834–843, 2015. https://doi.org/10.1016/j.scitotenv.2015.08.064

[9] J. Fields. Effect of Personal and Situational Variables on Noise Annoyance: With Special Reference to Implications for En Route Noise 243, 1992.

[10] R. Guski. Personal and social variables as co-determinants of noise annoyance. Noise Health 1, 45, 1999.

[11] D. Schreckenberg, S. Benz, J. Kuhlmann, M. Conrady, U., Felscher-Suhr. Attitudes towards authorities and aircraft noise annoyance: Sensitivity analyses on the relationship between non-acoustical factors and annoyance 12, n.d.

[12] ISO/TS 15666 Acoustics - Assessment of noise annoyance by means of social and socio-acoustic surveys, 2003.

[13] EU, Commission Implementing Regulation (EU) 2018/1048 - of 18 July 2018 - laying down airspace usage requirements and operating procedures concerning performance-based navigation. Off. J. Eur. Union, 2018.

[14] Health Canada. Health effects of airplane and aircraft noise, 2019. https://www.canada.ca/en/health-canada/services/health-risks-safety/radiation/everyday-things-emit-radiation/health-effects-airplanes-aircraft-noise.html (accessed 6.16.22).

[15] H.M.E. Miedema, H. Vos. Demographic and attitudinal factors that modify annoyance from transportation noise. J. Acoust. Soc. Am. 105, 3336–3344, 1999. https://doi.org/10.1121/1.424662

[16] M. van Smeden, K.G. Moons, J.A. de Groot, G.S. Collins, D.G. Altman, M.J. Eijkemans, J.B. Reitsma. Sample size for binary logistic prediction models: Beyond events per variable criteria. Stat. Methods Med. Res. 28, 2455–2474, 2019. https://doi.org/10.1177/0962280218784726

[17] NORAH - Noise-related annoyance and quality of life over time. http://www.laermstudie.de/en/results/results-of-the-quality-of-life-study/noise-re

TONAL NOISE PREDICTION OF SERRATED TRAILING-EDGE AIRFOILS

Yehia Salamav *[1], Basim Al Tluav †[2], and Johana Rocha ‡[2]
[1]Department of Mechanical and Aerospace Engineering, Carleton University, Ottawa, Ontario.

Résumé

Dans ce travail, des simulations intégrées de grandes turbulences sont utilisées en association avec le modèle Ffowcs Williams-Hawkings pour prédire les pics sonores des voilures NACA0012 ayant différentes configurations de bord de fuite anti-bruit. Différentes configurations de dentelure en dents de scie de plaques non plates sont étudiées et des essais expérimentaux en soufflerie sont réalisés. Les résultats sont validés puis comparés aux mesures expérimentales, et un accord qualitatif est obtenu en termes de statistiques d'écoulement et de spectres de bruit en champ lointain. Il est démontré que les dentelures en dents de scie TE modifient considérablement l'aérodynamique du sillage et améliorent le mélange à travers le profil aérodynamique. Les résultats expérimentaux confirment que les dentelures en dents de scie réduisent le bruit à large bande émis par le profilé au détriment de la génération d'un pic tonal, causé par le délestage tourbillonnaire associé à l'émoussement des extrémités de la dentelure. Des dentelures plus longues et des valeurs plus élevées d'émoussement des extrémités sont responsables de la force des tourbillons rejetés et de l'intensité du bruit tonal rayonné. La fréquence à laquelle les pics tonaux se produisent peut être contrôlée pour la même amplitude de dentelure et le même émoussement de l'extrémité de la dentelure, en modifiant la longueur d'onde. Des valeurs de longueur d'onde plus élevées pour une même amplitude de dentelure et un même émoussage de l'extrémité de la dentelure conduisent à des pics de fréquence tonale plus élevés, et des valeurs d'émoussage de l'extrémité de la dentelure plus élevées pour une même amplitude de dentelure et une même longueur d'onde conduisent à des pics de fréquence tonale plus bas accompagnés d'amplitudes de crête plus élevées.

Mots clefs : embedded large eddy simulation; bruits de bord de fuite; dentelures de bord de fuite, airfoil, soufflerie

Abstract

In this work, Embedded Large Eddy Simulations are employed in tandem with the Ffowcs Williams-Hawkings model to predict the tonal peaks of NACA0012 airfoils having different noise-suppressing trailing-edge configurations. Different non-flat plate sawtooth serration configurations are investigated and experimental wind tunnel testing is performed. Results are validated then compared with experimental measurements, and qualitative agreement is obtained in terms of flow statistics and the far-field noise spectra. TE sawtooth serrations are shown to significantly modify the aerodynamics of the wake and improve mixing across the airfoil. Experimental results confirm that sawtooth serrations reduce the broadband noise radiated by the airfoil at the expense of generating a tonal peak, caused by vortex shedding associated with the bluntness of the serration roots. Longer serrations, and higher values of root bluntness are responsible for the strength of the shed vortices and the intensity of the radiated tonal noise. The frequency at which the tonal peaks occur can be controlled for the same serration amplitude and root bluntness by modifying the wavelength. Larger wavelength values for the same serration amplitude and root bluntness lead to higher tonal peak frequencies, and larger values of root bluntness for the same serration amplitude and wavelength lead to lower tonal peak frequencies accompanied by higher peak amplitudes.

Keywords: embedded large eddy simulation; trailing-edge noise; trailing edge serration, airfoil, wind tunnel

1 Introduction

With the world growing increasingly noisier, aerodynamic noise reduction has been steadily gaining the attention of the research community. Over the past few decades, noise pollution has increased, disturbing the integrity of natural ecosystems and putting them at risk [1]. Humans are suffering from noise pollution as it impacts their quality of life and puts their mental and physical well-being at risk [2].

In parallel, global warming has led a universal push towards sustainability, promoting an increased interest in renewable power sources to replace coal and fossil fuels, and reduce greenhouse gas emissions. One of these sustainable resources is to harness the energy of wind through wind turbines. Despite their many advantages, the noise produced by such turbines is still of the most significant hindrance preventing their widespread use, and the largest contributor to this noise pollution is that generated by the trailing edge of wind turbine blades [3]. For those reasons, TE noise reduction has become a crucial challenge in many industrial sectors.

To investigate the possibility of having low-noise airfoils, researchers and engineers turned to nature, and in 1934, R. R. Graham [4] was the first to recognize the potential of using birds as a reference to render modern airplanes more efficient, and specifically identified owls as a biomim-

* Yehia.Salama@cmail.carleton.ca
† Basim.AlTlua@cmail.carleton.ca
‡ Joana.Rocha@carleton.ca

icry candidate to achieve silent flight. The wings of owls differ from those of all other groups of birds. Three main noise reduction peculiarities were observed in owl wings, which distinguish them from other birds:

- the leading-edge comb: A remarkably stiff comb-like fringe exists on the front margin of every feather.
- the trailing-edge fringe: A fringe resembling that of a shawl spans along the TE of the main wing.
- the downy upper surface: Certain parts of the upper surface are covered with a short, fine down.

Soon afterwards, more researchers followed the same path and were drawn to nature looking for inspiration. In 1998, Lilley [5] confirmed the three main noise suppression mechanisms in owl wings previously addressed by Graham [4]. The author then discussed the aerodynamic characteristics of each of these devices and proposed explanations as to how the flow dynamics vary, leading to large noise reduction in the range of frequencies above 2 kHz. According to him:

- the comb-shaped leading-edge feathers behave as closely spaced co-rotating vortex generators creating streamwise vortices which lead to a reduction in boundary layer (BL) thickness and in the volume of turbulence crossing the TE.
- the trailing-edge fringe resembles a serrated edge which suggests the reduction or even elimination of TE scattering.
- given the small diameter of its fibers, the compliant velvety surface of the wing acts as a bypass mechanism for energy dissipation at frequencies smaller than the conventional dissipation range of frequencies associated with viscous damping. In other words, the fibers absorb energy from the small-scale noise-emitting eddies, thus silencing them.

Following the work of these authors, further work has been using the owl as a biomimicry model. The proceeding step was to implement owl wing features in a practical way on solid airfoils to study their efficiency as noise suppressers and their effect on aerodynamic flow properties. Extensive experimental work has been conducted to confirm the applicability of TE extensions, serrations in particular, as noise suppression devices [6-9]. Chong et al. [8] experimentally investigated the feasibility of employing different serrated TE configurations to reduce the noise produced by a NACA0012 airfoil. For the case of an untripped boundary layer, testing velocities of up to 60 m/s and an angle of attack of 4.2°, it was shown that sound power reduction of up to 30 dB is possible for the instability tonal noise. When the airfoil surface is tripped, broadband sound power reduction of 6.5 dB was achieved. However, more significant narrowband noise is generated by the vortex shedding at the serration roots. The authors concluded even though smaller serration angles lead to better broadband noise reduction, larger angles are recommended to account for the unavoidable narrowband vortex shedding noise.

Numerical simulations were used to predict far-field noise radiation. In 2000, Manoha, Troff and Sagaut [10] successfully predicted the far-field noise generated by turbulence flowing over the blunt TE of a thick flat plate by coupling a Large Eddy Simulation (LES) with Curle's solution to the Lighthill equation, then the Ffowcs-Williams and Hawkings (FW-H) analogy. Agrawal et and Sharma [11] also assessed the effectiveness of biomimicry in reducing aerodynamic noise using LES. The interaction between the wake of a cylindrical rod and a downstream airfoil was simulated to investigate the effect of sinusoidal leading-edge serrations on radiated noise. Tang et al. [12] performed simulations employing LES using the Lighthill-Curle method in an attempt to reveal the variation in the hydrodynamic field and sound source associated with TE serrations on a NACA 0012 airfoil. It was confirmed that TE serrations reduce the radiated noise seeing that serrations impede the growth of spanwise vortices, i.e. decrease spanwise coherence, and promote streamwise ones near the wake. Zilstra and Johnson [13] demonstrated the ability of LES, combined with the FW-H acoustic analogy, to predict the flow field and acoustic results for a SD7037 airfoil at a Re of 43,000 and different angles of attack. Overall, the method proved to be an effective airfoil self-noise prediction tool at static angles of attack (AOAs).

Despite the increase in computing power over the last two decades, Large Eddy Simulations remain prohibitively expensive. Because of the impracticality of LES and the need for reliable short-response-time noise prediction methods for industrial design and optimization, some researchers resorted to statistical models based on steady RANS solutions in a sequential CFD/CAA approach. Markus [14] reviewed three different methods based on steady Reynolds-averaged Navier-Stokes (RANS) solutions to predict noise emitted from airfoils [15-17]. Validation studies showed decent agreement between the considered methods and results from experiments, a semi-empirical airfoil self-noise prediction code and LES. In another attempt to get accurate noise predictions at a reasonable computational cost, Quéméré and Sagaut [18] presented a novel zonal multi-domain RANS/LES method (also known as Embedded LES or ELES), where the full domain configuration was decomposed into several subdomains that can be treated with either RANS or LES. The same concept was later adopted by Teraccol [19], who investigated using ELES to represent aerodynamic noise sources. The method was applied to a flat plate with a blunt TE and a NACA0012 airfoil. In this approach, zonal LES is only performed close to the main elements responsible for sound generation, while the overall configuration is treated by a RANS. The most critical point was the numerical treatment performed at the inlet of the LES domain. CPU time reductions in the order of 40 were obtained and the method was found to be an attractive compromise between accuracy and computational cost. In 2008, Fröhlich and von Terzi [20] presented a generic review of the various ELES approaches along with different interface treatment strategies. The review provided information on how to distinguish between the different methods and to further the understanding of their inherent limitations as well as the encountered difficulties. Successful simulation results demonstrated the high potential of the approach. In the same year, Mathey [21] evaluated using the ELES approach for the prediction of broadband and tonal noise generated by the flow past an airfoil TE at a high Re. Two simulations were performed for a free stream velocity of 30.5 m/s and a chord based Re of 1,800,000. The first one used a random forcing method at the RANS/LES interface, and the second one used the Vortex Method. The far-field noise was calculated using the FW-H model. The results showed that the technique is capable of capturing the separated flow and reproducing the main characteristics of the aeroacoustic sources. Lastly, it was shown that the use of the Vortex Method (VM) for the generation of a synthetically turbulent flow field significantly improved the accuracy of the simulation. Kim et at. [22] used a segregated ELES approach to predict the aeroacoustic and aerodynamic properties of several flatback airfoils at high Re and compared the results to semi-empirical and experimental data. Synthetic turbulence was generated at the RANS/LES interface using the Vortex Method and far-field acoustics were computed using the FW-H analogy. The obtained frequency spectra of surface pressure fluctuations obtained is in good agreement with experimental measurements at the same observer location and the hybrid RANS-LES method is found to be adequate for predicting aerodynamic noise generation by vortical flow in the vicinity of a blunt TE airfoil over a range of frequencies. Lane, Croaker and Ding [23] tested and implemented ELES for the prediction of TE noise due to flow around a NACA 0012 airfoil. The obtained results were compared to a full LES simulation and to experimental data. Both simulations used the same mesh resolution and the same wall-modeled LES approach. For ELES, the mesh size was only about 13 million cells, compared to 40 million cells for the full LES. It was found that the results of both simulations were in good agreement. The ELES approach resulted in saving 55% of the computational cost of a full LES. Zuo et al. [24] performed flow simulations using ELES to analyze the aerodynamic and noise characteristics of a serrated-TE NACA0018 airfoil at a Re of 160,000 and an AOA of 6 degrees. Two airfoils having the same serration wave length and different serration amplitudes were considered and compared to a plain straight TE case. Predictions based on the FW-H acoustic analogy showed that longer serrations are more effective in decreasing the overall sound pressure levels.

In the present work, ELES is adopted to study the flow field around a flat-TE NACA0012 airfoil as well as three serrated-TE airfoils having different serration amplitudes and wavelengths, at zero AOA. The far-field noise is computed using the Ffowcs Williams–Hawkings (FW-H) model and attention is given to the tonal peaks generated by the serrated airfoils. The flow chord-based Reynold's number, Re_c, is approximately 500,000. The computational results are validated and compared with available experimental data. The used ELES configuration, where the LES region only partially covers the airfoil chord-length, hasn't been used to investigate bio-inspired TE designs yet. In this context, the main goals of this study are to provide a faster alternative to the currently-used computationally prohibitive simulation models and use it to visualize the flow field around TE serrations, as well as assess the effect of changing different serration parameters on the radiated tonal noise.

This paper is structured as follows. Section 2 presents the numerical methodology with the governing LES equations (Sec. 2.1), Section 2.2 describes the hybrid RANS/LES interface treatment and Section 2.3 presents the FW-H aeroacoustic analogy. Thereafter, Section 3 describes the flow configuration (Sec. 3.1), the computational mesh (Sec. 3.2) and the experimental setup (Sec. 3.3). All results are presented in Sec. 4.

2 Numerical methods

2.1 Governing equations

The governing equations used in the current study, termed the spatially-filtered Na-vier-Stokes equations, are obtained by applying a low pass filter on the time dependent Navier-Stokes equations in the physical space. The flow is assumed incompressible. In order to increase efficiency, the filter width is the same size as the mesh spacing used in the computational domain. The resulting equations describe the dynamics of large eddies [25, 26]. Field variables, such as pressure and velocity, are defined by their convolution with a filter function over the fluid domain:

$$\bar{\phi}(x) = \int_D \phi(x')G(x,x')dx' \; ; \tag{1}$$

where D is the fluid domain and G is the filtering function. The overbar indicates spatial filtering and not temporal averaging. After applying the filter to the mass and momentum conservation equations, the NS equations become:

$$\frac{\partial \rho}{\partial t} + \frac{\partial}{\partial x_i}(\rho \bar{u}_i) = 0, \tag{2}$$

$$\frac{\partial}{\partial t}(\rho \bar{u}_i) + \frac{\partial}{\partial x_j}(\rho \bar{u}_i \bar{u}_j) = \frac{\partial}{\partial x_j}(\sigma_{ij}) - \frac{\partial \bar{p}}{\partial x_i} - \frac{\partial \tau_{ij}}{\partial x_j}. \tag{3}$$

In order to obtain a close system of equations, the unknown SGS stresses are modeled by applying the Boussinesq eddy viscosity hypothesis [27], thus computing the sub-grid-scale turbulent stresses from

$$\tau_{ij} - \frac{1}{3}\tau_{kk}\delta_{ij} = -2\,\mu_t \bar{S}_{ij} \; ; \tag{4}$$

where μ_t is the subgrid-scale turbulent viscosity and τ_{kk} is the isotropic part of the SGS. The latter part is not modeled as it is added to the filtered static pressure term. S_{ij} is the strain-rate tensor of the resolved scale calculated from equation (5) using the filtered velocity components :

$$\bar{S}_{ij} = \frac{1}{2}\left(\frac{\partial \bar{u}_i}{\partial x_j} + \frac{\partial \bar{u}_j}{\partial x_i}\right) \tag{5}$$

For the Wall Adapting Local Eddy Viscosity (WALE) model [28], μ_t is modeled as:

$$\mu_t = \rho L_s^2 \frac{\left(S_{ij}^d S_{ij}^d\right)^{\frac{3}{2}}}{\left(\overline{S_{ij}}\,\overline{S_{ij}}\right)^{\frac{5}{2}}\left(S_{ij}^d S_{ij}^d\right)^{\frac{5}{4}}} \; ; \tag{6}$$

where L_s, the mixing length of the sub-grid scale, and S_{ij}^d, which is a function of the strain and rotation rate tensors, are defined in equations (7) and (8) as:

$$L_s = \min\left(\kappa d, C_w V^{\frac{1}{3}}\right), \tag{7}$$

$$S_{ij}^d = \frac{1}{2}\left(\overline{g}_{ij}^2 + \overline{g}_{ji}^2\right) - \frac{1}{3}\delta_{ij}\overline{g}_{kk}^2 ; \tag{8}$$

and g_{ij} is defined in equation (9) as :

$$\overline{g}_{ij} = \frac{\partial \overline{u}_i}{\partial x_j}. \tag{9}$$

In equation (7), d is the distance to the closest wall, V is the volume of the computational cell, κ = 0.41 is the von Kármán constant and C_w = 0.325 is the WALE constant.

2.2 RANS/LES Interface

In the present approach, the entire flow domain is decomposed into clearly identifiable regions for RANS and LES before the simulation is started. This is usually referred to as segregated modeling. The goal is to use each model where it is best suited. The flow is initialized using RANS equations, which provide stationary field statistics, and LES re-solves the unsteady high-resolution perturbations near the TE, where it is needed. The main difficulty is defining proper interface conditions, seeing that inappropriate coupling could lead to results contamination in the LES or RANS subdomains.

At the inflow interface, mass, momentum and energy are convected into the LES subdomain from the RANS region. The latter provides mean values which are to be coupled with the LES data. To obtain correct LES results, fluctuations must be provided at the interface and added to the mean flow computed by RANS. These fluctuations can be real, provided by precursor simulations or databases of similar flows, or synthetic, provided by Fourier modes, digital filters, random vortices...etc. The goal is to make the imposed fluc-tuation as close as possible to those present in a real physical flow.

The Vortex Method [29] was chosen as a means of adding artificial resolved turbulence at the RANS/LES interface. In this approach, a fluctuating vorticity field is added to the mean flow, consequently creating perturbations similar in behavior to realistic ones. The VM is based on the Biot-Savart law and the 2D evolution equation of vorticity. Vortex points, or particles, are distributed over the inlet interface perpendicular to the streamwise direction and are randomly convected, carrying information about the vorticity field. The amount of vorticity carried by a given particle "i" is represented by the circulation Γ according to equation (11), and the assumed spatial distribution is given by equation (12), such that:

$$\omega(\vec{x}, t) = \sum_{i=1}^{N} \Gamma_i(t)\,\eta(|\vec{x} - \vec{x}_i|, t)\,, \tag{10}$$

$$\Gamma_i(x,y) = 4\sqrt{\left(\frac{\pi A k(x,y)}{3N(2\ln(3) - 3\ln(2))}\right)}\,; \tag{11}$$

$$\eta(\vec{x}) = \frac{1}{2\pi\sigma^2}\left(2e^{\frac{-|x|^2}{2\sigma^2}} - 1\right)2e^{\frac{-|x|^2}{2\sigma^2}}; \tag{12}$$

where N is the number of vortex points, A is the inlet section area, k is the turbulence kinetic energy and σ controls the size of the vortex particles. The resulting discretization for the velocity field is given by:

$$\vec{u}(\vec{x}) = \frac{1}{2\pi}\sum_{i=1}^{N}\Gamma_i\frac{\left((\vec{x_i} - \vec{x}) \times \vec{z}\right)}{|\vec{x} - \vec{x_i}'|^2}\left(1 - e^{\frac{|\vec{x}-\vec{x}'|^2}{2\sigma^2}}\right)e^{-\frac{|\vec{x}-\vec{x}'|^2}{2\sigma^2}}\;; \tag{13}$$

where $\vec{z}$ is a unit vector in the streamwise direction and x_i is the location of the i-th vortex particle. The value of σ is calculated from a known profile of mean turbulence kinetic energy and mean dissipation rate at the inlet, such that:

$$\sigma = \frac{ck^{3/2}}{2\epsilon}\;; \tag{14}$$

where c = 0.16. The minimum value of σ is determined by the local mesh size to ensure that the vortices will always belong to the resolved scale. Furthermore, the sign of the circulation of each vortex is randomly changed every characteristic time scale, which is the time needed for a 2D vortex to travel n times its mean characteristic 2D size in the boundary normal direction, where n is set to equal 100 from numerical testing. Finally, a rescaling model is used, and the velocity fluctuations are expressed as:

$$u_i'^* = u_i'\frac{\sqrt{< u_i u_i >}}{\sqrt{\frac{2}{3k}}}\;; \tag{15}$$

where $u_i'^*$ and u_i' are the scaled and unscaled velocity fluctuations, and $< u_i u_i >$ represents the normal statistic velocity fluctuations.

2.3 The FW-H aeroacoustic analogy

To overcome the prohibitive cost of directly resolving the pressure fluctuations responsible for noise in the far-field, a method based on Lighthill's acoustic analogy [30] is used. In this approach, the nearfield flow is computed using the appropriate governing equations of ELES, and the far-field noise is predicted with the aid of an analytically de-rived integral solution to the wave equation. The acoustic analogy decouples sound generation from its propagation, thus allowing the separation of the flow solution from the acoustic analysis and the extraction of acoustic sources from the CFD domain.

The Ffowcs Williams and Hawkings (FW-H) formulation [31] adopts the most gen-eral form of Lighthill's acoustic analogy. The FW-H equation [31, 32] is nothing but an in-homogeneous wave equation derived by manipulating the continuity and Navier-Stokes equation. The FW-H equation can be expressed as:

$$\begin{aligned}\frac{1}{a_\infty^2}\frac{\partial^2 p'}{\partial t^2} - \nabla^2 p' = &\frac{\partial}{\partial t}\{[\rho_\infty v_n + \rho(u_n - v_n)]\delta(f)\}\\ &- \frac{\partial}{\partial x_i}\{[P_{ij} + \rho u_i(u_n - v_n)]\delta(f)\}\\ &+ \frac{\partial^2}{\partial x_i \partial x_j}\{T_{ij}H(f)\},\end{aligned} \tag{16}$$

$$T_{ij} = \rho u_i u_j + P_{ij} - a_\infty^2(\rho - \rho_\infty)\delta_{ij}\,; \quad (17)$$

where $p' = p - p_\infty$ is the sound pressure at the far-field, u_i is the fluid velocity component in the x_i direction, u_n is the velocity component normal to the surface $f = 0$, v_i is the surface velocity component in the x_i direction, v_n is the surface velocity component normal to the surface, $\delta(f)$ is the Dirac delta function and $H(f)$ is the Heaviside function. The subscript "∞" denotes free-stream parameters. The $f = 0$ surface is a mathematical surface representing the source surface. n_i is a unit vector normal pointing towards the exterior region of the source (f>0), a_∞ is the speed of the sound at the far field, T_{ij} is the Lighthill stress tensor defined in equation (17) P_{ij} is the compressive stress tensor. The first term on the RHS of equation (16) represents the monopole or thickness source, modeling the sound generated by the displacement of a fluid as a body passes through it. The second term is the dipole or loading source, resulting from the unsteadiness of the forces acting on the body's surface. The third term is the quadrupole source term, representing the non-linear fluctuations in the local sound speed and fluid velocity near the body surface. Monopole and dipole sources are dominant in low Mach number flows. By integrating equation (16) assuming free-space flow and no obstacles between the sound source and receiver, a full solution consisting of surface and volume integrals is obtained [32]. In the present case, the volume integral is neglected as it is only significant in high Mach number flows. Thus, the far-field sound pressure can be expressed as :

$$p'(\vec{x},t) = p'_T(\vec{x},t) + p'_L(\vec{x},t) \quad (18)$$

where:

$$4\pi p'_T(x,t) = \int_{f=0} \left[\frac{\rho_\infty(\dot{U_n} + U_{\dot{n}})}{r(1-M_r)^2}\right] dS + \int_{f=0} \left[\frac{\rho_\infty U_n\{r\dot{M}_r + a_\infty(M_r - M^2)\}}{r^2(1-M_r)^3}\right] dS \quad (19)$$

$$4\pi p'_T(x,t) = \frac{1}{a_\infty}\int_{f=0} \left[\frac{\dot{L_r}}{r(1-M_r)^2}\right] dS + \int_{f=0} \left[\frac{L_r - L_M}{r^2(1-M_r)^2}\right] dS + \frac{1}{a_\infty}\int_{f=0} \left[\frac{L_r\{r\dot{M}_r + a_\infty(M_r - M^2)\}}{r^2(1-M_r)^3}\right] dS \quad (20)$$

$$U_i = v_i + \frac{\rho}{\rho_\infty}(u_i - v_i) \quad (21)$$

$$L_i = P_{ij}\,\hat{n}_j + \rho u_i(u_n - v_n) \quad (22)$$

A dot over a variable indicates the source-time derivative of that variable, while the subscripts "n", "r" and "M" denote the dot product with the unit normal vector, the unit radiation vector and surface velocity vector normalized by the speed of sound, respectively.

3 Flow configuration and computational setup

3.1 Flow configuration

The airfoil selected for the present study is a NACA0012 symmetric airfoil to isolate the effect of lift generation on the radiated noise. The chord length of the airfoils c is $0.3\ m$. The airfoil is placed in a square $10c \times 10c$ domain. The flow domain is divided into two regions as seen in figure 1. RANS equations are employed in a coarse RANS domain, while LES equations are employed in a refined LES region near the TE. It's important to note that only the noise radiated by the flow within the LES region is predicted in the numerical simulations. Since the presented work is focused on TE noise predictions, it is reasonable to neglect the noise generated by other airfoil sections, such as the leading edge. All airfoil geometric parameters are shown in table 1. s is the span of the flow domain. Two embedded configurations were tested. For cases C1.1 and C1.2, the LES domains in the streamwise direction extend from $x/c = 0.5$ and $x/c = 0.7$, respectively, to $1c$ downstream of the TE. The letter "C' stands for computational. The origin is defined at the airfoil leading edge. In the transverse direction, the LES domain extends $0.25c$ above and below the airfoil. Two serration configurations are also tested. A general model of the serration characteristics is presented in figure 2. Table 2 summarizes the flow parameters of the simulations. Computations are carried out at a free stream velocity $u_\infty = 24$ m/s and a free stream Mach number $M_\infty = 0.071$, resulting in a chord-based Reynolds number, $Re_c = \rho u_\infty D/\mu$, of approximately $500{,}000$, where ρ is the fluid density, μ is the dynamic viscosity and D is the characteristic length, which is the airfoil chord in this case.

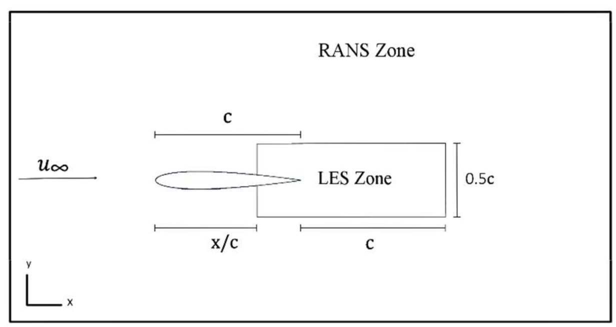

Figure 1: Schematic illustration of the segregated modeling domains.

Table 1: Geometric parameters of simulated aifoils.

Case	c [mm]	s [mm]	$2h$ [mm]	λ [mm]	ϵ [mm]
C1.1	300	18	–	–	–
C1.2	300	30	–	–	–
C2.1	300	30	30	10	7.4
C2.2	300	30	60	7.5	16.3
C2.3	300	30	60	10	16.3

Table 2: Flow parameters.

u_∞	24 m/s
M_∞	0.071
Re_c	500,000
μ	$1.7894 * 10^{-5}$ kg/m/s
ρ	1.225 kg/m^3
AOA	0

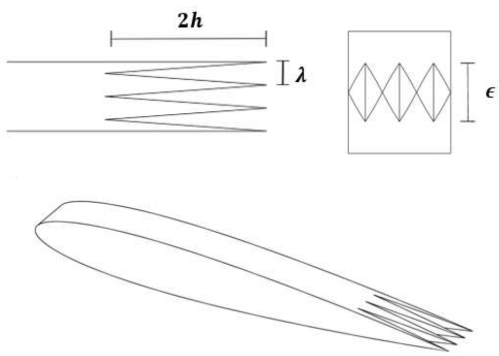

Figure 2: General serration configuration, not to scale.

3.2 Computational mesh and setup

A predominantly hexahedral mesh is generated following the cartesian cut-cell method (figure 3). This meshing technique, which has received a significant development in recent years [33]**Erreur ! Source du renvoi introuvable.**, was found ideal for the current study seeing that it results in a smaller number of elements for the same resolution compared to other methods, thus significantly reducing the simulation time. In addition, the resulting elements are characterized by their high orthogonal quality and low skewness, which minimizes truncation errors [33, 34]. Element size is restricted to $25.6\,mm$ in the coarse RANS zone, $0.8\,mm$ in the refined LES zone and $0.2\,mm$ on the airfoil surface in the vicinity of the TE. Elements in the airfoil wake of the RANS zone have a size of $5\,mm$. The grid resolution in terms of wall-normal units is defined by:

$$\Delta x^+ = \frac{u_\tau \Delta x}{\nu}, \Delta y^+ = \frac{u_\tau \Delta y}{\nu} \text{ and } \Delta z^+ = \frac{u_\tau \Delta z}{\nu},$$

where u_τ is the frictional velocity and ν is the kinematic viscosity. 40 inflation layers (figure 3c) are generated around the airfoil with the thickness of the first layer set to $7.6 * 10^{-3}$ mm and a growth factor of 1.08, thus ensuring $y^+ < 0.5$ everywhere on the airfoil surface (figure 4), at least 3 layers in the viscous sublayer and overall accurate boundary layer resolution. Table 3 lists mesh statistics for all simulated cases. The chosen computational grid has a maximum resolution $\Delta x^+_{max} \leq 20$ and $\Delta z^+_{max} \leq 20$ in the streamwise and spanwise directions, respectively [35, 36]. Case C2.3 is simulated using two different meshes to investigate the effect of the mesh on the predicted tonal peak. A steady-state mesh convergence study was carried out by

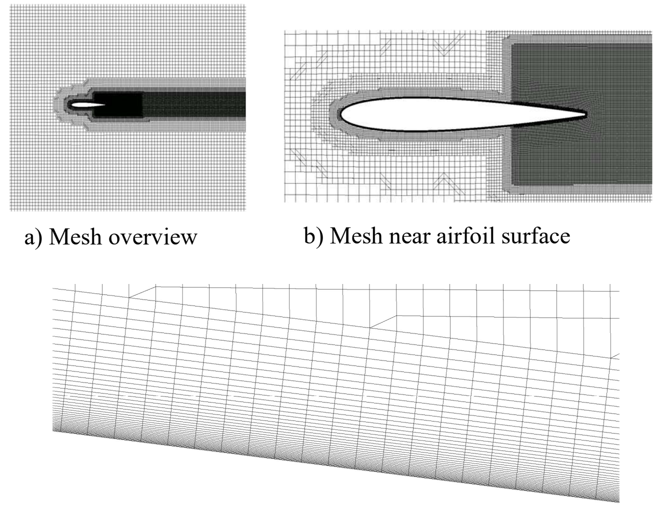

a) Mesh overview

b) Mesh near airfoil surface

c) Inflation layers around airfoil

Figure 3: Computational mesh.

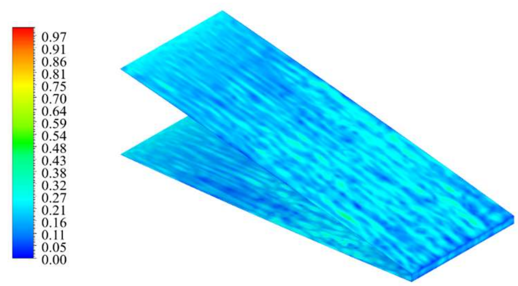

Figure 4: Instantaneous $\boldsymbol{y^+}$ distribution.

Table 3: Mesh elements.

Case	RANS	LES	Total
C1.1	456,353	4,586,780	5,043,133
C1.2	976,300	5,690,368	6,666,668
C2.1	976,300	6,134,898	7,111,198
C2.2	976,300	5,896,422	6,872,722
C2.3, Mesh 1	976,300	5,647,833	6,624,133
C2.3, Mesh 2	1,050,433	6,173,725	7,224,158

progressively refining the mesh, creating three meshes having 6,666,668 elements, 7,606,083 elements and 9,011,531 elements respectively. The values of integrated output parameters, such as lift and drag coefficients, were compared and the maximum error is found to be less than 0.4%, demonstrating mesh convergence. Furthermore, the first two meshes were carried over for a transient simulation analysis. The lift-history coefficients were evaluated for each mesh at every time step and their RMS values were computed. Both meshes yield the same lift-coefficient RMS value, $c_{L_{RMS}} = 0.0013$. Consistent results in terms of integrated flow parameters, for both steady-state and transient simulations, are a strong indication of the convergence of the used computational mesh, i.e. the mesh directly resolves enough flow structures for the results not to change with mesh refinement.

The boundary conditions used are demonstrated in figure 5. A velocity inlet boundary condition is specified at the domain entrance, where $u_\infty = 24$ m/s. Periodic boundary conditions (PBCs) are applied on the right and left side walls of the domain in the spanwise direction to allow the flow to develop naturally. No-slip boundary conditions are applied on the airfoil surface and a zero gauge-pressure outlet boundary condition is used. The inlet turbulence is set to 0.3%. The SIMPLE pressure-velocity coupling scheme is used. All results are second order accurate in time and space.

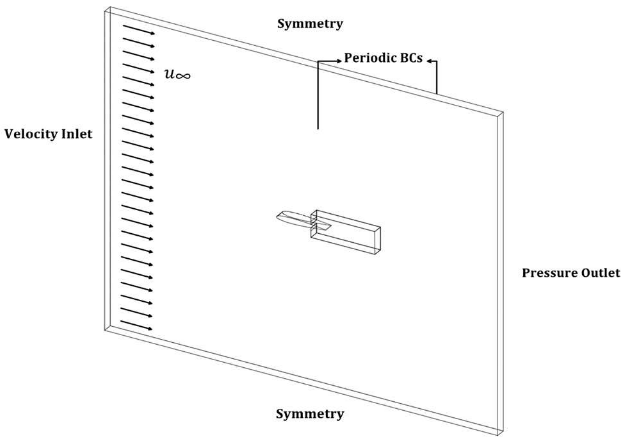

Figure 5: Boundary conditions.

The flow is initialized using the k-ω SST model developed by Menter [37], as it gives accurate separation predictions for external flows. The VM is then used to inject turbulence at the RANS/LES interface and the simulation is run for $4T_{TF}$ "Through-flow time" to obtain a fully developed flow, where $T_{TF} = L_{CFD}/u_\infty$ [36]. L_{CFD} is the LES domain length in the streamwise direction. WALE subgrid-scale (SGS) modelling is employed in the LES region as it is designed to return correct asymptotic wall behavior for wall-bounded flows [25]. The time step $dt = 1.2 * 10^{-5}$ seconds. With these values, the Courant-Friedrichs-Lewy (CFL) number achieved is ≤ 1 everywhere in the domain, meaning the flow particles don't travel more than the length of one mesh element every time step. Residuals are reduced by three orders of magnitude each time step. Lastly, acoustic data is gathered for $3T_{TF}$. All convergence residuals are set to 10^{-5}. Pressure and velocity monitoring points were placed in the airfoil wake and statistical convergence is achieved. Statistical convergence is also achieved for the coefficients of lift and drag. All simulations are carried out using the commercial CFD software FLUENT 2019R3 and run on Intel Xeon L5410 2.33 GHz platform of 60 cores.

3.3 Experimental setup

Experiments were conducted in the medium-speed, subsonic, closed-loop wind tunnel at Carleton University (figure 6). The airflow is powered by a 37.3 kW (50 HP) variable-speed DC motor driving a 1.2 m axial propeller at speeds as high as 900 RPM. A variable frequency drive (VFD) modulates the rotational frequency of the fan at a resolution of 1.0 Hz. A series of turbulence grids precede a 9:1 contraction, which reduces the turbulence intensity levels in the center of the test section to less than 0.27%. The tunnel has a removable, rectangular test section along with the surrounding anechoic chambers was completed to be used for aeroacoustic testing. This test section is a 0.78 m × 0.51 m rectangular section, 1.83 m long. The upper and lower walls of the test section are each composed of two aluminum sheet panels and contain hardware (circle aluminum material) for the vertical mounting of a two-dimensional airfoil in the midway, and 0.45 m from the upstream end of the test section [38, 39].

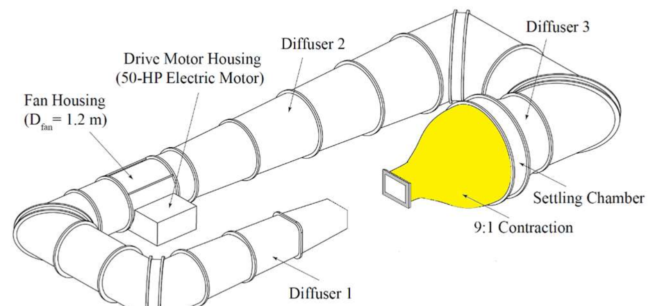

Figure 6: Wind tunnel configuration at Carleton University.

The airfoil wing is mounted vertically in the test section (figure 7) with its leading edge (at zero AOA) 0.45 m downstream of the test section entrance. The airfoil under investigation is a NACA0012 airfoil with a sawtooth TE serration cut directly into the main body of the airfoil (as shown in figure 8). The chord length of the airfoil is 300 mm, and the width is 510 mm. Between the leading-edge ($x/c = 0$), and $x/c = 0.73$ mm, the original NACA0012 airfoil profile is unmodified, where x is the streamwise direction. Further downstream, $0.73 \leq x/c \leq 1.0$, is a section that can be removed and replaced by either an unmodified or modified TE profile. Once attached, the TE section forms a continuous profile giving the appearance that the serrations are cut into the main body of the NACA0012 airfoil. Typical parameters including the serration amplitude, $2h$, and serration wavelength, λ, are defined as specified in figure 2. A prominent feature for airfoil that this type of serrated TE is the exposure of a significant bluntness ϵ at the root region. A photograph of the sawtooth serrated TEs used is shown in figure 8.

Table 4 shows the summary of geometrical parameters of the two TE serration tested in the present paper, according to $2h$, λ and ϵ, in which E0 represents the baseline sharp trailing-edge. The letter "E" stands for experimental. Far-field noise measurements in the mid-span were performed by a calibrated Brüel & Kjær microphone, which is installed at a distance of 1.4 m for an observer angle $\alpha = 90°$. The analysis was carried out between 100 Hz and 5 kHz.

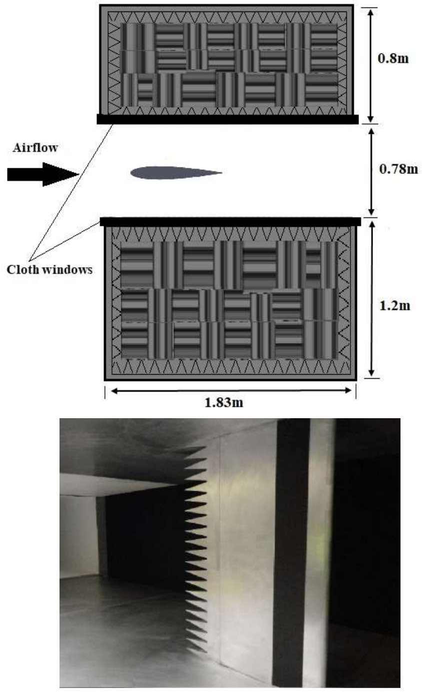

Figure 7: Cross section through the aeroacoustic test section and anechoic chamber as seen from above (top) and photograph of serrated-TE airfoil mounted in test section (bottom).

Figure 8: From left to right: NACA0012 main body, TE of case E0, TE of case E1 and TE of case E2.

Table 4: Geometric parameters of all experimental cases.

Case	c [mm]	s [mm]	$2h$ [mm]	λ [mm]	ϵ [mm]
E0	300	500	–	–	–
E1	300	500	70	25	18.2
E2	300	500	60	10	16.6

4 Results

4.1 Surface pressure

The pressure coefficient distribution around the airfoil is an important parameter, since it determines the lift coefficient and the development of the boundary layer [40-42]. In addition, the BL is responsible for the majority of the generated sound. C_p distributions for cases C1.1 and C1.2 are computed for validation and compared against experimental results obtained by Lee and Kang [43] for a NACA 0012 airfoil at a Re = 600,000, and full LES results published by Marsden, Bogey and Bailly [44] at $Re_c = 500{,}000$ (figure 9). Excellent agreement is found between the computational and experimental results. Of importance is the fact that from $x/c = 0.15$ down to the TE, the boundary layer is subject to an adverse pressure gradient. Both cases C1.1 and C1.2 are validated against existing literature. The LES domain in C1.1 is longer in the streamwise direction as it starts at a $x/c = 0.5$, while it starts at $x/c = 0.7$ in C1.2 (see tables 1 and 3). Even though both configurations yield acceptable results, the configuration of case C1.2 is chosen for the succeeding simulations as the LES domain covers a larger span.

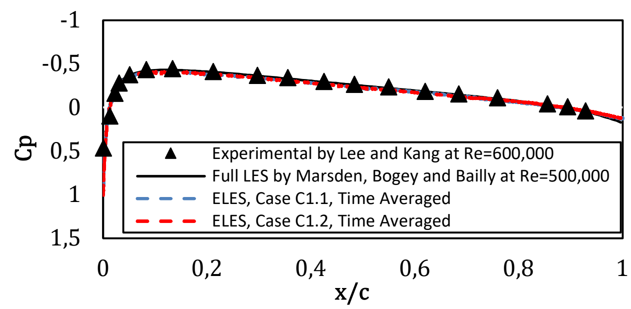

Figure 9: C_p distribution on airfoil surface.

Figure 10 shows the locations of maximum pressure fluctuation, where P_{RMS} is maximum for cases C1.2, C2.1, C2.2 and C2.3. For case C1.1, the location of maximum P_{RMS} is close to the sharp TE, seeing that that is where the discontinuity occurs and the BLs on the upper and lower sides clash. The introduction of serrations concentrated the maximum pressure fluctuation region from the extremity of the TE to downstream of the serration roots. This is where the pressure fluctuations are most violent, which suggests that aeroacoustic improvement to this design would require a modification of the flow field at that area, because regions with the highest P_{RMS} emit the most noise. The presence of serrations mitigates the sudden interaction between the BLs on the pressure and suction sides, thus allowing for progressive mixing and affecting the radiated sound. By comparing the maximum P_{RMS} values for C2.1, C2.2 and C2.3, the maximum P_{RMS} increases as the serration amplitude, and subsequently the root bluntness, are increased. C2.2 and C2.3 share the same root bluntness, ϵ, and serration amplitude, $2h$, and are subject to comparable P_{RMS} values.

4.2 Wake characteristics

By calculating the coefficient of lift, $c_L = L/(0.5 * \rho v^2 A)$, for every timestep of flow simulation, the lift-coefficient history can be plotted. L is defined as the lift force and A is the airfoil area. The lift-coefficient history is commonly used as an indicator of statistical convergence in transient simulations. Furthermore, it's a non-dimensional representation of the fluctuating forces acting normal to the airfoil surface due to the turbulence of air flow. To demonstrate the

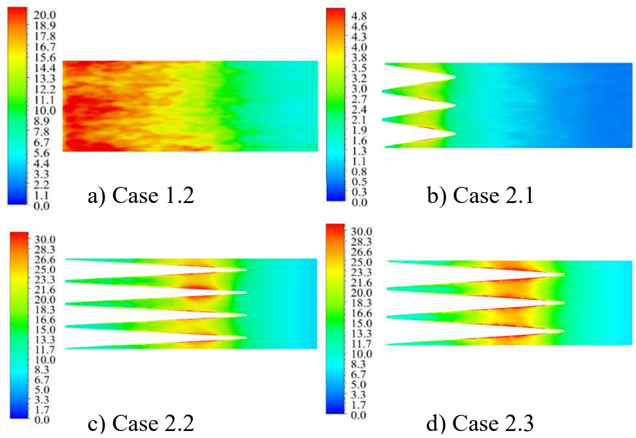

Figure 10: P_{RMS} distribution near airfoil TE.

convergence of the computational mesh, C2.3 is simulated twice, using two different meshes having 6,624,133 and 7,224,158 elements, respectively. The obtained lift-coefficient history plots are presented in figure 11. Both simulations yield the same lift-variation amplitude and frequency once the flow is initialized. The only observable difference is a phase shift, which is normal and simply means each simulation started from a different point in the periodic cycle. Both simulations also predict the same Strouhal number, $St = 0.168$. Figure 12 shows the lift-coefficient history plots of all the presented cases. All axes are kept constant and aligned for the sake of clarity and comparison. For case C1.2, the lift monitor is random and irregular, characterized by a relatively small amplitude. With the introduction of serrations, the lift monitors adopt sinusoidal shapes having different wavelengths and frequencies. C2.1 is characterized by the smallest amplitude and highest frequency, $f = 388$ Hz. C2.2 and C2.3 are almost subject to the same fluctuation amplitude, but their lift-coefficients vary with distinct frequencies equal to 218 Hz and 248 Hz, respectively. This behavior is attributed to the vortices shed in the wake of the airfoil. The dominant frequencies of the periodic plots were obtained by applying discrete Fast-Fourier Transform (FFT) on the propagated presented lift-coefficient history plots. Figure 13 shows the instantaneous flow fields in the airfoil wake in term of iso-surfaces of the Q-criterion, which is defined as the second invariant of the instantaneous velocity gradient tensor [45]. The iso-surfaces are used to identify and portray the turbulent coherent structures of the wake, which are inherently three-dimensional. The iso-surfaces are colored by the spanwise vorticity, ω_z, and demonstrate how the wake behavior changes as standard serrations are introduced then their geometrical parameters modified. For the case of a flat TE (C1.2), the wake is non-uniform and has almost no observable coherent structures, while serrated cases (C2.1, C2.2 and C2.3) are clearly subject to vortex shedding.

For the case of a flat TE (C1.2), the wake is turbulent but has no identifiable coherent structures. For the cases of standard serrations (C1.2, C2.2 and C2.3), the wake is characterized by sinusoidal vortex shedding. The amplitude and frequency of the observed phenomenon change as the serrations amplitude and wavelengths are varied. C2.1 is subject

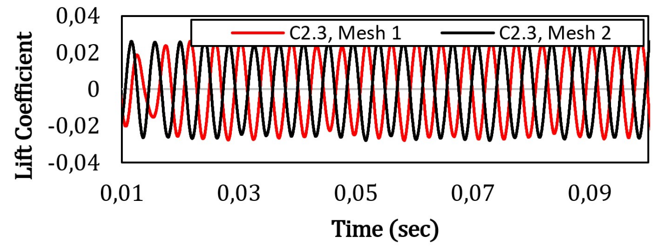

Figure 11: Lift-coefficient history of C2.3 using two different meshes.

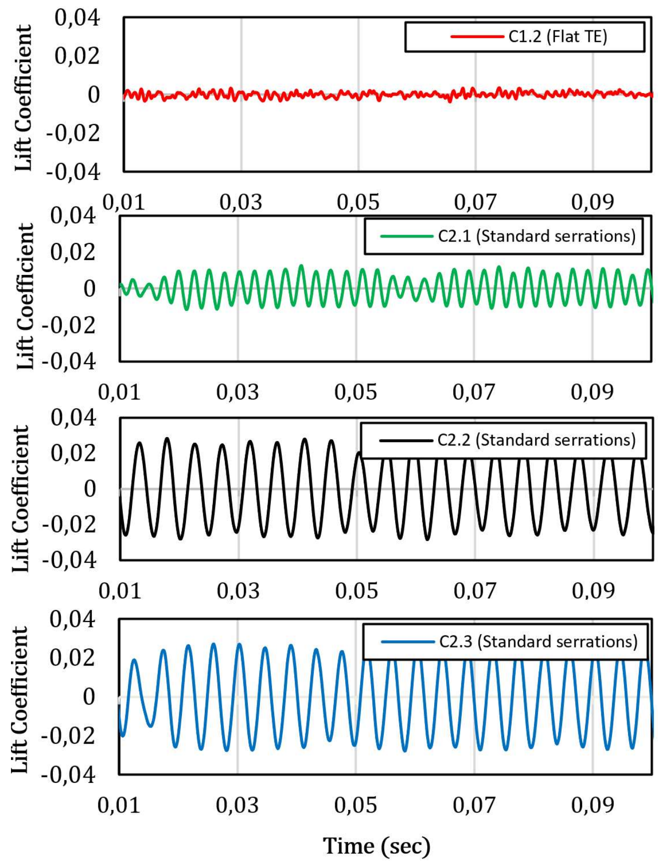

Figure 12: Lift-coefficient history for cases C1.2,C2.1,C2.2, and C2.3.

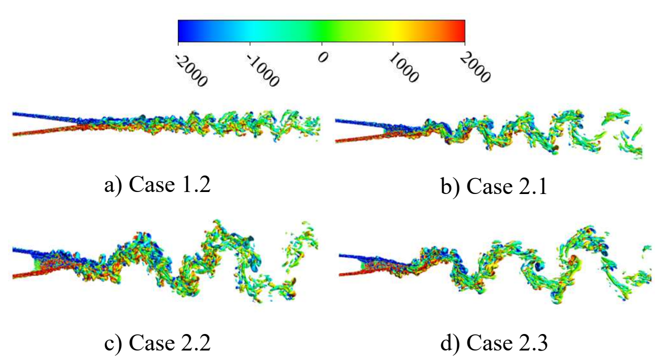

Figure 13: Instantaneous Q-Criterion colored by ω_z.

to the highest shedding frequency and the smallest amplitude. C2.2 and C2.3 are subject to similar vortex shedding amplitudes, but the frequency is higher in C2.3. The vortex shedding frequency can also be approximated by counting the number of full periodic cycles in the airfoil wake and dividing it by the through-flow time (T_{TF}). Vortex shedding is caused by the interaction of two shear layers as they leave the airfoil surface. Because of the inherent instability of the turbulent boundary layer, alternating low pressure zones are generated downstream of the airfoil, giving rise to fluctuating forces acting normal to the wind direction, which in turn explains the sinusoidal lift coefficient variation (figure 12). The frequencies at which vortices are shed from the airfoil TEs are equal to those at which the non-dimensional lift forces acting on the airfoil vary, and can thus be accurately calculated by applying a discrete FFT on the lift-coefficient history plots. Then, cases C2.1, C2.2, C2.3 and C4 are subject to vortex shedding frequencies of 388 Hz, 218 Hz, 248 Hz, and 210, respectively. A generated vortex is initially growing and fed by circulation from the separated shear layer, until it becomes strong enough to roll up and draw the opposing shear layer across the wake. At that point, this vorticity of opposite sign interrupts any further supply of circulation to the growing vortex, which then stops increasing in strength. As a result, that vortex is shed and convected downstream while a new one of opposite vorticity takes its place and the cycle keeps going [46, 47]. As the serration amplitude ($2h$) is reduced, the root bluntness (ϵ) is also reduced and the shear layers are brought closer together. Subsequently, the interaction between the two shear layers is facilitated and the periodic time is shortened, giving rise to a higher vortex shedding frequency [47].

In order to study the dynamics of vortex shedding, the Strouhal number, $St = f_s L/u_\infty$, is often used [48], in which f_s is the vortex shedding frequency in Hz, L is the characteristic length separating the shear layers in meters, which is equal to ϵ, and u_∞ is the free-stream velocity. St represents the ratio of inertial forces due to the local acceleration of the flow to the inertial forces due to the convective acceleration. The first is a product of turbulence and how the velocity of a fluid particle changes due to the inherent instability of the TBL, while the latter is an indication of how much the velocity changes as the flow moves across the fluid domain. St is particularly helpful for flows characterized with periodic motion as it associates the oscillations of the flow due to the inertial forces to the changes in velocity due to the convective acceleration of the flow field. In the case of a flat TE, the oscillations are not prominent, seeing that they are swept by the fast-moving fluid (figure 13a). When changing the serration amplitude ($2h$) from 30 mm (C2.1) to 60 mm (C2.2), the observed vortex shedding frequency (figures 13b and 13d) is reduced and St increases ($St_{2.1} = 0.119$ and $St_{2.3} = 0.168$). Increasing λ while keeping $2h$ constant leads to an increase in vortex shedding frequency and St ($St_{2.2} = 0.148$ and $St_{2.3} = 0.168$). The observed trend is in good agreement with the work of Hu et al.[49], as well as the aforementioned findings. Different airfoils will have different root bluntness for the same serration amplitude depending on their profile, and subsequently different vortex shedding frequencies. Wake vorticity is also dissipated faster in cases C2.3 and C2.2 than C2.1 and C1.2, which can be seen by inspecting the vorticity magnitude in the wake, shown in figure 14. Lastly, figure 15 gives the streamwise vorticity, $\omega_x = \partial u_y/\partial z - \partial u_z/\partial y$, contours for all the simulated cases. The two limits of the contour correspond to fluid particles having equal vorticity but in opposite directions. For the case of a flat TE (C1.2), turbulent, counter-rotating coherent structures are observed at the TE. For the cases having standard serrations (C2.1, C2.2 and C2.3), the turbulent coherent structures are allowed to pass between the serrations, across the airfoil surface.

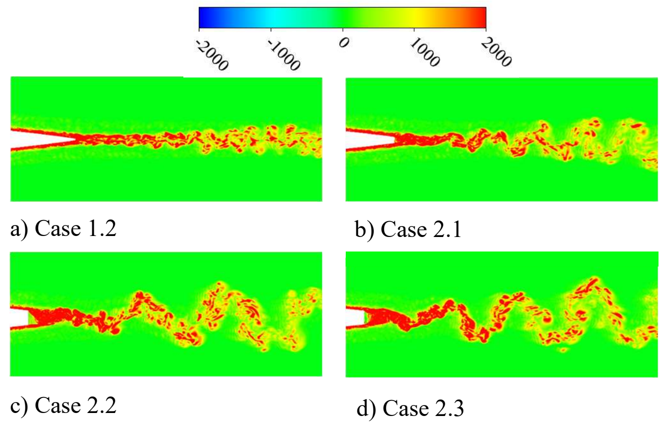

Figure 14: Instantaneous vorticity magnitude contours.

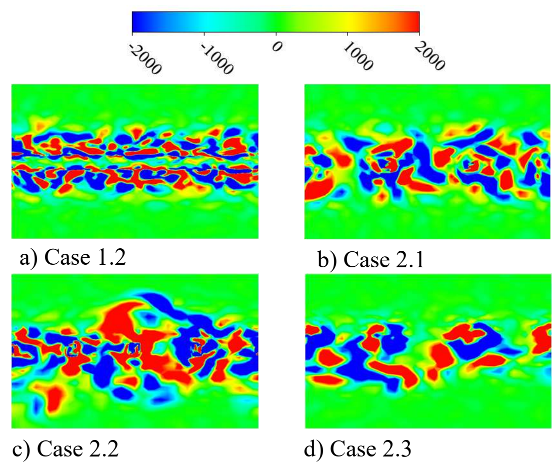

Figure 15: Instantaneous ω_x contours at $x/c = 1$.

4.3 Far field noise

The FW-H aeroacoustic analogy [30, 31] is used to compute the radiated far-field noise for the computational cases C1.2, C2.1, C2.3. In order to keep the computational cost reasonable, the span of the simulation domains is kept smaller than that of the experimental testing. Acoustic data is sampled every 2 flow-timesteps and data sampling is performed for $3T_{FT}$ after the flow is fully developed, resulting in a sampling frequency of 41.67 kHz and a frequency resolution of 28.4 Hz, where the frequency resolution is defined as the inverse of the sampling period. Pressure fluctuations are propagated to receivers placed midspan at a distance of 1.5 meters directly above the airfoils' TEs, as seen in figure 16. Cases C2.1, C2.2 and C2.3 show periodic patterns, where the amplitude is highest in C2.2 and C2.3, and the periodic frequency is highest in C2.1. Discrete FFT is performed on the resulting time signals seen to compute the sound pressure level (SPL) signal in the frequency domain, as shown in figure 17. The Hanning window is applied to the time signal to reduce numerical leakages associated with the discrete FFT [50]. Case C1.2 only exhibits broadband behavior. Tonal peaks are observed for C2.1, C2.2 and C2.3 at 397 Hz, 198 Hz and 240 Hz, respectively. The tonal peak amplitudes are equal for C2.2 and C2.3. The peak amplitude is 3.3 dB lower in C2.1, meaning the tonal noise is louder for the cases having longer serrations. The narrowband peaks are fundamentally justified by the vortex shedding caused by the serration root bluntness discussed in subsection 4.2 [51]. Figure 18 presents the far-field spectra obtained from simulating design C2.3 using two meshes, as previously mentioned. Both simulations predict the same narrow-band tonal peak amplitude and frequency, as well as comparable broad-band behavior at frequencies higher than the tonal peak.

As part of the current study, and in addition to the numerical predictions, wind tunnel testing has been performed to measure the noise of a NACA0012 airfoil with a straight TE and a serrated sawtooth TE. The airfoil has a chord length c of 300 mm, and the width is similar to the width of the nozzle exit at 510 mm. The airfoil AOA is set to zero and fixed to the nozzle exit by two side plates. The microphone was placed at about 1.4 m from the TE at a polar angle of 90°. The free jet velocity was set to 24 m/s and the flow, parameters and chord length are similar to the computational cases, yielding a Re_c of approximately 500,000. The fluctuating pressure-time signals for the used microphone are recorded and then used to calculate the SPL spectrum. The data sampling frequency is set to 20 kHz and the data sampling period is 30 seconds, corresponding to a frequency resolution of 0.033 Hz. The obtained signal is also passed through a time-domain filter to remove the low and high frequency contamination, caused by the microphone's low frequency roll off and high-frequency aliasing. The band-pass filter used is a Butterworth filter with the first and second stopband frequencies of 100 and $f_s/2$ Hz respectively, where f_s is the sampling frequency. The sound pressure level, SPL, is computed using the root mean square (RMS) of filtered pressure signal using the following equation:

$$SPL = 10log_{10}\left(\frac{P_{RMS}^2}{P_{ref}^2}\right) \quad (23)$$

where P_{ref} is the standard reference pressure in air, 20 μPa. Figure 19 shows the turbulent broadband noise spectra (SPL) radiated by a straight TE and a serrated TE, respectively. Note that the serrated TE is a non-flat plate type where a certain degree of bluntness exists at each sawtooth root for all experimental and computational cases. Vortex shedding has been shown to be emanated from the blunt roots, which then proceeds to generate the tonal noise. A tonal peak is observed at 290 Hz in case E2 and broadband reduction occurs at frequencies higher than the tonal component (350 Hz to 5 kHz).

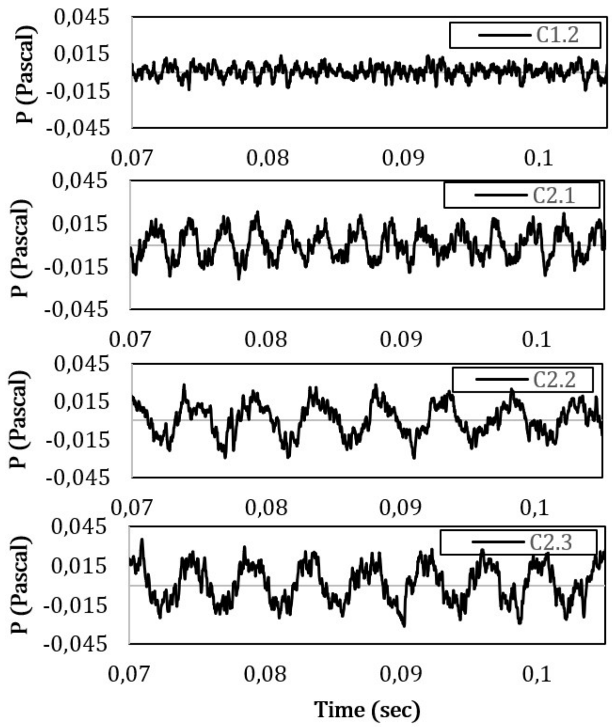

Figure 16: Time-domain noise signals propagated to receiver.

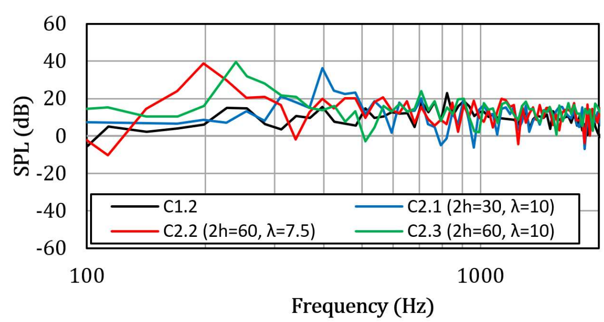

Figure 17: Frequency-domain noise signals of C1.2, C2.1, C2.2 and C2.3.

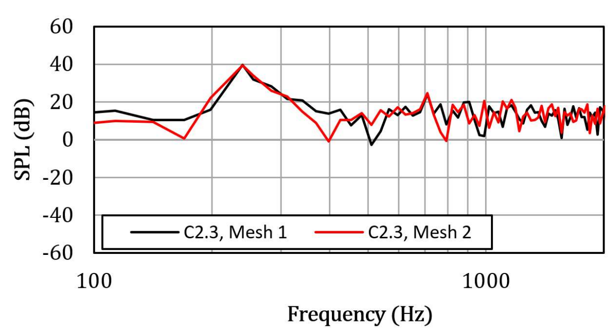

Figure 18: Frequency-domain noise signals of C2.3 using 2 meshes.

The numerical simulations and the wind tunnel experiments predict comparable acoustic behavior; by comparing C1.2 to E0 and C2.3 to E2, the numerically simulated and experimentally obtained SPL levels follow similar acoustic spectra shapes, but with different amplitude. This is mainly caused by limited computational domain span, compared to

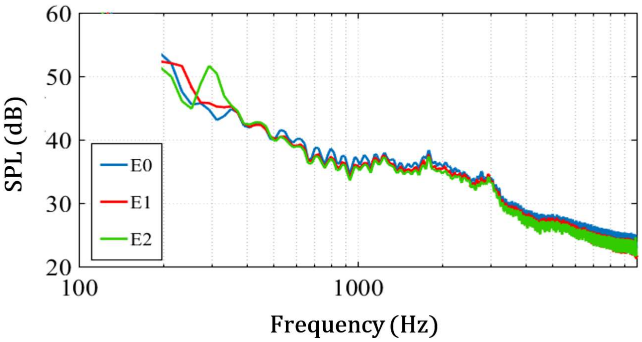

Figure 19: Experimentally obtained SPL.

the experimental one ($span_{ELES} = 30$ mm, compared to $span_{Experimental} = 500$ mm), and the noise source contribution of the airfoil leading edge, which is not accounted for in the used ELES configuration. Since the work is focused on TE noise, it is reasonable to neglect the noise radiated by other sections of the airfoil. Narrowband tonal peaks are predicted in both numerical and experimental far-field spectra for the case of sawtooth serrations having $2h = 60$ mm and $\lambda = 10$ mm (C2.3 and E2). The difference in the predicted tonal frequencies is consistent with the results of Kim et al.[22]. The difference in the tonal peak frequencies is attributed to the subtle differences that exist between the numerical and experimental geometric models and inflow conditions, such as turbulence, and the limited LES domain size.

Experimental results confirm that sawtooth serrations reduce the generated broadband noise at the expense of adding a narrow-band tonal peak, caused by vortex shedding associated with the bluntness of the serration roots. The broadband reduction was not captured in the numerical simulations. Increasing the sensitivity of the simulation would require a finer mesh and longer simulation time, which would render the simulations unfeasible. For the broadband reduction to be captured without significantly increasing the simulation run-time, more powerful computer clusters are required to allow for a larger LES domain and a higher frequency resolution (longer sampling period). The obtained accuracy is found to be satisfactory for the purposes discussed in this paper, when compared to the corresponding reduction in computing effort. ELES successfully predicted the narrowband tonal noise component at a relatively low computational cost, and was used to assess the effect of different serration parameters on the tonal peak and frequency.

5 Conclusion

Embedded Large Eddie Simulations as well as experimental wind tunnel testing are carried out for NACA0012 airfoils having different TE configurations. Different sawtooth serrations having various serration amplitudes and wavelengths were investigated for a freestream flow velocity $u_\infty = 24$ [, $AOA = 0$ and Re_c of approximately $500{,}000$. A mesh convergence study is performed and the obtained pressure coefficient distribution is validated. Results show excellent agreement with experimental data and full LES predictions. The validated computational approach is employed to gain an improved understanding of the flow characteristics of serrated-TE airfoils, as well as predict any acoustic tones, while experimental testing is conducted to obtain highly accurate acoustic results.

The introduction of serrations is shown to strongly affect the flow field, mitigating the sharp TE discontinuity and improving mixture between the upper and lower sides of the airfoil. Serrations are shown to concentrate the maximum pressure fluctuation region to downstream of the serration roots. Due to the introduced bluntness of these non-flat plate type sawtooth serrations, vortices are shed from the serration roots, generating narrowband tonal peaks. Narrow-band tonal peaks are observed in the far-field noise spectra at 397 Hz, 198 Hz and 240 Hz for C2.1, C2.2 and C2.3, respectively. The tonal peak amplitudes are equal for C2.2 and C2.3, which share the same $2h = 60$ mm and $\epsilon = 16.3$ mm. The peak amplitude was lower in C2.1 by $3.3\ dB$, suggesting that the tonal noise is louder for cases having longer serrations and increased root bluntness. Longer serrations, and higher values of ϵ are responsible for the strength of the shed vortices and the intensity of the radiated tonal noise. The frequency at which the tonal peaks occur can be controlled for the same 2h and ϵ by modifying the wavelength, λ. Larger values of λ for the same $2h$ and ϵ lead to higher tonal peak frequencies, and larger values of ϵ for the same $2h$ and λ lead to lower tonal peak frequencies accompanied by higher peak amplitudes.

Experimental results confirm that sawtooth serrations reduce the broadband generated noise at the expense of adding a tonal peak. Qualitative comparisons are made between computational results and experimental measurements and satisfactory agreement is achieved. The numerical simulations and the wind tunnel experiments predict similar acoustic behavior and shape of the far-field noise spectra. In combination with the FW-H analogy, ELES successfully captures the narrowband peaks of the radiated far-field noise, which are associated with vortex shedding. The results of this investigation illustrate how ELES can be used as a reasonable alternative to the more computationally demanding full LES or direct numerical simulation approaches. Future work aims to utilize the aforementioned methods for the development of new noise-suppressing TE designs.

References

[1] Chapter 2: Effects of Noise Pollution on Birds: A Brief Review of Our Knowledge. Ornithol. Monogr. 2012, 74 (1), 6–22. doi: 10.1121/1.4784049

[2] Bronzaft, A. L. Noise Pollution: A Threat to Our Mental and Physical Well-being. J. Acoust. Soc. Am. 2004, 115 (5), 2567–2567. doi: 10.3390/wsf-00623

[3] Jianu, O.; Naterer, G.; Rosen, M. Noise Polution Prevention in Wind Turbines: Status and Recent Advances. In Proceedings of The 1st World Sustainability Forum; MDPI: Basel, Switzerland, 2011. dio: 10.3390/wsf-00623

[4] Graham, R. R. The Silent Flight of Owls. J. R. Aeronaut. Soc. 1934, 38 (286), 837–843.

[5] Lilley, G. A Study of the Silent Flight of the Owl. In 4th AIAA/CEAS Aeroacoustics Conference; American Institute of Aeronautics and Astronautics: Reston, Virigina, 1998. doi: 10.1017/s0368393100109915

[6] Herr, M.; Dobrzynski, W. Experimental Investigations in Low-Noise Trailing Edge Design. AIAA J. 2005, 43 (6), 1167–1175. doi: 10.2514/1.11101

[7] Gruber, M.; Joseph, P.; Azarpeyvand, M. An Experimental Investigation of Novel Trailing Edge Geometries on Airfoil Trailing Edge Noise Reduction. In 19th AIAA/CEAS Aeroacoustics Conference; American Institute of Aeronautics and Astronautics: Reston, Virginia, 2013. doi: 10.2514/6.2013-2011

[8] Chong, T. P.; Vathylakis, A.; Joseph, P. F.; Gruber, M. Self-Noise Produced by an Airfoil with Nonflat Plate Trailing-Edge Serrations. AIAA J. 2013, 51 (11), 2665–2677. doi: 10.2514/1.j052344

[9] Chen, E.; Ma, Y.; Yang, A.; Zhao, G. Experimental Investigation on Noise Emissions of an Airfoil with Non-Flat Plate Trailing Edge Serrations. J. Mech. Sci. Technol. 2019, 33 (7), 3069–3074. doi: 10.1007/s12206-019-0601-x

[10] Manoha, E.; Troff, B.; Sagaut, P. Trailing-Edge Noise Prediction Using Large-Eddy Simulation and Acoustic Analogy. AIAA J. 2000, 38 (4), 575–583. doi: 10.2514/2.1015

[11] Agrawal, B. R.; Sharma, A. Numerical Investigations of Bio-Inspired Blade Designs to Reduce Broadband Noise in Aircraft Engines and Wind Turbines. In 54th AIAA Aerospace Sciences Meeting; American Institute of Aeronautics and Astronautics: Reston, Virginia, 2016. doi: 10.2514/6.2016-0760

[12] Tang, H.; Lei, Y.; Fu, Y. Noise Reduction Mechanisms of an Airfoil with Trailing Edge Serrations at Low Mach Number. Appl. Sci. (Basel) 2019, 9 (18), 3784. doi: 10.3390/app9183784

[13] Zilstra, A.; Johnson, D. LES and FW-H Prediction of Aeroacoustic Noise for a SD 7037 Airfoil for Wind Turbine Applications. In 25th AIAA/CEAS Aeroacoustics Conference; American Institute of Aeronautics and Astronautics: Reston, Virginia, 2019. doi: 10.2514/6.2019-2537

[14] Rumpfkeil, M. P. Using Steady Flow Analysis for Noise Predictions. Comput. Fluids 2017, 154, 347–357. doi: 10.1016/j.compfluid.2017.03.003

[15] Hosder, S.; Schetz, J. A.; Mason, W. H.; Grossman, B.; Haftka, R. T. Computational-Fluid-Dynamics-Based Clean-Wing Aerodynamic Noise Model for Design. J. Aircr. 2010, 47 (3), 754–762. doi: 10.2514/1.29105

[16] Albarracin, C.; Doolan, C.; Jones, R.; Hansen, C.; Brooks, L.; Teubner, M. D. A RANS-Based Statistical Noise Model for Trailing Edge Noise. In 18th AIAA/CEAS Aeroacoustics Conference (33rd AIAA Aeroacoustics Conference); American Institute of Aeronautics and Astronautics: Reston, Virigina, 2012. doi: 10.2514/6.2012-2181

[17] Remmler, S.; Christophe, J.; Anthoine, J.; Moreau, S. Computation of Wall Pressure Spectra from Steady Flow Data for Noise Prediction. In 16th AIAA/CEAS Aeroacoustics Conference; American Institute of Aeronautics and Astronautics: Reston, Virigina, 2010. doi: 10.2514/6.2010-4000

[18] Quéméré, P.; Sagaut, P. Zonal Multi-Domain RANS/LES Simulations of Turbulent Flows: ZONAL RANS/LES SIMULATIONS. Int. J. Numer. Methods Fluids 2002, 40 (7), 903–925. doi: 10.1002/fld.381

[19] Terracol, M. A Zonal RANS/LES Approach for Noise Sources Prediction. Appl. Sci. Res. 2006, 77 (1–4), 161–184. doi: 10.1007/s10494-006-9042-6

[20] Fröhlich, J.; von Terzi, D. Hybrid LES/RANS Methods for the Simulation of Turbulent Flows. Prog. Aerosp. Sci. 2008, 44 (5), 349–377. doi: 10.1016/j.paerosci.2008.05.001

[21] Mathey, F. Aerodynamic Noise Simulation of the Flow Past an Airfoil Trailing-Edge Using a Hybrid Zonal RANS-LES. Comput. Fluids 2008, 37 (7), 836–843. doi: 10.1016/j.compfluid.2007.04.008

[22] Kim, T.; Jeon, M.; Lee, S.; Shin, H. Numerical Simulation of Flatback Airfoil Aerodynamic Noise. Renew. Energy 2014, 65, 192–201. doi: 10.1016/j.renene.2013.08.036

[23] Lane, G.; Croaker, P.; Ding, Y. Embedded Large Eddy Simulation Method for Predicting Flow-Induced Noise. Proceedings of ACOUSTICS. 2019.

[24] Zuo, Z. G.; Huang, Q.; Liu, S. An Analysis on the Flow Field Structures and the Aerodynamic Noise of Airfoils with Serrated Trailing Edges Based on Embedded Large Eddy Flow Simulations. J. Appl. Fluid Mech. 2019, 12 (2), 327–339. doi: 10.29252/jafm.12.02.29142

[25] ANSYS Fluent 2019 Theory Guide, ANSYS, Inc 2019

[26] Leonard, A. Energy Cascade in Large-Eddy Simulations of Turbulent Fluid Flows. In Turbulent Diffusion in Environmental Pollution, Proceedings of a Symposium held at Charlottesville; Elsevier, 1975; pp 237–248. doi: 10.1016/s0065-2687(08)60464-1

[27] Hinze, J. O. Turbulence, 2nd ed.; McGraw-Hill: New York, NY, 1976.

[28] Nicoud, F.; Ducros, F. Embedded Large Eddy Simulation Method for Predicting FlowInduced Noise. Flow, Turbulence and Combustion 62, 183–20, 1999. https://doi.org/10.1023/A:1009995426001

[29] Mathey, F.; Cokljat, D.; Bertoglio, J; Sergent, E. Specification of LES Inlet Boundary Conditions Using Vortex Method. Progress in Computational Fluid Dynamics, vol. 6, 2006. https://doi.org/10.1142/s0219887821501644.

[30] Lighthill, M. J. On Sound Generated Aerodynamically I. General Theory. Proc. R. Soc. Lond. 1952, 211 (1107), 564–587. doi: 10.1098/rspa.1952.0060

[31] Williams, J. E. F.; Hawkings, D. L. Sound Generation by Turbulence and Surfaces in Arbitrary Motion. Philos. trans. R. Soc. Lond. 1969, 264 (1151), 321–342. doi: 10.1098/rsta.1969.0031

[32] Brentner, K. S.; Farassat, F. Analytical Comparison of the Acoustic Analogy and Kirchhoff Formulation for Moving Surfaces. AIAA J. 1998, 36 (8), 1379–1386. doi: 10.2514/2.558

[33] Berger, M.; Aftosmis, M. Progress towards a Cartesian Cut-Cell Method for Viscous Compressible Flow. In 50th AIAA Aerospace Sciences Meeting including the New Horizons Forum and Aerospace Exposition; American Institute of Aeronautics and Astronautics: Reston, Virigina, 2012. doi: 10.2514/6.2012-1301

[34] Ghmati, R. E.; Jawad, B. A.; Koutsavdis, E. An Investigation of CutCell Meshing Strategies for Accurate Aerodynamic Performance Prediction. SAE Int. J. Passeng. Cars - Mech. Syst. 2012, 5 (1), 369–380. doi: 10.4271/2012-01-0499

[35] ANSYS Fluent 2019 User Guide, ANSYS, Inc 2019

[36] Menter, F. R., "Best Practice: Scale-Resolving Simulations in ANSYS CFD," 2015, ANSYS Germany GmbH

[37] Menter, F. R. Two-Equation Eddy-Viscosity Turbulence Models for Engineering Applications. AIAA J. 1994, 32 (8), 1598–1605. doi: 10.2514/3.12149

[38] Al Tlua, B., and Rocha, J., “Development and Testing of an Aeroacoustic Wind Tunnel Test Section,” Canadian Acoustics, vol. 47, 2019.

[39] Al Tlua, B., and Rocha, J., “Optimization and Testing of Flat-Plate Trailing-Edge Serration Geometry for Reducing Airfoil Self-Noise,” Canadian Acoustics, vol. 48, 2020.

[40] Clauser, F. H. Turbulent Boundary Layers in Adverse Pressure Gradients. J. Aeronaut. Sci. (Inst. Aeronaut. Sci.) 1954, 21 (2), 91–108.

[41] Falkner, V. M., and Skan, W. Some approximate solutions of the boundary layer equations. A.R.C Reports and Memoranda, 1930, no. 1314.

[42] Ludwieg, H., and Tillmznn, W. Investigations of the wall shearing stress in turbulent boundary layers. NACA T.M., 1950, no. 1285.

[43] Lee, H.; Kang, S.-H. Flow Characteristics of Transitional Boundary Layers on an Airfoil in Wakes. J. Fluids Eng. 2000, 122 (3), 522–532. doi: 10.1115/1.1287592

[44] Marsden, O.; Bogey, C.; Bailly, C. Direct Noise Computation around a 3-D NACA 0012 Airfoil. In 12th AIAA/CEAS Aeroacoustics Conference (27th AIAA Aeroacoustics Conference); American Institute of Aeronautics and Astronautics: Reston, Virigina, 2006. doi: 10.2514/6.2006-2503

[45] Chong, M. S.; Perry, A. E.; Cantwell, B. J. A General Classification of Three-dimensional Flow Fields. Phys. Fluids 1990, 2 (5), 765–777.

[46] Green, R. B.; Gerrard, J. H. Vorticity Measurements in the near Wake of a Circular Cylinder at Low Reynolds Numbers. J. Fluid Mech. 1993, 246 (1), 675–691. doi: 10.1017/s002211209300031x

[47] Gerrard, J. H. The Mechanics of the Formation Region of Vortices behind Bluff Bodies. J. Fluid Mech. 1966, 25 (2), 401–413. doi: 10.1017/s0022112066001721

[48] Blevins, R. D., Flow-induced vibration, Malabar (Fl.): Krieger publ., 2001.

[49] Hu, J.; Wang, Z.; Zhao, W.; Sun, S.; Sun, C.; Guo, C. Numerical Simulation on Vortex Shedding from a Hydrofoil in Steady Flow. J. Mar. Sci. Eng. 2020, 8 (3), 195. doi: 10.3390/jmse8030195

[50] William H. Press; Teukolsky, S. A.; Vetterling, W. T.; Flannery, B. P. Numerical Recipes; Cambridge University Press: Cambridge, England, 1986.

[51] Strouhal, Vincenz. Über eine besondere Art der Tonerregung. Stahel, 1878.

The Effect of Mouth Opening Levels on Acoustic Parameters of Voice Signal

Mahtab Rasi Mahmoudi *[1], Fatemeh Abnavi †[2], Leila Ghasisin ‡[3], and Shirin Saberi ♦[4]
[1]Student Research Committee, School of Rehabilitation, Isfahan University of Medical Sciences, Isfahan, Iran
[2]Audiology and Speech-Language Pathology Program, School of Rehabilitation Sciences, University of Ottawa
[3]Department of Speech Therapy, School of Rehabilitation Sciences, Isfahan University of Medical Sciences, Isfahan, Iran
[4]Musculoskeletal Research Center, School of Rehabilitation, Isfahan University of Medical School, Isfahan, Iran

Résumé

Cette étude examine l'effet de trois niveaux différents d'ouverture de la bouche sur : la fréquence fondamentale, le « jitter », le « shimmer », le rapport harmoniques/bruit, la fréquence du premier formant, la fréquence du second formant et le rapport des deux premiers formants lors de la production de la voyelle /a/. Une stratégie d'échantillonnage aléatoire simple a été utilisée pour recruter 36 participants. Au total, 18 femmes et 18 hommes âgés de 18 à 29 ans ont été recrutés. Les participants ont soutenu la voyelle /a/ pendant 7 secondes. La première et la dernière seconde de la voyelle ont été omises afin d'éliminer du signal audio l'effet d'initiation et de terminaison de la voyelle, et les 5 secondes du milieu ont donc été analysées pour en déduire les paramètres acoustiques. Sept caméras infrarouges ont enregistré l'ouverture de la bouche et les mouvements de la tête. Les résultats ont montré que le niveau d'ouverture de la bouche n'a d'effet que sur la fréquence fondamentale ($p=0{,}009<0{,}05$), le shimmer ($p=0{,}033<0{,}05$) et la fréquence du premier formant ($p=0{,}004<0{,}05$). Une posture de mâchoire ouverte place le larynx dans une position plus basse, ce qui entraîne une phonation plus détendue qui réduit la fréquence fondamentale et augmente le shimmer. Le niveau d'ouverture de la bouche a une relation inverse avec la fréquence du premier formant.

Mots clefs : niveaux d'ouverture de la bouche, fréquence fondamentale, fréquences des formants, jitter, shimmer, rapport harmoniques/bruit, voyelle /a/.

Abstract

This study examined the effect of three different mouth opening levels on fundamental frequency, jitter, shimmer, harmonic to noise ratio, first formant frequency, second formant frequency and first two formants ratio in Producing vowel /a/.simple random sampling strategy was used to recruit 36 participants. 18 females and 18 males between age 18 to 29 years were recruited. the participants sustained vowel /a/ 7 seconds. The first 1 second and the last 1 second of the vowel were omitted in order to eliminate the vowel initiation and termination effect from the audio signal and, thereby, the middle 5 seconds were analyzed to derive acoustic parameters. Seven infrared cameras recorded mouth opening and head movements. The results showed that mouth opening level is only effective on fundamental frequency ($p=0.009<0.05$), shimmer ($p=0.033<0.05$) and first formant frequency ($p=0.004<0.05$).An open jaw posture places the larynx in a lower position which causes a more relaxed phonation that reduce fundamental frequency and increase shimmer. Mouth opening level has an inverse relationship with first formant frequency.

Keywords: mouth opening levels, fundamental frequency, formant frequencies, jitter, shimmer, harmonic to noise ratio, vowel /a/.

1 Introduction

The speech production system, according to the source-filter theory, is composed of two main parts, the source (larynx) and the filter (articulators). Based on this theory, features of the vocal tract can be inferred from its acoustic output. In other words, different postures in the articulators produce different sounds. If the Supraglottic part of the vocal tract (supraglottis) is assumed as the acoustic resonator, different postures will change the shape of this acoustic resonator and, subsequently, the acoustic features of the produced signal will change as well. While producing the speech, the source or the larynx produces the harmonics and then the filter selectively enhances or attenuates the amplitude of harmonics [1]. The shape of the filter is influenced by the changes in the postures of the articulators. One of these articulators is the lower jaw. By changing its posture, the length and width of the vocal tract changes and, thereby, affects the signal produced by the larynx.

The larynx has a cartilage-muscular structure suspended from the hyoid bone. When the jaw is lowered (i.e. the open jaw posture), the hyoid bone is placed in the lower position too and, subsequently, the larynx is placed at a lower position as well. The placement of the jaw in the lower position reduces the muscular tension, improves approximation of the

* m.rasimahmoudi@gmail.com
† f.abnavi@gmail.com
‡ ghasisin@rehab.mui.a.ir ou ghasisin@gmail.com
♦ shirin.saberi69@gmail.com

vocal folds [2], and increases the vocal folds adduction [3] which causes a more relaxed voicing pattern [4]. On the contrary, the tense phonation is associated with the higher position of the hyoid bone and, subsequently, the placement of the larynx in the higher position.

1.1 Mouth opening as a voice therapy technique

Mouth opening is also used as a voice therapy technique to reduce muscular tension. The yawn-sigh technique and Froeschels' chewing method are two treatment methods that are used by opera singers [5]. The treatment methods focusing on the reduction of muscular tension, which have been used for singers, have improved the phonation among this group of patients [6]. The use of the Lee Silverman Voice Training (LSVT) method among patients with Parkinson's disease reduced the vocal cord bowing and increased vocal loudness. In this therapeutic method, the increase in the vocal effort is followed by an increase in the mouth opening [7]. Using LSVT method in dysarthria group changes formant frequencies of vowels and improves vowel goodness which is checked through perceptual vowel ratings [8].

1.2 Mouth opening and acoustic parameters

Studies have been conducted aiming to investigate the effect of the posture of the lower jaw on fundamental frequency. Lim et al. showed that the amount of mouth opening is inversely related with fundamental frequency [9]. Zawadzki & Gilbert showed that the fundamental frequency is related to the position of the lower jaw but the exact relationship was not reported [10]. Other studies have been conducted on the effect of the posture of the lower jaw on the filter-related parameters. Tasko et al. showed that as the mouth opening increases and the jaw is in a lower position, the first and second formant of the diphthongs are increased [11]. In another study, Mercer et al. investigated the effect of the lower mandible maneuver on the aerodynamic and acoustic parameters. They showed that the lower mandible maneuver results in a higher aerodynamic efficiency, higher SPL and also lower values of the first and second formants [12]. The effect of mouth opening on the parameters related to the source and filter were studied simultaneously by Mautner. In this study, it was shown that the mouth opening helps to increase the fundamental frequency, first formant, and the vowel space area and to reduce the jitter and the difference between the amplitude of first tow harmonics [13].

Science findings about mouth opening and frequency, first formant and second formant are in contrast in previous studies and mouth opening amount is mostly reported in a qulititative manner, the aim of this study was to investigate the effect of mouth opening in a quantitative and normalized manner on acoustic parameters of voice signal. The studied acoustic parameters included the fundamental frequency, jitter, shimmer, harmonic-to-noise ratio, the first formant, the second formant, and the first two formants ratio.

The hypothesis of the current study is that acoustic parameters of voice will be different in three mouth opening levels.

2 Method

The present study has been approved by the Isfahan University of Medical Sciences under the Ethical Code IR.MUI.RESEARCH.REC.1399.509.

2.1 Participants

The study participants included 18 males and 18 females aged between 18-29 years old. All participants met the inclusion criteria for this study: The mother tongue of the participants was Persian (Farsi). None of the participants had a history of smoking, drinking alcohol, gastrointestinal disease and voice disorder based on their own report and also didn't have temporomandibular joint problems. Based on diagnostic criteria of temporomandibular joint problems [14] if the researcher doubted the existence of signs or reported symptoms of the temporomandibular joint problems, the participant was eliminated from the study. On the sampling day none of the samples showed signs of allergy and cold.

2.2 Materials

To investigate the acoustic parameters of interest in the present study, the production of the vowel /a/ was used. For this purpose, the samples were asked to produce the vowel /a/ for 7 seconds. The first 1 second and the last 1 second of the pronunciation of the vowel were omitted in order to eliminate the vowel initiation and termination effect from the audio signal and, thereby, the middle 5 seconds were examined.

2.3 Procedures

Once the necessary permits were obtained from the Isfahan University of Medical Sciences, in order to invite people to participate in this study, an invitation was published on the relevant pages of the journals of the colleges of the Isfahan University of Medical Sciences. In these pages, the research objectives were described. Then, the applicant entered the sampling process. When the number of applicants from each gender reached 36, a number was assigned to each of them based on the table of random numbers. Next, using The Hat software, 18 participants were selected from each group. Again, the research objectives were explained to the selected participants. Then, they filled in the ethical consent form of the Isfahan University of Medical Sciences. These participants were examined in terms of the inclusion criteria and if qualified, they entered the next stage. In the next stage perceptual and acoustic voice assessment was done. The voice perceptual assessments were performed using the GRBAS scale. For this purpose, the participants read the rainbow text [15]. Also, they were asked to produce the vowel /a/ for 7 seconds and, then, scoring was done based on these two speech tasks. The cut of point was 0. To perform the voice acoustic assessment, which was done using the PRAAT (V.6.1.08), the samples were asked to produce the vowel /a/ for 7 seconds. Then, the middle 5 seconds were selected to perform the voice acoustic analyses. jitter, shimmer, and harmonic-to-noise ratio were analyzed. The cut off point for shimmer was less than 2/6, for jitter was less than 1 and for harmonic-to-noise ratio was greater than 12Db. The participants who had all inclusion criteria and proved healthy in the perceptual and acoustic assessments entered the sampling process. If each of the participants couldn't achieve the intended score in acoustic or perceptual assessment they were excluded from the study and another participant substituted the eliminated one. Accordingly, two participants were eliminated from the study at this stage.

In order for sampling, the participants were asked to open their mouth as wide as possible without feeling pain. Then, their mouth opening amount was measured by a caliper in mm and the 1/3 and 2/3 values of the measurements were calculated and recorded. Then, 4 markers were placed on the bone landmarks nasion, pogonion and porion according to the Fig. 1 with double sided glue. The participants sat in front of the cameras of the Qualisys system equipped with 7 infrared cameras. These cameras and QTM software (version 7.5; the Qualisys, Göteborg, Sweden) recorded the data of the mouth opening fixedness and head fixedness through the markers placed on the bone landmarks.

To collect the acoustic signal sample, a Zoom H1 recorder (Model 2016 made by ZOOM Company, Japan) was used. The microphone was connected to a headset and then the headset was placed at a distance of 5cm from the mouth and at a 45o angle at the right side of the mouth. The participants were asked to open their mouth as wide as possible. Then their mouth opening was measured again by a caliper to make sure that it is equal to the first amount. Afterward, the participants were asked to keep their mouth opening fixed and produce the vowel /a/ with a loudness of 75dB for 7 seconds while they had to avoid moving their head during sampling process. The voice loudness was examined using Sound Level Meters. Meanwhile, the cameras and QTM software recorded the data of the mouth opening fixedness and head fixedness through the markers placed on the bone landmarks. Camera data for each marker was reported in three-dimension x, y and z. the difference between the position of the nasion and pogonion markers was used to check mouth opening movements and the difference between the positon of left and right porion markers was used to check head movement. In the case that, considering the data obtained from the cameras, the mouth openness had changed or the participant had moved his/her head, the sample taken from that participant was eliminated and another sample from another participant was replaced. This process was repeated for the 1/3 and 2/3 values of the mouth opening. Once the process was finished, the data collected from the cameras was examined and the outlier was calculated. The audio signals were checked before data analysis and if any sample had abrupt loudness changes, the sample was eliminated.

The data obtained from the analysis of the audio signal of the participants were imported into the SPSS-25 software. The analysis of the collected data was performed using the ANOVA test and Bonferroni post hoc test. Also, the data obtained from the cameras were imported into the SPSS-25 software. Then, the outlier data were calculated and, accordingly, the samples with excessive head or mouth movement were eliminated from the sampling process.

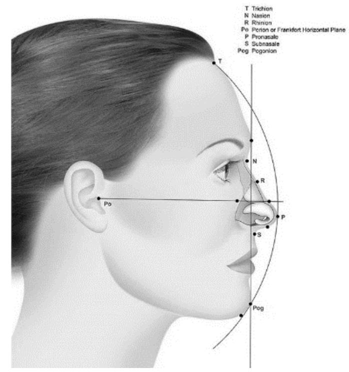

Figure 1: Bone landmarks, where markers are placed.

3 Results

The result obtained from descriptive statistics of marker's position at each level of the mouth opening are presented in-Tab. 1.

Table 1: Descriptive Statistics of difference in position of nasion-pogonion markers and left and right porion markers.

	N	Mean	SD	Max	Min
Nasion-pogonionx1/3	36	-10.05	5.00	0.00	-22.00
Nasion-pogo-niony1/3	36	-5.00	4.00	7.00	-16.00
Nasion-pogo-nionz1/3	36	-134.09	11.00	118.00	-161.00
Porionx1/3	36	-6.00	4.00	0.03	-14.00
Poriony1/3	36	-145.00	49.00	137.00	-188.00
Porionz1/3	36	-6.00	4.00	0.08	-16.00
Nasion-pogo-nionx2/3	36	-10.00	5.00	1.00	-22.00
Nasion-pogo-niony2/3	36	-7.09	4.00	0.06	-17.00
Nasion-pogo-nionz2/3	36	-164.00	234.0	143.00	147.00
Porionx2/3	36	-5.00	3.00	0.09	19.00
Poriony2/3	36	-141.00	51.00	156.00	-163.00
Porionz2/3	36	-6.00	3.00	2.00	-14.04
Nasion-pogo-nionx3/3	36	-8.00	6.00	12.00	-20.00
Nasion-pogo-niony3/3	36	-6.00	4.00	2.09	-16.00
Nasion-pogo-nionz3/3	36	-182.00	170.0	133.00	-147.00
Porionx3/3	36	-4.00	2.00	0.00	-9.00
Poriony3/3	36	-142.00	52.00	162.00	-165.00
Porionz3/3	36	-6.08	3.00	1.00	-13.00

N: Number SD: Standard Deviation Max: Maximum Min: Minimum

The results obtained from descriptive statistics, including the mean and the standard deviation, at each level of the mouth opening are presented in Tab. 2

Table 2: Mean and standard deviation for each of the seven experimental measures in three different mouth opening levels.

Measures		1/3 Mouth opening		2/3 Mouth opening		3/3 Mouth opening	
		Mean	SD	Mean	SD	Mean	SD
F0	male	127.98	16.44	124.08	14.09	125.75	21.57
	Female	250.10	32.97	245.40	30.35	243.19	34.59
Jitr		.271	.142	.266	.125	.276	.097
Shimer		2.076	.914	2.039	.746	2.550	1.156
HNR		23.76	2.83	24.30	3.16	23.10	2.85
F1		758.95	104.09	778.61	100.79	795.43	114.37
F2		1164.05	139.43	1174.76	129.65	1197.67	117.96
F1/F2		.648	.046	.658	.056	.659	.058

Also, the ANOVA test results concerning the effect of the mouth opening level on the fundamental frequency, separated based on the gender, jitter, shimmer, harmonic-to-noise ratio, the first formant, the second formant, and the first two formant ratio, are presented in Tab. 4.

Table 3: Results of Anova test performed on the seven experimental measures in three different mouth opening levels.

Agent	Measure		F	df1	df2	sig	η^2
Mouth opening	F0	male	2.884	2	16	.085	.265
		Female	6.360	2	16	.009*	.443
	% Jit		.113	2	34	.893	.007
	% Shim		3.791	2	34	.033*	.182
	HNR		2.628	2	34	.087	.134
	F1		6.647	2	34	.004*	.281
	F2		1.911	2	34	.164	.101
	F1/F2		.939	2	34	.401	.052

As indicated by the results in Tab. 3, the mouth opening level has a significant effect on the fundamental frequency in the women's group. According to the results of Bonferroni post hoc test (Tab. 4).

Table 4: Results of Bonferroni test performed on F0, % Shim and F1.

Measure	Mouth opening level	Mouth opening level	Mean difference	P value
F0	1/3	2/3	4.704	.018*
	1/3	3/3	6.914	.021*
	2/3	3/3	2.210	.933
Shim	1/3	2/3	.037	.99
	1/3	3/3	-.474	.029*
	2/3	3/3	-.511	.038*
F1	1/3	2/3	-19.66	.02*
	1/3	3/3	-36.478	.004*
	2/3	3/3	-16.819	.231

In the 1/3 mode of mouth opening, the average fundamental frequency is significantly higher than that in the 2/3 and 3/3 modes of mouth opening. Since the eta-squared in women's group is 0.443, 44.3% of the fundamental frequency variations in the women's group at these three levels is due to the mouth opening level. The mouth opening level also affects the shimmer ($p=0.033<0.05$). According to the results of the Bonferroni post hoc test (Tab. 4), the shimmer in the 1/3 mode of mouth opening is significantly lower than the shimmer in the 2/3 mode of mouth opening. Also, the shimmer in the 2/3 mode of mouth opening is significantly lower than that I the 3/3 mode of mouth opening. Considering the fact that the obtained eta-squared value is 0.182, 18.2% of the shimmer percentage variations at these three levels is due to the mouth opening level. The mouth opening level also affects the value of the first formant ($p=0.004<0.05$). The Bonferroni post hoc test (Tab. 4) shows that the average first formant in the 1/3 mode is significantly lower than that in the 2/3 mode and significantly lower than that in the 3/3 mode. Since the eta-squared value of 0.281, 28.1% of the first formant variations at these three levels is due to the mouth opening size. As for the jitter ($p=0.893>0.05$), the harmonic-to-noise ratio ($p=0.078>0.05$), the second formant ($p=0.146>0.05$), and the first two formant ratio ($p=0.401>0.05$) don't affect the mouth opening level. As shown in Tab. 2, the jitter has the highest average in the 3/3 mode of mouth opening and the lowest average in the 2/3 mode of mouth opening, but such a difference is not significant according to Tab. 3. According to Tab. 2 the harmonic-to-noise ratio has the lowest value in the 2/3 mode of mouth opening and the highest value in the 3/3 mode of mouth opening. However, such a difference is not significant (Tab. 3). As shown in Tab. 2, the average second formant has the highest average value in the 3/3 mode of mouth opening and the lowest average value in the 1/3 mode of mouth opening, but this difference is not significant (Tab. 4). The first two formant ratio has the highest average value in the 3/3 mode of mouth opening and the lowest average value in the 1/3 mode of mouth opening (Tab. 2), but such a difference is not significant according to Tab. 4.

4 Discussion

4.1 Mouth opening and fundamental frequency

The present study aimed to investigate the effect of the mouth opening level on the parameters of the produced acoustic signal. According to the findings, with an increase in the mouth opening level, the fundamental frequency reduced in both groups of men and women. This difference was insignificant in men's group so that the statistical tests exhibited no significant difference while this difference was significant in women's group. In women's group, the average fundamental frequency in the 1/3 mode of mouth opening was higher than that in the 2/3 and 3/3 modes. The increased mouth opening causes the larynx to be placed in a lower position [4]. Furthermore, the vertical movements of the larynx are directly related to the control of the fundamental frequency [16]. The placement of the larynx in a higher position results in a higher fundamental frequency and a lower position of the larynx leads to a lower fundamental frequency. with an increase in the mouth opening level and, subsequently, placement of the larynx in a lower position, the fundamental frequency is reduced. This phenomenon, which is well known, has no clear cause-and-effect explanation. In a study in this regard, Kakita & Hiki investigated the vertical movements of larynx and electromyography of the infrahyoid muscles (sternohyoid, sternothyroid, thyrohyoid, and omohyoid) and found a strong relationship between the fundamental frequency, the vertical movements of larynx, and contraction of the infrahyoid muscles. Based on these findings, they designed an anatomical model in which the thyrohyoid and sternothyroid muscles controlled the vertical position of larynx. In this model, the effect of the larynx's vertical position on the fundamental frequency was attributed to the vertical movements of the cricothyroid joint [17]. With the rotation of the cricothyroid joint, the cricothyroid muscle is stretched and changes the vocal cord’s tension, in this way affects the fundamental frequency. In the following studies, as for the probable cause of the effect of the larynx's vertical movements on the fundamental frequency, Hirai et al. explained that the larynx's movements in vertical direction result in the rotation of the cricoid cartilage. The rotation of this cartilage affects the length of the vocal cords and controls the voice fundamental frequency [18]. As such, the position of the larynx in the neck affects the fundamental frequency.

Studies have reported that the thickness of the vocal cords in men in 20% more than that in women. Such a difference in thickness affects the voice frequency so that in the individuals undergoing SRS surgery (sex reassignment surgery), the thickness of vocal cords must be changed by 20% in order that the fundamental frequency of voice can be changed from a male voice into a female voice [19]. As mentioned above, the rotation of the cricoid cartilage following the change in the vertical position of the larynx results in the stretch of the vocal cords and also the increase in the muscular tension leads to the increased fundamental frequency. In men who have thicker vocal cords, probably the force imposed on the vocal cords following the placement of the larynx in a higher position will be slighter and will result in a slighter stretch of the vocal cords. Accordingly, the increase in the produced frequency will be slighter in the men's group.

In a study on patients with mutational falsetto, Salturk et al. showed that in the case of using lower mandible maneuver and, subsequently, the placement of the larynx in a lower position, the fundamental frequency decreased significantly [20]. Findings of this study were consistent with those of the study conducted by Lim et al. [9]. Also, Gilbert and Zawadzki obtained similar results [10]. However, findings of Mautner et al.'s study [13] were not consistent with results of the present work since in their study, the fundamental frequency increased with an increase in the mouth opening level. Regarding the fact that the mouth opening level in this study was qualitative and it was not exactly known how wide the subjects had opened their mouth when producing the vowel, the results of these two studies cannot be compared appropriately.

4.2 Mouth opening and jitter, shimmer and harmonic to noise ratio

In this study, the average shimmer in the 1/3 mode of mouth opening was significantly lower than that in the 3/3 and in 2/3 was lower than 3/3 mode of mouth opening. Nevertheless, the increase in the mouth opening level didn't cause the shimmer to exceed its normal value, which was 2.6 [2]. As the mouth opening level increases, the larynx is placed in a lower position and its normal state, which is followed by a reduced glottal tension and, thus, the voice is heard a bit breathy. The voice breathiness degree is correlated with the closeness of the vocal cords. The endoscopic studies on the yawn-sigh method have shown that with the placement of the larynx in a lower position and the expansion of the pharyngeal space, the degree of the vocal folds adduction is reduced so that in the closed phase, in which the vocal cords must be completely closed, there will be a small gap between two vocal cords resulting in an increased perturbation level, an increased shimmer, and a breathy voice quality [4]. Shimmer findings of the present study are consistent with those of the above-mentioned study. Also, other studies in this regard have shown that an increase in the fundamental frequency would lead to a reduction in the average shimmer. In fact, with an increase in the fundamental frequency, the vibrational regularity of the vocal cords is increased and the average shimmer is reduced [21, 22]. Therefore, the reduction in the shimmer observed in the 1/3 mode of mouth opening can be due to the increased frequency observed at this mouth opening level. In the study conducted by Mautner, the increase in the mouth opening was associated with a reduced average shimmer [13]. In 2007, in a study conducted on the effect of mouth opening on the speech production and voice characteristics of children with hearing loss and healthy children, Lee showed that the exaggerative mouth opening would result in a lower shimmer percentage and an increased voice stability [23]. In both of these two studies, the mouth opening level has not been examined quantitatively and since the subjects' mouth opening level is not clearly known, the obtained results cannot be compared to the findings of the present work. Furthermore, studies have shown that the voice loudness is a confounder variable for the parameters related to the acoustic signal disturbances (i.e. jitter, shimmer, and harmonic-to-noise ratio). This means that an increased voice loudness would improve these parameters even in individuals with voice disorders. Therefore, when these parameters are used to investigate the quality of the acoustic signals, the voice loudness must be controlled as a confounding variable [24]. Thus, the improvement in the shimmer observed in these studies might be due to the increased voice loudness since in both of these studies, the voice loudness has not been controlled and merely the subjects have been asked to produce the given vowels and syllables with their habitual voice loudness. In the present study, the jitter and the harmonic-to-noise ratio exhibited no significant relationship with the mouth opening level. On the other hand, in Mautner's study on the effect of mouth opening level on the above-mentioned parameters, it was shown that the increased mouth opening would reduce these two parameters. As mentioned earlier, such an improvement might be due to the increased voice loudness and the effect of the increased SPL (sound pressure level) on these parameters, not due to the direct effect of the increased mouth opening.

4.3 Mouth opening first formant, second formant and first two formants

Results of the present study showed that the first formant is significantly related to mouth opening level while the second formant and the first tow formant ratio don't have a significant relationship with mouth opening. In this study, with an increase in the mouth opening, the frequency of the first formant increased. The first formant has a reverse relationship with the tongue height so with a reduction in the tongue height, the value of the first formant increases. Since the tongue and the lower jaw mainly move together, it is expected that the movements of the lower jaw affect the frequency of the formants because the lowering of the jaw results in the lowering of the tongue and elongation of the oral cavity. As the mouth opening increases, the tongue is placed in a lower position and the frequency of the first formant increases. In Mautner's study, the frequency of the first formant increased with an increase in the mouth opening [13]. Lee et al. obtained the same findings. They studied the relationship between the position of the tongue on the X-Y axis and the values of the first and the second formants and found a very strong reverse relationship between the tongue's position on the Y-axis and the value of the first formant. Accordingly, the highest the position of the tongue on the Y-axis, the lower the frequency of the first formant [25]. Results of this study confirm the results of the previous works.

The theory states that the value of the second formant is related to the tongue's posterior and anterior position in the mouth so the more posterior the position of the tongue, the smaller the value of the second formant. Furthermore, studies have shown that as the mouth is opened wider, the tongue moves backward and the vowel constriction finds a more posterior position [26]. Based on the findings, it is expected that with an increase in the mouth opening, the value of the second formant decreases. There are studies with findings that confirm the above claim [12, 13]; whereas, in the present work, no significant relationship was found between the frequency of the second formant and the mouth opening level. This can be probably attributed to the relationship between the frequency of the second formant and the height and forward movement of the tongue at the same time. Findings of a new study show that the second formant is identically related to the tongue's position on the X-axis and the Y-axis. In this study, it has been shown that the frequency of the first formant is clearly related to the height of the tongue or, in other words, the tongue's position on the Y-axis. On the other hand, for the second formant, the relationship between the tongue's position on the X-axis and the Y-axis and is a bit more complex. This study showed that the second formant is dependent not only on the tongue's position on the X-axis or the posterior and anterior position of the tongue but also on the tongue's position on the Y-axis or, in other words, the tongue's height [25].

The first tow formants ratio determines the quality of the vowel. Accordingly, the longer the distance of the first and second formants of a vowel, the higher the quality of that vowel. Also, as the anterior part of the oral cavity gets smaller and the posterior part of the oral cavity expands, the first and second formants of the vowel get farther and, thereby, the quality of the vowel increases [1]. However, as the mouth opening level increases, the case gets reversed. Accordingly, with an increase in the mouth opening level, the anterior part of the oral cavity expands while with the backward movement of the tongue, the posterior part of the oral cavity gets smaller.

Findings of the present study about fundamental frequency and shimmer shows that with opening the mouth in 3.3 level, which is the maximum mouth opening level without pain, fundamental frequency decreases the most. In treatment of voice disorders such as mutational falsetto and muscle tension dysphonia increasing mouth opening level in maximum amount (3/3) can be helpful in frequency decrease without exceeding the shimmer from its normal value. First formant frequency also increases as the mouth opening increase. Studies have shown first formant frequency in people with dysarthria decreases [27, 28]. Findings of the present study shows that first formant frequency has its normal value in 1/3 of maximum mouth opening. Therefore, it seems exaggerated amounts of mouth opening doesn’t improve vowel quality in people with dysarthria. Further studies are needed to determine which level of mouth opening can improve vowel quality in people with dysarthria.

5 Conclusion

The results in this study show that by increasing the amount of mouth opening level, fundamental frequency decrease, while shimmer and the first formant frequency increase. Other acoustic parameters didn’t have significant relationship with mouth opening level.

Acknowledgments

This work was supported by the musculoskeletal research center, university of medical science, Isfahan, iran. Authors would like to thank all participants who took part in this study.

References

[1] Behrman A. Speech and voice science: Plural publishing; 2017.

[2] Boone DR, McFarlane SC, Berg SLV. The voice and voice therapy: Pearson Education; 2014.

[3] Cookman S, Verdolini K. Interrelation of mandibular laryngeal functions. Journal of voice : official journal of the Voice Foundation. 1999;13(1):11-24. DOI: 10.1016/s0892-1997(99)80057-5

[4] Boone DR, McFarlane SC. A critical view of the yawn-sigh as a voice therapy technique. Journal of Voice. 1993;7(1):75-80. DOI:10.1016/s0892-1997(05)80114-6

[5] Sundberg J, Skoog J. Dependence of jaw opening on pitch and vowel in singers. Journal of Voice. 1997;11(3):301-6. DOI: 10.1016/S0892-1997(97)80008-2

[6] Sabol JW, Lee L, Stemple JC. The value of vocal function exercises in the practice regimen of singers. Journal of Voice. 1995;9(1):27-36. DOI: 10.1016/s0892-1997(05)80220-6

[7] Smith ME, Ramig LO, Dromey C, Perez KS, Samandari R. Intensive voice treatment in Parkinson disease: laryngostroboscopic findings. Journal of Voice. 1995;9(4):453-9. DOI: 10.1016/s0892-1997(05)80210-3

[8] Sapir S, Spielman JL, Ramig LO, Story BH, Fox C. Effects of intensive voice treatment (the Lee Silverman Voice Treatment [LSVT]) on vowel articulation in dysarthric individuals with idiopathic Parkinson disease: acoustic and perceptual findings. 2007. DOI: 10.1044/1092-4388(2007/064)

[9] Lim M, Lin E, Bones P. Vowel effect on glottal parameters and the magnitude of jaw opening. Journal of voice. 2006;20(1):46-54. DOI: 10/1016/j.jvoice.2004.09.003

[10] Zawadzki PA, Gilbert HR. Vowel fundamental frequency and articulator position. Journal of Phonetics. 1989;17(3):159-66. DOI:10.1016/S0095-4470(19)30425-5

[11] Tasko SM, Greilick K. Acoustic and Articulatory Features of Diphthong Production: A Speech Clarity Study. Journal of Speech, Language, and Hearing Research. 2010;53(1):84-99. DOI: 10.1044/1092-4388(2009/08-0124)

[12] Mercer E, Lowell SY. The Low Mandible Maneuver: Preliminary Study of Its Effects on Aerodynamic and Acoustic Measures. Journal of Voice. 2019. DOI: 10.1016/j.jvoice.2018.12.005

[13] Mautner HD. An Acoustic and Electroglottographic Study of the Aging Voice With and Without an Open Jaw Posture. Journal of voice : official journal of the Voice Foundation. 2015;29(4):518.e1-11 DOI: 10.1016/j.jvoice.2014.09.024

[14] Steenks MH. Temporomandibular joint damage in juvenile idiopathic arthritis: Diagnostic validity of diagnostic criteria for temporomandibular disorders. Journal of Oral Rehabilitation. 2019;46(10):883-4. DOI: 10.1111/joor.12811

[15] Memarian A, Ghorbani A, Torabi Nejad F, Keyhani MR. Designing a Farsi text for the assessment of adult voice features and determining its validity and reliability in measuring the fundamental frequency and intensity of speech. Journal of Research in Rehabilitation Sciences. 2010;4(2). DOI:10.22122/JRRS.V4I2.44

[16] Chiba T, Kajiyama M. The vowel: Its nature and structure: Phonetic society of Japan Tokyo; 1958.

[17] Kakita Y, Hiki S, editors. A study on laryngeal control for pitch change by use of anatomical structure model. ICASSP'76 IEEE International Conference on Acoustics, Speech, and Signal Processing; 1976: IEEE.

[18] Honda K, Hirai H, Masaki S, Shimada Y. Role of vertical larynx movement and cervical lordosis in F0 control. Language and Speech. 1999;42(4):401-11. DIO:10.11770023830999042004030l

[19] Kim H-T. Vocal feminization for transgender women: current strategies and patient perspectives. International journal of general medicine. 2020;13:43. DOI:10.2147/IJGM.S205102

[20] Saltürk Z, Doğanay T, Üstün O, Tutar B, Akgün MF, Uyar Y. Efficacy of low mandible maneuver on mutational falsetto. Folia Phoniatrica et Logopaedica. 2021;73(5):442-8. DOI: 10.1159/000506631

[21] Pyo H-Y, Sim H-S. Shimmer Change According to Fundamental Frequency Variation of Korean Normal Adults. Speech Sciences. 2003;10(1):143-52.

[22] Verstraete J, Forrez G, Mertens P, Debruyne F. The effect of sustained phonation at high and low pitch on vocal jitter and shimmer. Folia Phoniatrica et Logopaedica. 1993;45(5):223-8. DOI: 10.1159/0002266266

[23] Lee C-C. Relationship Between Jaw Opening and Phonetic Complexity: A Cross-Language Study. 2007.

[24] Brockmann-Bauser M, Bohlender JE,Mehta DD. Acoustic Perturbation Measures Improve with Increasing Vocal Intensity in Individuals With and Without Voice Disorders. Journal of voice : official journal of the Voice Foundation. 2018;32(2):162-8. DOI: 10.1016/j.jvoice.2017.04.008

[25] Lee J, Shaiman S, Weismer G. Relationship between tongue positions and formant frequencies in female speakers. The Journal of the Acoustical Society of America. 2016;139(1):426-40. DOI:10.1121/1.4939894

[26] Stevens KN, House AS. Development of a quantitative description of vowel articulation. The Journal of the Acoustical Society of America. 1955;27(3):484-93. DOI: 10.1121/1.1907943

[27] Byeon H. An Acoustic Analysis of the Korean Diphthong in Speakers with Dysarthria.

[28] Sapir S, Ramig LO, Spielman JL, Fox C. Formant centralization ratio: A proposal for a new acoustic measure of dysarthric speech. 2010. DOI: 10/1044/1092-4388(2009/08-0184)

SOUNDSCAPE ADDITIONS FROM VESSELS RELATED TO TRANSIT SPEED, DIRECTION AND MANOEUVRES

Brody Granger *[1], Rianna Burnham †[2] and Svein Vagle ‡[2]
[1]University of British Columbia, BC, Canada
[2]Institute of Ocean Sciences, Fisheries and Oceans Canada, Sidney, BC, Canada

Résumé

Les changements de niveaux sonores sous-marins lors de la navigation des navires commerciaux sur les couloirs de navigation dans les eaux intérieures autour du Golfe de Géorgie et des îles San Juan ont été évalués. Ces mesures in-situ s'appuient sur des évaluations antérieures plus expérimentales. Les enregistrements de trois mouillages acoustiques à Boundary Pass, Turn Point et Haro Strait, dans le sud de l'île de Vancouver, en Colombie-Britannique, ont été utilisés pour comparer les mesures du champ acoustique au point d'approche le plus proche des navires avant, pendant et après un virage. Les types de navires évalués comprenaient des pétroliers, des vraquiers, des transporteurs de véhicules, des porte-conteneurs et des navires à passagers. Une régression linéaire multi-variable a confirmé la relation entre la vitesse du navire et les niveaux sonores, montrant que la trajectoire du navire avait également une influence. Les vitesses de transit les plus lentes, mais aussi les niveaux sonores à large bande (10 Hz à 100 kHz) et les niveaux sonores les plus élevés des navires ont été enregistrés lors de leurs manœuvres à Turn Point. Les émissions sonores dérivées des navires dans les moyennes et hautes fréquences étaient également considérables.

Mots clefs : bruit des navires, navigation commerciale, virages et manœuvres, bruit anthropique

Abstract

The changes in underwater sound levels as commercial vessels navigate through shipping lanes in the inland waters around the Gulf of Georgia and San Juan Islands were assessed. These in-situ measures build on previous, more experimental evaluations. Recordings from three acoustic moorings at Boundary Pass, Turn Point and Haro Strait, southern Vancouver Island, British Columbia, were used to compare sound field measures at vessels' closest point of approach before, during, and following a turn. Vessel types assessed included tankers, bulkers, vehicle carriers, containerships, and passenger vessels. A multi-variate linear regression confirmed the relationship between vessel speed and sound levels, showing that the course of the vessel was also influential. The slowest transit speeds, yet highest broadband (10 Hz to 100 kHz) and vessel noise levels were recorded as they manoeuvred at Turn Point. Vessel-derived sound emissions in the mid- to high-frequencies were also considerable.

Keywords: vessel noise, commercial shipping, turning and manoeuvres, anthropogenic noise

1 Introduction

Anthropogenic noise is quickly becoming an ubiquitous contribution to oceanic soundscapes. Increases in the ambient sound levels compared to those in pre-industrial conditions have been found to be significant [1,2]. This is particularly true for the low-frequency (< 1000 Hz) component of the vessel noise emissions, as these tonal components of the signal are able to propagate over long distances, with low absorption rates and transmission losses compared to higher frequencies [3,4]. These sound level increases have occurred simultaneously to an increase in the number, size and travel speed of merchant vessels in the global fleet. Additions from shipping can propagate to regions far removed from the source, however the additions from commercial vessels are particularly concentrated in areas near the coast, on shipping routes, and in ports [5-8].

Understanding the additions and impacts of commercial shipping on ocean soundscapes is complex. Additions from commercial and recreational vessels can dominate the soundfields at times and/or in places [1]. Commercial vessel passages can elevate the ambient sound levels substantially [9]. Acoustic signals of specific vessels and vessels during particular manoeuvres has so far been addressed by experimental recordings in controlled conditions [3, 10-12]. For example, Trevorrow et al. [10] showed the acoustic additions and its directionality from vessels manoeuvring. In addition, a linear relationship between vessel speed and noise emissions has been established from vessels transiting a monitored area [9]. During manoeuvres vessels slow, and so we might expect that the noise levels adding to the soundscape from these vessels may be reduced as per this established relationship [9]. However, mechanical adjustments and increased hydrodynamic drag during the turn, as well as potentially greater engine power being applied to maintain speed during the manoeuvre, may lessen any potential reductions.

Elevation of ambient underwater sound levels, particularly resulting from vessel noise additions, is increasingly

* grangerb@mail.ubc.ca
† rianna.burnham@dfo-mpo.gc.ca (corresponding author)
‡ svein.vagle@dfo-mpo.gc.ca

being recognised as a stressor for marine mammals who rely on acoustics to send and receive information about their surroundings. Also, critical habitat of at-risk species can overlap with areas of high human use.

The Salish Sea is the collective name for the inland waters around southern Vancouver Island, the San Juan Islands, and Puget Sound in Washington State. These waterways lead to ports in Vancouver, Seattle, Tacoma, Port Angeles, Nanaimo and Victoria (Figure 1). However, these waters are also designated as critical habitat for endangered southern resident killer whales (*Orcinus orca*, SRKW). The international shipping lanes in this area overlap with SRKW foraging habitat [13-14]. Acoustic disturbance in frequencies used for communication calls or echolocation could, for example, reduce SRKW ability to navigate, find and capture prey, or retain group contact. Additionally, this area is frequently used by humpback whales (*Megaptera novaeangliae*) and several dolphin and porpoise species [15-16].

To lessen the acoustic disturbance, in particular for SRKW, voluntary slowdown measures have been introduced for portions of the shipping lanes at Swiftsure Bank, at the western entrance to Juan de Fuca Strait, and around the southern Gulf Islands through Haro Strait and Boundary Pass (Figure 1) through the Enhanced Cetacean Habitat and Observation (ECHO) program [17]. These measures were first introduced in 2017, and have shown vessel participation rates to be high, demonstrating this to be an effective means to reduce underwater vessel noise [17]. The slowdown measure is initiated with a confirmed observation (visual or acoustic) of SRKW in the area following June 1, and continues until at least the middle of October or until SRKW have been absent from the Salish Sea for a number of weeks after this time.

Following on from the experimental work by Trevorrow et al. [10], we examined in-situ recordings from vessels transiting to and from ports in the Salish Sea. Comparisons of received vessel noise levels from recordings made before, during, and following a vessel turning and manoeuvring were made to ascertain how vessel acoustic signals change during these types of manoeuvres. As well as underwater broadband (10 Hz to 100 kHz) sound level changes, variations in sound levels in frequencies pertinent to species in the Salish Sea, in particular the SRKW, who are frequently sighted in this area [13-14] were given focus. The recordings were evaluated to establish how vessel signals may make acoustic additions during transit and turning which may impact on SRKW communication and echolocation frequencies. Our study area and period were part of a slowdown trial, and so the changes between pre- and during trial for vessel emissions from manoeuvres will also be examined.

2 Method

2.1 Acoustic data

Acoustic recordings

Calibrated Autonomous Multichannel Acoustic recorders (AMAR G4, JASCO Applied Sciences) with omnidirectional hydrophones (M36-100, GeoSpectrum Technologies) were deployed in Haro Strait, Turn Point and Boundary Pass in the Salish Sea (Figure 1).

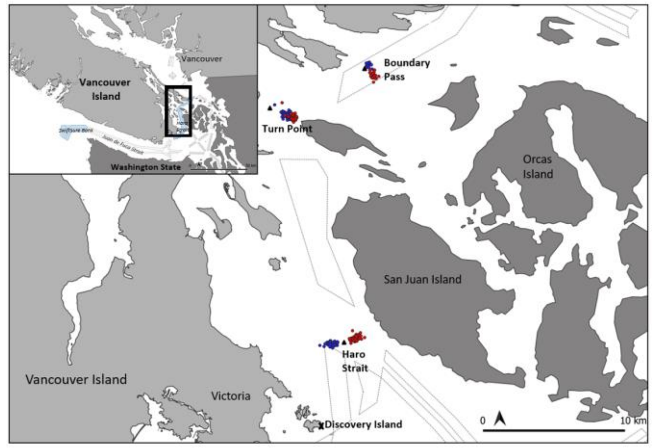

Figure 1: Study area map, with the inset showing vessel transit lanes and the recording locations at Boundary Pass, Turn Point and Haro Strait. Locations marked in red represent inbound vessels and outbound in blue. In the inset, the blue shaded areas are where the seasonal slowdown measures were in place.

Equipment was mounted onto specially designed quiet mooring systems manufactured by Oceanetic Measurement Ltd. The hydrophone was positioned 2 m from the sea floor with the deployment location in Haro Strait being 226 m, Turn Point 193 m and Boundary Pass 178 m deep. Each system was calibrated by the manufacturer and then again before the deployments using a 250 Hz piston phone. Recordings were made simultaneously at these locations from June 1 to August 18, 2019. The sampling rate was 256 kHz with 24-bit resolution. Data were stored on internal SD memory cards as wav files. On retrieval, these files were processed using custom Python scripts modified from Merchant et al. [18] to form 1-minute power spectra in 1-Hz bands of the full domain using 1 s Hanning window with 50% overlap and Welch's averaging.

Acoustic analysis

Changes in the underwater sound levels were considered through examining the sound pressure levels (SPL) in a broadband frequency range (10 Hz to 100 kHz). Vessel presence acoustic metrics (10-100 Hz, 53-71 Hz, 113-141 Hz [18-19]) were also examined to capture the low-frequency additions from commercial vessel traffic, while a 1-kHz frequency band centered at 50 kHz was used as an acoustic marker for smaller, recreational vessel presence [20-21]. These band metrics are consistent with previous studies and the EU Marine Strategy Framework [18-19].

To consider the potential impact on cetacean species the frequency range of 500-15000 Hz was considered for the potential acoustic masking of low- to mid-frequency calls of humpback (*Megaptera novaeangliae*) and killer whales (*Orcinus orca*), and 15-100 kHz for dolphin and porpoise echolocation. The 49.5-50.5 kHz band represents the centre frequency of the bimodal echolocation clicks used by SRKW [22], and so examination of this range might help estimate the potential for masking of these signals by vessels turning.

Comparisons were made between the received SPL at the recorders to evaluate the vessel noise additions before, during and after the manoeuvre at Turn Point. The L_{25}, L_{50} or median, and L_{75} SPL were examined. Non-parametric tests were used for comparisons of noise levels, and Student t-tests used for comparison of average vessel speed or distance from the mooring to a given vessel.

2.2 Vessel Data

Vessel transit data were obtained from terrestrial Automatic Identification System (AIS) receivers. The use of AIS transceivers is mandated for international vessels over 150 gross tons (GT) carrying more than 12 passengers, vessels over 300 GT engaged in an international voyage, or any vessel over 500 GT. This encompasses the commercial vessel traffic transiting to and from ports in the Salish Sea. A vessel's location, identity, type, and intended destination is transmitted every 5-30 seconds. For this analysis, commercial vessels were grouped into five classes: Passenger ships, vehicle carriers, tankers, containerships and bulkers.

The AIS data for the study period were cleaned and binned from the received time intervals into 1-minute periods for each vessel. Speed over ground (SOG) and acceleration over ground (AOG) were calculated using the distance between GPS locations and the time elapsed. Any data that appeared erroneous, for example expressing an excessive vessel SOG or AOG (>50 knots or >100 knots/s, respectively) or a GPS location on land, were removed. Any missing data were interpolated from adjacent data points. Locational data were converted to an orthogonal co-ordinate system, and then vessel travel direction and distance from each of the moorings as it transited, and its closest point of approach (CPA, Figure 1), were all obtained. This established a course over ground (COG) for each vessel. Vessel speed through water (STW) was derived from the SOG by correcting for tidal velocity and direction (WebTide model, [23]). Examining STW was used to determine whether a vessel was slowing down to turn. Maximum received levels (RL) of vessel noise additions in the vessel metrics were obtained from recordings when a vessel was at its CPA to the recorder. These RL and CPA distances were used to estimate the source levels (SL) of each vessel passing a hydrophone. Near spherical spreading losses were assumed, as:

$$SL\ (1\ \mu\text{Pa @ 1 m}) = RL + 18.6 \log_{10}(r), \qquad (1)$$

where r is the CPA distance in meters. A previous study in the same region found that an empirically-based transmission loss coefficient of 18.6 +/- 0.4 dB/decade worked for $r < 3$ km [9]. Range dependent water absorption for all metrics was not included when calculating this for broadband (10 Hz to 100 kHz) and low-frequency vessel metrics due to the limited distances being considered, but for the 49.5 – 50.5 kHz metric a narrow-band absorption (αr) term was added to Equation 1 to form:

$$SL\ (1\ \mu\text{Pa @ 1 m}) = RL + 18.6 \log_{10}(ar), \qquad (2)$$

where α is the absorption coefficient at 50 kHz [24].

Some vessels made multiple transits through the study area during the study period. The five most recurring vessels in the AIS records, noted as passing through Haro Strait-Boundary Pass during the six weeks of this study from each of the five vessel classes, were selected for the acoustic analysis. The minute-wise acoustic and AIS data were matched manually. Also, periods of low wind (<15 km/h), as measured at a weather station at Discovery Island (Figure 1), and low tidal current speeds (<0.3 m/s), established using WebTide [22] measures, were used. Times when small vessels were absent in the AIS Class B data were also used; however, it is recognised that this represents the minimum presence of recreational vessels as this AIS transceiver if carried voluntarily by this vessel type. A comparison of the data recorded during the day (05:00-21:00) and night (from 21:00 to 05:00) was made to establish the potential contributions of smaller vessels that may not be seen in the AIS data, but could still be influential on the underwater sound levels, especially in the higher frequencies. It was presumed for this comparison that these smaller recreational vessels would be absent overnight when it is dark. This presumption of absence at night was made based on findings by Burnham et al. [20] from the Salish Sea.

A voluntary vessel slowdown was in place for commercial vessels from July 5 onwards, and continued throughout the latter part of the study period. These measures requested that bulker, tankers, ferries and government vessels limit their speed to 11.5 kts and vehicle carriers, cruise ships and containerships to 14.5 kts. Comparisons of underwater sound levels and received SPL from vessel transits from before and during the slowdown trial were considered as part of this analysis.

3 Results

The AIS data helped identify 245 1-minute acoustic recordings from the three moorings where a vessel was passing within 3 km of a mooring during the study period. These were then categorised by their direction of travel (inbound to ports or outbound away from ports) and then into the five vessel classes. These recording intervals were of the five most recurring vessels for each vessel class. They represented 46 full tracks of passage, and 47 partial tracks, due to the Boundary Pass recorder not recording between July 3- August 17, 2019.

3.1 Vessel passage and speed

During the study period the number of transits for container ships, bulkers and tankers averaged 11.21 +/- 5.90 vessels/day, with a maximum of 60 passages/day.

Tanker and bulker transit speeds tended to be slower, and vehicle carriers and containerships the fastest. Vessels transiting inbound were also typically slower compared to the outbound vessels. Of the three mooring locations, greater speeds were seen as the vessels were passing the Boundary Pass mooring, and most reduced as they were manoeuvring at Turn Point. For inbound transits to ports, vessel speeds were similar at both Boundary Pass and Haro Strait and reduced at Turn Point (Figure 2). Significant increases were seen for outbound passenger vessels compared to inbound passenger vessels at two of the three locations (Figure 2). Vehicle carriers leaving port transited significantly slower than when they were approaching as they manoeuvred at Turn Point. For outbound transits the greatest speeds were noted at Boundary difference between the pre- and during trial speeds may be less than in other areas of the trial zone for other vessel types.

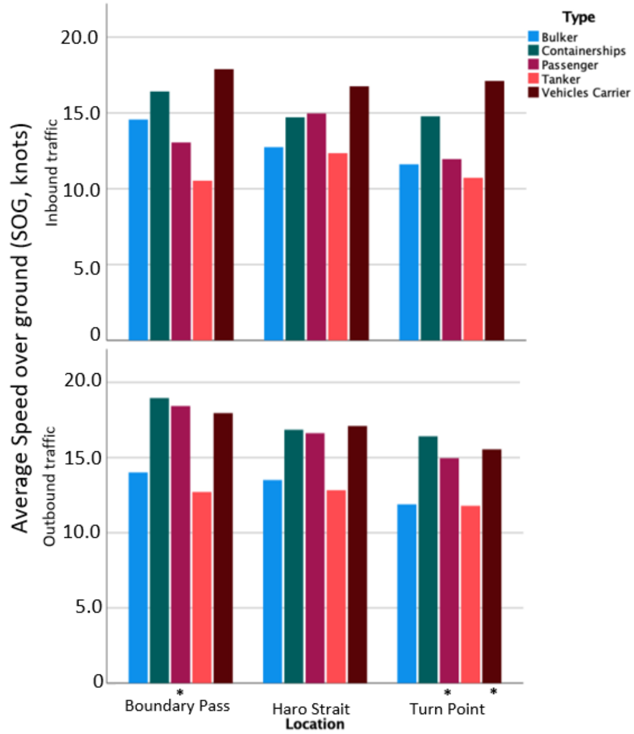

Figure 2: Comparison of SOG for each vessel type as they pass each of the moorings for inbound and outbound transits. Significantly different values between inbound and outbound are indicated by an asterisk on the lower x axis, established through Student t-test at the level p<0.05

Pass, and were increased at Haro Strait following the manoeuvre at Turn Point, but did not match speeds seen prior to the turn (Figure 2).

The voluntary slowdown initiation on July 5, 2019 was evident in the AIS data for vessel transit speed. Comparing vessel speeds by type, overall SOG was reduced for transits during the trial compared to pre-trial speeds in all cases except for tankers, and significantly for all vessel types except tankers and passenger vessels (Table 1). The average speed of all vessels through the area was reduced by 1.4 knots, with the greatest change from outbound transits (pre-trial $\bar{x}$ = 16.5 ± 2.9, trial $\bar{x}$ =13.9 ± 2.0), whereas the change in inbound transits on average was 0.7 knots, with less variation in speed during the trial (pre-trial $\bar{x}$ = 14.0 ± 4.0, trial $\bar{x}$ =13.3 ± 2.1). Comparing each vessel type at each location by direction of travel showed most reduction in both SOG and broadband (10 Hz to 100 kHz) underwater sound levels from vehicle carriers transiting inbound (Table 1).

The requested speeds are specified in SOG, however we also examined the change in STW. Significant changes in STW were only seen for inbound bulkers (t(8)=-3.894, p=0.005) and outbound containerships (t(12.485)=-4.965, p<0.001) between the pre-trial and trial passage average speeds. An average reduction in speed of more than 2 kts for bulkers and containerships were seen to meet the slowdown requirements [17, 21]. Vessel speeds may have been reduced through the Haro Strait-Boundary Pass slowdown area (Figure 1) for the turning/manoeuvring needed, and so the

Table 1: Difference in SOG and broadband underwater sound levels from before to during the slow down trial. The average change of SOG (SOG diff.) and SPL (SPL diff.) is shown. Significant changes are indicated with an asterisk (*) established through a Student T-test at p<0.05. BP= Boundary Pass, TP= Turn Point and HS= Haro Strait.

Vessel	SOG diff. (kts)	SPL diff. . (dB)
Bulker	-2.04 *	-2.96
BP- In	-	-
BP-Out	-	-
TP- In	-	-
TP-Out	-0.72	-0.24
HS-In	-4.39	-4.39
HS-Out	-0.63	+1.64
Tanker	+0.46	-4.41 *
BP- In	-	-
BP-Out	-	-
TP- In	+1.19	-1.98
TP-Out	-0.32	+0.42
HS-In	+1.96	-2.99
HS-Out	+0.01	-6.55 *
Container	-2.19 *	-2.0
BP- In	-	-
BP-Out	-	-
TP- In	-2.68	-1.84
TP-Out	-1.86	-2.55
HS-In	-0.78	-1.51
HS-Out	-2.31	+1.65
Vehicle	-2.41 *	-7.92 *
BP- In	-	-
BP-Out	-	-
TP- In	-2.84 *	-9.99 *
TP-Out	-0.37	-5.37
HS-In	-4.08 *	-7.11 *
HS-Out	-1.83	-6.10 *
Passenger	-0.73	-2.39
BP- In	-	-
BP-Out	-	-
TP- In	+0.26	+1.50
TP-Out	-2.49 *	-4.57
HS-In	+0.64	+2.41
HS-Out	-3.29 *	-9.47 *

Vessels on average passed the moorings at a distance of 1.4 km. Typically, the distance at CPA was less for vessels transiting outbound from Boundary Pass to Juan de Fuca Strait than for inbound vessels (Figure 3). At this location the recorder was placed more towards the outbound lane (Figure 1). The difference between the centroid of the CPA locations for in- and outbound vessels locations was greatest here at 579 m.The difference between the inbound and outbound CPA distances were significantly reduced on average for each of the vessel classes when passing the Boundary Pass mooring, and for tankers, containerships, vehicle carriers and passenger vessels transiting Turn Point (Figure 3). The distance to the inbound centroids of vessel CPA locations was 445 m greater than the outbound at Turn Point. The mooring was located to the west of both the out and inbound transits (Figure 1). Differences in the CPA distances were not found to be significant at Haro Strait (Figure 3). The difference between the centroids of CPA vessel locations were the least here, with inbound traffic transiting 118 m closer to the mooring than outbound vessels. The mooring is located midway between both transit lanes (Figure 1). Vessel passages were generally closest to the Boundary Pass mooring (Figure 3), which was situated under the outbound shipping lane. However, a significant (t(82.112)=9.891, $p<0.001$) increase in CPA distance of, on average, 420 m was seen at Turn Point when comparing inbound to outbound transits during turning manoeuvres.

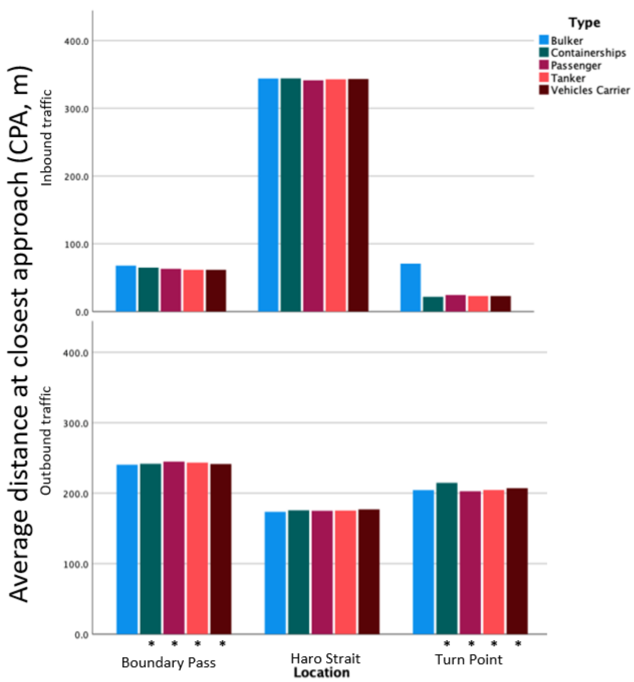

Figure 3: Comparison of distance from the mooring at closest point of approach (CPA) for each vessel type for inbound and outbound transits. Significantly different values are indicated by an asterisk on the lower x-axis, established by a Student T-test at $p<0.005$

3.2 Acoustic analysis

The estimated vessel SL were greatest during passages of containerships and bulk carriers at the Haro Strait and Boundary Pass mooring locations (Figure 4). This suggests they are the principal anthropogenic noise sources at these locations, in line with previous research which noted each passage can elevate the ambient sound levels up to 20 dB per transit [9, 12, 20].

The SL obtained from the measured SPLs were also in line with previous reporting [9, 24]. SL of outbound vessels showed elevated underwater noise levels in the broadband

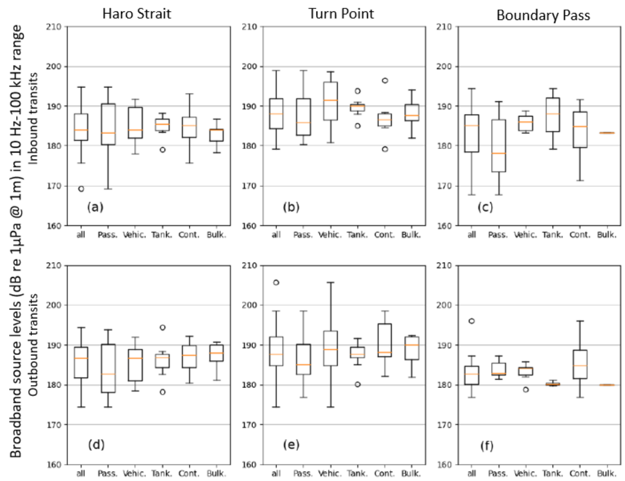

Figure 4: Estimated broadband SL (10-100,000 Hz) during the passage of each vessel type, mooring location and direction of travel.

frequency range (10-100,000 Hz) compared to inbound vessels (Figure 4). This is consistent with the differences in speed, where the higher outbound transit speeds would be expected to result in greater acoustic additions. The recordings at Boundary Pass and Turn Point showed this difference in SL to also be significant in the frequencies used to represent vessel noise (Table A-1 in Appendix).

Overall, the SL (10-100,000 Hz) were greater at Turn Point when the vessels were slowing and preparing to turn, or while manoeuvring. Comparing median SL by vessel type between the three locations showed an approximate 3 dB difference between Turn Point and Haro Strait, and 5 dB difference between Turn Point and Boundary Pass for all vessel passages (Figure 4). Aggregating all vessel data, median SL (10-100,000 Hz) at Haro Strait with vessels passing was 185 dB re 1 µPa @ 1 m, while at Boundary Pass it was 183 dB re 1 µPa @ 1m and at Turn Point it was 188 dB re 1 µPa @ 1 m. The differences between inbound vessels and outbound vessels were minimal in both median and inter-quartile SL despite there being a difference in average speed of 1.4 kts (Figure 2, Tables 1-2). The difference was more pronounced when considering the passage of vessels by type at each location in the vessel related metrics. In this case, the median low-frequency vessel metrics (10-100 Hz, 100-1000 Hz) were most elevated at Boundary Pass, and least at Turn Point.

A comparison between day and night measured SPL, to determine the potential influence of smaller non-commercial vessels on the soundscape showed no significant differences between periods, suggesting that these smaller vessels were not adding notably to sound levels for the 1-minute time periods used for this analysis in the broadband and lower-frequency vessel metrics.

The measured SPL and derived SL for the high-frequency component of the vessel noise centered at 50 kHz, were greatest at Turn Point compared to Boundary Pass and Haro Strait. This suggests that manoeuvring could elevate the vessel noise emissions throughout the frequency range (49.5-50.5 kHz) considered here. Higher outbound speeds increased the SL of the vessels per transit (Figure 5).

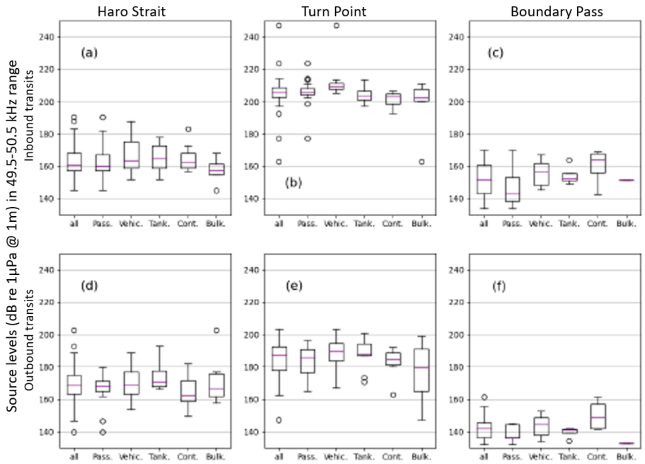

Figure 5: SL (49.5 – 50.5 kHz) by vessel class, mooring location and direction of travel. Median SL was determined to be 172 dB re 1 µPa @ 1m.

The linear regression (F(3,491)=71.845, p<0.001) of all vessels found that the directional change, speed, and distance between a vessel and a mooring, significantly influenced the received sound levels.

Travel speed through water influenced the SL most highly (coefficient 0.750, p<0.001). Significant negative coefficients between COG, and distance from the mooring (COG coefficient: -0.005, p=0.020; CPA coefficient: -0.003, p<0.001) were also found. The significance of the influence of speed on vessel noise emissions was consistently seen when vessel type and direction of travel were considered (Tables A2-6 in Appendix). Considered by vessel type, STW and CPA were seen to be the most influential variable to the broadband sound levels, with course direction also significant for bulkers (Table A-2 in Appendix). Distance from the mooring was not significant for container ships and tankers (Table A-3, A-6 in Appendix), which are the vessel types with the greatest passage rate in this area [9].

3.3 Marine Mammal Impacts

Elevated broadband underwater sound levels have potential to cause behavioural modification and increase physiological stress levels in cetaceans [e.g., 25], increases were seen in species-specific frequency ranges. Increases were seen in the mid- to high-frequency band of 500 Hz to 15 kHz during vessel transits. These increases could be impactful for SRKW and other whale species, such as humpback whales that are also frequently seen in the Salish Sea. Also, sound level increases were found to correlate with the number of vessel transits (500-15000 Hz, Boundary Pass: r_s=0.451, p<0.001, Haro Strait: r_s=0.407, p<0.001; 15-100 kHz Boundary Pass r_s=403, p<0.001, Haro Strait r_s=0.301, p<0.001). Inbound traffic showed the strongest correlation coefficient, albeit mild, to 1000-10000 Hz (rs=0.463, p=0.001), while outbound transits were most strongly correlated to 500-15000 Hz (r_s=0.326, p=0.04). Higher frequency additions were correlated with speed in Haro Strait, in frequency ranges above 15000 Hz for inbound transits (1500-10000 Hz, r_s=0.694, p<0.001), whereas outbound transits were most strongly correlated with 10-100 Hz (r_s=0.398, p=0.010). Short transmission distances were highlighted when high frequency SL were correlated with CPA distances. High-frequency signals are absorbed more rapidly than those in lower frequencies; this was demonstrated in the significant negative correlations found between the distance from the mooring (CPA) and SL in the 49.5-50.5 kHz band (Boundary Pass r_s=-0.710, p<0.001; Turn Point r_s=-0.287, p=0.06; Haro Strait r_s=-0.337, p=0.001). This, and the interpolation of the high frequency vessel SL, suggest that vessel turning and associated manoeuvres can have implication for marine mammal species in the area, elevating vessel additions to the soundscape. Also, the impact would be greater the closer the animals were to the shipping lanes.

4 Discussion

Vessel noise is the dominant anthropogenic addition to soundscapes. This analysis shows the impact that commercial vessels can have throughout a broad frequency range, including into the higher frequencies, not typically associated with these vessel types.

The Salish Sea is a high traffic area. The upper bound of our average value of passage rate is comparable to Veirs et al. ([9], 19.5 ships/day). However, Veirs et al. [9] derived this value from averaging all vessel passages noted by AIS divided by the study length in days, and not examining each day independently or limiting vessel classes, as we have done here. Veirs et al. [9] suggest that bulk carriers and containerships account for a little more than half these vessels, which does make our average rates comparable. However, averaging a total vessel count by the number of days of the study does not allow for examination of variability in passage rate, which we found to be up to 60 vessels a day at the maximum. Veirs et al. [9] also report that vessel passages in these waters can increase underwater sound levels by up to 20 dB, suggesting a substantial impact on sound fields especially on days when passage rate is high [26-29]. The impact of commercial traffic on ambient soundscape levels is a subject of ongoing work broadly [26-38], and in the Salish Sea [see e.g., 20, 26, 32].

We found the broadband underwater sound levels were at their greatest when vessels were slowed and completing manoeuvres at Turn Point. This was common to all vessel types. Indeed, the comparison of the median broadband SL at each site ranked the sites in reverse to what would be expected if one was to use speed of the vessel alone as a predictor. That is, vessels speeds were most reduced at Turn Point, but sound levels were most elevated. The highest vessel speeds were recorded at Boundary Pass, yet the recordings at this mooring showed the lowest median SL. Typically, the outbound traffic showed the most elevated underwater noise levels. This likely resulted from vessels typically running at higher speeds and having reduced distances at CPA. Noise additions in the higher frequency ranges considered mirrored the patterns seen in the broadband levels, with the greatest SL levels seen at Turn Point during vessel turns. In low frequencies (<1000 Hz) SL were greatest at Boundary Pass, perhaps reflecting vessels' increased speed. The underwater noise levels and

CPA distances from the mooring, for both in- and outbound traffic, were also the greatest at Turn Point.

This analysis represents an in-situ determination of vessel noise inputs to the soundscape, while also taking into account the behaviours of vessel operators as they transit through the Salish Sea. Distinct differences were seen between inbound and outbound traffic (Table 3, Figure 2). The increased broadband and high-frequency SL found in our measures are in agreement with the initial experimental work by Trevorrow et al. [10], where a rapid rise in noise emissions, up to 10 dB, was seen as a ship set its rudder and began to heel into the turn with the propeller speed increased to maintain consistent vessel speed through water. We confirmed a link between radiated vessel noise and ship speed, with underwater sound levels elevated in the broadband and vessel metrics frequency ranges. At Turn Point, it was also possible that acoustic signatures from propeller and machinery caused the observed increases in the higher frequency noise [10].

The addition of vessel noise to ocean soundscapes is a pressing issue for managers devising conservation actions aimed at reducing anthropogenic impact. Elevated underwater noise levels resulting from shipping reduces the effectiveness of calling for cetaceans, hindering, for example, their ability to navigate and forage. Elevated broadband noise levels can induce stress or behavioural modification [e.g., 25, 32]. Also, we found additions in more species-specific frequencies [20-22, 27, -32]. This has the potential to hinder the acoustics use of the species in social communications or echolocation signals [e.g., 30, 32]. Our data suggests that when vessels slow to turn, they add considerably more to these ranges, particularly in the frequencies used by SRKW and humpback whales for conspecific communication or social calling (500-15000 Hz), but also into echolocation frequencies of killer whales, dolphins and porpoises (15-100 kHz [27, 32]).

Operational measures implemented in this area, such as vessel slowdowns have been shown to be effective in reducing vessel noise emissions [17, 21, 33-34]. Participation rates of the slowdown trial during the study period were high, and the relationship between vessel speed and source level is well established (see [9]). The results of linear regression analysis substantiated this relationship, showing it to be formative to received sound levels. However, a reduction in speed to turn did not generate the same effect, showing that the disturbance from vessels does not decline in the same linear relationship as the one described by Veirs et al. [9] when vessels are manoeuvring. Furthermore, variables including hull shape, load, and draft, not accounted for in this analysis, also influence vessel signatures within each category. The influence of sea state or sea surface roughness [35], and multiple vessels transiting together, on manoeuvrability, and the resulting emissions, was also not considered in this study.

Detection and classification of vessels from sound signatures is one means to monitor maritime traffic. However, databases [3, 29, 35-38] are still in their infancy, and principally developed under controlled conditions. However, measured levels have shown up to a 20 dB difference in vessel noise emissions depending on the class of vessel [3, 28], predominantly from differing cavitation. Our recordings add to this work, suggestive of the impact that larger vessels can have over a broad frequency range [also see 26, 30, 36-37], including into the higher frequencies while maneuvering. More insitu and realistic determinations of vessel noise will derive improved measures of the acoustic inputs to the sound field. This is the subject of ongoing work in the Salish Sea.

The global shipping fleet is expected to grow in both vessel number and capacity as a greater volume of material is shipped over greater distances [38-39]. In the absence of mitigation, this trend will potentially increase the maximum noise level of the fleet by a factor of 1.9, or an average of 102% in noise emissions, in the next 10 years [38]. Our results add a nuance that will help identify areas that will be most highly impacted. The consideration of change in vessel speed and direction highlighted the different components of vessel noise. Also, the proximity of vessel transits, and in particular regions of vessel turning or manoeuvring near to areas of importance to threatened species may also need to be considered, given the results seen in the difference in SPL when CPA to the mooring was reduced. Haro Strait, for example, is an area where SRKW have been frequently sighted foraging, and so increased noise in that areas could lessen their ability to find or capture prey through acoustic masking effects [32, 40]. Greater high frequency components of noise, perhaps from generators, engines and blade harmonics, add to propeller cavitation when manoeuvring to elevate SPL. Adding more detail to how vessel-derived noise changes throughout its transit will create for more spatially explicit estimates of sound field levels of ocean regions. Mitigation measures such as re-routing vessels, or the design and designation of protected areas should look to how vessel signatures vary throughout their transit to maximise their efficacy.

5 Conclusion

This work adds to observations of received vessel noise from commercial vessels quantified in controlled settings, which can be used to refine vessel noise models. The impacts of human-use on marine wildlife are increasingly realised, and mitigation measures are considered for noise in high vessel traffic areas, this will have implications for shipping lane design or redesignation, or marine protected area design. Difference in vessel types and travel direction was considered for the potential for acoustic disturbance. Our results suggest the focus of these measures should be on outbound container ships and bulk carriers if the application of measures were more limited. Additions to broadband ambient noise may instigate stress responses or modification to swimming/diving patterns, and ultimately area abandonment. The consideration of more species-specific frequencies allows us to estimate the potential interference the vessel noise additions could have in the use of communication calls or echolocation signals of the species present in the Salish Sea, through masking, and start to quantify the potential impact of vessel noise even in the absence of observable behavioural changes.

Acknowledgments

The officers and crew on CCGS VECTOR for all their help with servicing our hydrophone moorings in the Salish Sea, and Caitlin O'Neill for equipment preparation and data download.

Appendix

Table A-1: Results of a Student T-test to compare sound pressures levels (SPL) for the study period before (June 1-July 5, 2019) and during (July 5-August 18, 2019) a vessel slowdown trial through Haro Strait and Boundary Pass.

DF	T-value	Sign.
Boundary		
100-1000	-5.247	<0.001
113-141	-5.771	<0.001
57-71	-4.116	<0.001
Turn Pt		
100-1000	-3.727	<0.001
113-141	-4.028	<0.001
57-71	-0.695	0.488
Haro St		
100-1000	-2.389	0.018
113-141	-1.619	0.107
57-71	0.288	0.774

Table A-2: Multivariate linear regression for bulkers considering the SL (10-100,000 Hz) resulting from changes in vessel transit direction (course over ground, COG), speed (speed through water, STW) and distance (closest point of approach, CPA). Model summary for inbound: $F(3,26) = 3.247$, $p=0.038$ and outbound $F(3,24) = 25.143$, $p<0.001$. Significant results are indicated with bold text

Variable	Coeff.	Sign.
Inbound		
COG	**-0.015**	**0.010**
STW	0.123	0.732
CPA	**-0.004**	**0.010**
Outbound		
COG	0.047	0.250
STW	**2.391**	**<0.001**
CPA	-0.001	0.640

Table A-3: Multivariate linear regression for container ships considering the SL (10-100,000 Hz) resulting from changes in vessel transit direction (course over ground, COG), speed (speed through water, STW) and distance (closest point of approach, CPA). Model summary for inbound: $F(3,33)=7.364$, $p=0.001$ and outbound $F(3,40) = 7.848$, $p<0.001$. Significant results are indicated with bold text.

Variable	Coeff.	Sign.
Inbound		
COG	0.009	0.180
STW	**1.526**	**<0.001**
CPA	-0.001	0.640
Outbound		
COG	-0.005	0.165
STW	**1.678**	**<0.001**
CPA	**-0.003**	**0.041**

Table A-4: Multivariate linear regression for passenger vessels considering the SL (10-100,000 Hz) resulting from changes in vessel transit direction (course over ground, COG), speed (speed through water, STW) and distance (closest point of approach CPA). Model summary for inbound: $F(3,142) = 26.937$, $p<0.001$ and outbound $F(3,41)=18.365$, $p<0.001$. Significant results are indicated with bold text

Variable	Coeff.	Sign.
Inbound		
COG	-0.005	0.165
STW	**1.084**	**<0.001**
CPA	**-0.002**	**0.025**
Outbound		
COG	0.050	0.111
STW	**1.678**	**<0.001**
CPA	**-0.002**	**0.048**

Table A-5: Multivariate linear regression for vehicle carriers considering the SL (10-100,000 Hz) resulting from changes in vessel transit direction (course over ground, COG), speed (speed through water, STW) and distance (closest point of approach CPA). Model summary for inbound: $F(3,48) = 5.282$, $p=0.003$ and outbound $F(3,34) = 5.480$, $p=0.004$.

Variable	Coeff.	Sign.
Inbound		
COG	-0.001	0.813
STW	**1.136**	**0.003**
CPA	**-0.002**	**0.048**
Outbound		
COG	0.066	0.093
STW	-0.134	0.763
CPA	-0.003	0.075

Table A-6: Multivariate linear regression for tankers considering the SL (10-100,000 Hz) resulting from changes in vessel transit direction (course over ground, COG), speed (speed through water, STW) and distance (closest point of approach CPA). Model summary for inbound: $F(3,45)=7.303$, $p<0.001$ and outbound $F(3,22) = 5.371$, $p=0.006$.

Variable	Coeff.	Sign.
Inbound		
COG	-0.007	0.170
STW	-0.374	0.218
CPA	-0.004	<0.001
Outbound		
COG	0.034	0.349
STW	-0.227	0.576
CPA	-0.004	0.016

References

[1] Richardson WJ, Greene Jr. CR, Malme CI, Thomson D (1995) Marine Mammals and Noise. Academic Press, San Diego, CA.

[2] Hildebrand J (2009) Anthropogenic and natural sources of ambient noise in the ocean. Mar Ecol Prog Ser 395:5–20. 10.3354/meps08353.

[3] Arveson PT, Vendittis DJ (2000) Radiated noise characteristics of a modern cargo ship. J Acoust Soc Am. 107: 118.

[4] Aktas B, Atlar M, Turkmen S, Shi W, Sampson R, Korkut E, Fitzsimmons P (2016) Propeller cavitation noise investigations of a research vessel using medium size cavitation tunnel tests and full-scale trials. Ocean Engin.120: 122-135.

[5] Andrew RK, Howe BM, Mercer JA, Dzieciuch MA (2002) Ocean ambient sound: comparing the 1960s with the 1990s for a receiver off the California coast. Acoust Res Let Online 2002; 3(2):65-70

[6] National Research Council, NRC. Ocean Noise and Marine Mammals. Washington, DC: The National Academies Press 2003; doi:10.17226/10564

[7] Ross D (2005) Ship sources of ambient noise. IEEE J Ocean Engin.30 (2): 257-261. https://doi.org/10.1109/JOE.2005.850879

[8] McDonald MA, Hildebrand JA, Wiggins SM (2006) Increases in deep ocean ambient noise in the Northeast Pacific west of San Nicolas Island, California. J Acoust Soc Am 2006; 120(2), 711-718.

[9] Veirs S, Veirs V, Wood J (2016) Ship noise in an urban estuary extends to frequencies used for echolocation by endangered killer whales. PeerJ PrePrints. 1–36.

[10] Trevorrow MV, Vasiliev B, Vagle S (2008) Directionality and maneuvering effects on a surface ship underwater acoustic signature. J Acoust Soc Am. 124: 767–778.

[11] Wladichuk J, Hannay D, MacGillivray A, Li Z, Thornton S (2018) Systematic source level measurements of whale watching vessels and other small boats. J Ocean Tech. 14(3):110-126.

[12] MacGillivray AO, Li Z, Hannay DE, Trounce KB, Robinson O (2019) Slowing deep-sea commercial vessels reduces underwater radiated noise. J Acoust Soc Am. 146: 340-351.doi: 10.1121/1.5116140

[13] Olson JK, Wood J, Osborne RW, Barrett-Lennard L, Larson S (2018) Sightings of southern resident killer whales in the Salish Sea 1976−2014: the importance of a long-term opportunistic dataset. Endang Species Res 37:105-118. DOI: 10.3354/esr00918.

[14] Department of Fisheries and Oceans Canada, DFO (2021). Identification of areas for mitigation of vessel-related threats to survival and recovery for Southern Resident Killer Whales. DFO Can. Advis. Sec. Sci. Advis. Re. 2021/025.

[15] Baird RW (2003) Update COSEWIC status report on harbour porpoise (*Phocoena phocoena*) in British Columbia. Committee on the Status of Endangered Wildlife in Can.

[16] Dalla Rosa L, Ford JKB, Trites AW (2003) Distribution and relative abundance of humpback whales in relation to environmental variables in coastal British Columbia and adjacent waters. Cont Shelf Res 2012; 36:89-104.

[17] Burnham RE, Vagle S, O'Neill C, Trounce K (2021) The Efficacy of Management Measures to Reduce Vessel Noise in Critical Habitat of Southern Resident Killer Whales in the Salish Sea. Front. Mar. Sci. 8:664691. doi: 10.3389/fmars.2021.664691

[18] Merchant ND, Fristrup KM, Johnson MP, Tyack PL, Witt MJ, Blondel P, Parks S (2015) Measuring acoustic habitats. Method Ecol Evol. 6: 257–265, doi: 10.1111/2041-210X.12330

[19] Merchant ND, Witt MJ, Blondel P, Godley BJ, Smith GH (2012) Assessing sound exposure from shipping in coastal waters using a single hydrophone and Automatic Identification System (AIS) data. Mar Poll Bull. 64: 132-1329.

[20] Burnham RE, Vagle S, O'Neill C (2021b) Spatiotemporal patterns in the natural and anthropogenic additions to the soundscape in parts of the Salish Sea, British Columbia, 2018-2020. Mar Poll Bull. 170, 112647. doi: 10.1016/j.marpolbul.2021.112647

[21] Joy R, Tollit D, Wood J, MacGillivray A, Li Z, Trounce K, et al. (2019) Potential benefits of vessel slowdowns on endangered southern resident killer whales. Front Mar Sci. 6:344. doi: 10.3389/fmars.2019.00344

[22] Au WWL, Ford JKB, Horne JK, Allman KAN (2004) Echolocation signals of free- ranging killer whales (*Orcinus orca*) and modeling of foraging for chinook salmon (*Oncorhynchus tshawytscha*). J Acoust Soc Am. 115: 901–909. doi: 10.1121/1.1642628

[23] Hannah CG, Dupont F, Collins AK, Dunphy M, Greenberg D (2008) Revisions to a Modelling System for Tides in the Canadian Arctic Archipelago. Can. Tech. Rep. Hydrogr. Ocean Sci. 259: 6–62.

[24] Francois R, Garrison G (1982) Sound absorption based on ocean measurements. Part II: Boric acid contribution and equation for total absorption. J Acoust Soc Am. 72(6): 1879-1890

[25] Erbe C, MacGillivray A, Williams R (2012) Mapping cumulative noise from shipping to inform marine spatial planning. J Acoust Soc Am. 132: EL423–EL428.

[26] Rolland RM, Parks SE, Hunt KE, Castellote M, Corkeron PJ, Nowacek DP, Wasser SK, Kraus SD (2012) Evidence that ship noise increases stress in right whales. Proceedings of the Royal Society B: Biological Sciences 279(1737): 2363-2368.

[27] Heise KA, Barrett-Lennard LG, Chapman NR, Dakin DT, Erbe C, Hannay DE, Merchant ND, Pilkington JS, Thornton SJ, Tollit DJ, Vagle S, Veirs VR, Vergara V, Wood JD, Wright BM, Yurk H (2017) Proposed Metrics for the Management of Underwater Noise for Southern Resident Killer Whales. Coastal Ocean Report Series (2), Ocean Wise, Vancouver, 30pp.

[28] Wales SC, Heitmeyer RM (2002) An ensemble source spectra model for merchant ship-radiated noise J Acoust Soc Am. 111:1211-1231.

[29] McKenna MF, Ross D, Wiggins S, Hildebrand JA (2012) Underwater radiated noise from modern commercial ships J Acoust Soc Am. 131(1): 92-103.

[30] Hatch LT, Fristrup KM (2009) No barrier at the boundaries: implementing regional frameworks for noise management in protected natural areas. Mar Ecol Prog Ser. 395, 223–244. doi: 10.3354/meps07945

[31] Williams R, Erbe C, Ashe E, Clark CW (2015) Quiet(er) marine protected areas Mar Poll Bull. 10(1), 154-161.

[32] Burnham RE, Vagle S, Thupaki P, Thornton SJ (2023) Implications of wind and vessel noise on the sound fields experienced by southern resident killer whales *Orcinus orca* in the Salish Sea. Endang Species Res. 50: 31-46. https://www.int-res.com/prepress/n01217.html

[33] Vagle S, Neves M (2019) Evaluation of the effects on underwater noise levels from shifting vessel traffic away from Southern Resident Killer Whale foraging areas in the Strait of Juan de Fuca in 2018. Can Tech Rep Hydrogr Ocean Sci. 329: vi + 64 p.

[34] Vagle, S (2020) Evaluation of the efficacy of the Juan de Fuca lateral displacement trial and Swiftsure Bank plus Swanson Channel interim sanctuary zones, 2019. Can Tech Rep Hydrogr Ocean Sci. 332: vi + 60 p

[35] Gaggero T, Traverso F (2017) On the possibility of estimating parameters using acoustical Lloyds mirror effect. 24th International Congress on Sound and Vibration, ICSV London 2017.

[36] Santos-Domínguez D, Torres-Guijarro S, Cardenal-López A, Pena-Gimenez A (2016) ShipsEar: An underwater vessel noise database. Applied Acoust. 113: 64-69.

[37] Wales SC, Heitmeyer RM (2002) An ensemble source spectra model for merchant ship-radiated noise J Acoust Soc Am. 111:1211-1231.

[38] Kaplan MB, Soloman S (2016) A coming boom in commercial shipping? The potential for rapid growth of noise from commercial ships by 2030. Mar Pol. 73:119-121

[39] Lloyds Register Group, Global Marine Trends 2030, 2013.

[40] Sato M, Trites AW, Gautier S (2021) Southern resident killer whales encounter higher prey densities than northern resident killer whales during the summer. Canada J Fish Aquat Sci. 78(11). https://doi.org/10.1139/cjfas-2020-0445


Getting it right
has never been
so predictable.
DataKustik

Remembering Ken Barron
A Pioneer of Acoustics in Canada

In December 2022, Ken Barron passed away. He was 89. Through his design work, entrepreneurial vision, and technical innovations, Ken was a pioneer of acoustics in Canada. Notably, alongside Bob Strachan, Ken co-founded Western Canada's first acoustical consultancy, Barron and Strachan, Consulting Engineers in Acoustics, in 1966.

During his 40-year career, Ken worked with and inspired many fellow acousticians, some of whom went on to found their own firms across Canada and the United States. Ken leaves an enduring legacy, one that finds its beginnings at a spare desk in an accountant's office in Vancouver.

The Early Days of Canadian Acoustics

In the 1960s, while working for Hoyles Niblock, a telecommunications consulting firm, Ken and Bob began providing acoustical advice on radio control rooms, schools, and universities, on top of their regular telecommunications design and field work. Within a couple of years, they compiled a library of acoustical texts and a collection of instrumentation for measuring and analyzing noise and vibration.

Word spread about the two acoustical practitioners at Hoyles Niblock, and calls came in from a variety of potential clients, including Dino's Pizza, whose neighbours had complained about Dino's noisy ovens. With his Leo Beranek texts by his side, Ken designed a muffler for the ovens and helped appease the parlour's neighbours.

Hoyles Niblock wanted to send Ken and Bob overseas for telecommunications projects, yet the pair were starting families and preferred to work closer to home. Meanwhile, architects Thompson Berwick and Pratt asked Hoyles Niblock to provide acoustical advice on the UBC Health Sciences Centre. It was the perfect job for Ken and Bob.

Bob's wife, Cheryl, suggested they buy the acoustical practice. In 1966, Barron and Strachan was born, and Canada had its first independent acoustical consulting firm. Ken and Bob paid $10,000 to Hoyles Niblock over 10 years, interest free. They got the library, instruments, and their first project—the UBC Health Sciences Building. They set up shop in a spare room at their accountant's office, before moving to Heather Street in Vancouver in 1967.

In addition to the UBC Health Sciences Building, Barron and Strachan's early projects included the award-winning Westcoast Transmission Building; a noise survey of the Greater Vancouver Regional District, which informed the development of noise bylaw limits in the surrounding municipalities; and a residential building noise control project that would shape how municipalities in Greater Vancouver addressed the potential effects of noise on proposed developments.

Ken worked with the noise control departments at both the City of Burnaby and City of Vancouver and encouraged them to adopt North American community noise standards. The two municipalities were among the first in Western Canada to include noise control criteria in their residential development bylaws, which governed new residential construction exposed to noise from road and rail traffic, airports, and industry.

Barron and Strachan also advised on office acoustics, and were featured in an article in the July 1968 issue of Office Equipment and Methods about finding the right level of noise at offices to promote health, privacy, and productivity.

In the early 1970s, Barron and Strachan bought a Digital Equipment Corporation PDP8, making them one of the first engineering firms in Vancouver to have an in-house computer. They built analog-to-digital boards to connect their Hewlett-Packard one-third octave band filter set to the PDP8 and Bob wrote machine code to create a real-time analyzer that calculated reverberation time, equivalent sound levels, one-third octave band levels, and exceedance levels.

While Bob left the firm in 1975 for post-graduate acoustical studies with Tom Siddon at UBC, Ken continued as the sole principal. In 1988, he merged with Doug Kennedy and Dan Lyzun to form what is today BKL Consultants Ltd.

An Ear for Performance Spaces

Throughout his career, Ken contributed to the design of notable performance spaces in Western Canada. His portfolio included multi-purpose spaces like Unchagah Hall in Dawson Creek, which was acclaimed by the Victoria Symphony, and the Winnipeg Concert Hall.

In 1973 he investigated the acoustics at the Orpheum Theatre in Vancouver and joined the design team that restored the venue, which is now a popular spot for concerts and home to the Vancouver Symphony Orchestra.

Ken and BKL designed new acoustical reflectors for the Queen Elizabeth Theatre, and was commended by the Vice President of the Vancouver Bach Choir in 1990, after the choir performed Gustav Mahler's Symphony No. 8, which

included 650 musicians. The Vancouver Sun's (Michael Scott's) review of the performance said it was "an evening of music to treasure for many years to come."

Acoustical Influence

Ken supported the development of numerous technical innovations for the acoustical consulting industry using in-house staff and resources, such as Doug Whicker and David Brown's DUCTs mechanical and system noise prediction software, Marcel Rivard and Gordon Hall's portable noise source capable of testing STC 60 partitions (later licensed to Tracoustics as the NS-100) and Sound Beam acoustic flashlight for aligning theatre panels, and John Walsh's (with UBC's Norman Dadoun) Godot room acoustics modelling software, a precursor to modern ray-tracing room acoustics software.

During the 1980s, Ken presented on acoustical measurements at UBC's School of Architecture, demonstra-ting techniques and equipment for students taking professor Chuck Tiers's Architectural Acoustics course. Ken presented in class, welcomed students at his office on field trips, and even loaned out his equipment for student projects.

In 1985, Ken partnered with Transport Canada (J Bertok) to publish a paper in the Canadian Geotechnical Journal (National Research Council Canada) on vibration isolation of building foundations, detailing tests comparing different foundation types for the extension of the Area Control Centre at YVR considering the sensitive electronic equipment inside.

Throughout his career, Ken worked with and inspired many acousticians.

Dan Lyzun worked with Ken as a young acoustician right after graduation and again later, when their firms merged. He said, "Ken took a chance on a recent graduate, and it turned into a successful near 50-year career. I thank Ken for whatever it was he saw in me and for his encouragement along the way."

Michel Morin of MJM Acoustical Consultants also started his career at the firm after Leslie Doelle made the introductions. He really appreciated that Ken put faith in him to take on new responsibilities, pursue new business opportunities, and develop innovative solutions, despite challenging circumstances like the early 1980s economy crash and 20% interest rates.

Doug Kennedy described how Ken helped make the merger between their firms a success.

"It soon became apparent that Ken would be an excellent business partner," Doug said. "He was very knowledgeable on both technical and management issues and always receptive to discussing new ideas."

BKL and the Legacy of Ken Barron

We thank Ken and Bob for laying the foundation for our firm all those decades ago. As we celebrate Ken's life, we also look ahead and continue to build on his legacy of hard work and passion for acoustics, to a time when acoustics is embraced in all the places we live, work, and play in.

Personal Details

Ken Barron was born in Trail, BC, and grew up there with his family. He graduated with a bachelor of applied science in electrical engineering from UBC in 1956. Before founding Barron and Strachan, Ken worked for Hoyles, Niblock and Associates, operating their acoustical division; Northern Electric Co.; and BC Telephone Company.

Ken was a Professional Engineer licensed to practice in BC, Alberta, Saskatchewan, Manitoba, and Yukon. He was a founding director of Consulting Engineers of British Columbia and a member of the National Council of Acoustical Consultants, the Acoustical Society of America, the Canadian Acoustical Association, the Institute of Noise Control Engineering, and the Association of Consulting Engineers of Canada.

Ken retired in 1997 and moved to Penticton where he enjoyed golf, gardening, cross-country skiing, and Astronomy. In 1999 he met his second wife, Peggy. (Barbara had passed away in 1996)

From the Acoustical Consulting Industry

From all of us at BKL, other firms, or retired, we express our condolences to Ken's family and loved ones. He will be missed.

Thank you to Mark Bliss, David Brown, Doug Kennedy, Dan Lyzun, Michel Morin, Bob Strachan, and Doug Whicker for contributing to this tribute.

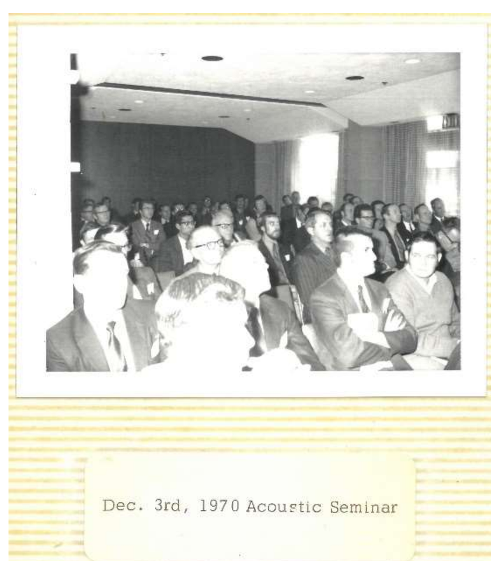

Acoustics Week in Canada

Montréal, Québec, October 3-6, 2023

The **Acoustics Week in Canada will be held from October 3-6, 2023** in downtown Montreal, Quebec. You are invited to be part of this three days conference featuring the latest developments in Canadian acoustics and vibration. The keynote talks and technical sessions will be framed by a welcome reception, conference banquet, ASTM Building Acoustics Standards Committee meeting, technical tour and an exhibition of products and services relating to the field of acoustics and vibration.

Montréal's congress center

Take a few days before or after the conference to enjoy the area! Quebec is famous for its fall colors, when trees all over the place turn bright shades of red, orange, and yellow before losing their leaves. It's an annual spectacle that draws tourists from around the world and remains impressive even to those of us who see it every year! Montreal still has important events to offer at this time of year such as the OFF Jazz Festival and the Festival du nouveau cinema.

Venue and Accommodation

The conference will be held at the Plaza in downtown Montreal (https://plazapmg.com/plaza-centre-ville/). A block of rooms is available at the Bonaventure hotel which is 5-minute walk from the conference center. A special conference rate will be offered for reservations made under "AWC2023 conference" codename. Extend your stay and enjoy the local area at the same special rate. Please refer to the conference website for further registration details: https://awc.caa-aca.ca

Jacques Cartier's Bridge

Montréal Downtown

Plenary, technical sessions.

Plenary, technical, and workshop sessions are planned throughout the conference. Each day will begin with a keynote talk of broader interest and relevance to the acoustics community. Technical sessions are planned to cover all areas of acoustics including:

ACOUSTICAL MATERIALS AND METAMATERIALS / AEROACOUSTICS / ARCHITECTURAL AND BUILDING ACOUSTICS/ ARTIFICIAL INTELLIGENCE IN ACOUSTICS / BIO-ACOUSTICS AND BIOMEDICAL ACOUSTICS / MUSICAL ACOUSTICS / NOISE AND NOISE CONTROL / PHYSICAL ACOUSTICS / PSYCHO- AND PHYSIO-ACOUSTICS / SHOCK AND VIBRATION / SIGNAL PROCESSING / SPEECH SCIENCES AND HEARING SCIENCES / STANDARDS AND GUIDELINES IN ACOUSTICS / ULTRASONICS / UNDERWATER ACOUSTICS

If you would like to organize a session on a specific topic please contact the Technical Chair as soon as possible.

Abstracts

Abstract for technical papers are due before June 15, 2023 through the conference web site. **Two-page summaries for publication in the proceedings are due July 15, 2023**.

Exhibition and sponsorship.

The conference offers opportunities for suppliers of products and services to engage the acoustic community through exhibition and sponsorship.

The tabletop exhibition facilitates in-person and hands-on interaction between suppliers and interested individuals. Companies and organizations that are interested in participating in the exhibition should contact the Exhibition and Sponsorship coordinator for an information package. Exhibitors are encouraged to book early for best selection.

The conference will be offering sponsorship opportunities of various conference features. In addition to the diamond, gold and silver levels, selected technical sessions, social events and coffee breaks will be available for sponsorship. Sponsors can have their logo placed on the conference web site within 10 days of their sponsorship. Additional features and benefits of sponsorship can be obtained from the Exhibition and Sponsorship coordinator or the conference web site.

Students.

Students are strongly encouraged to participate. Students presenting papers will be eligible for one of three $500 prizes to be awarded. Conference bursaries will also be available to those students whose papers are accepted for presentation (see conditions on the conference web site).

Registration details.

Please refer to the conference web site: https://awc.caa-aca.ca

Contacts.

Conference Chair:

Olivier Doutres (ÉTS)
(conference@caa-aca.ca)

Technical Chair:

Thomas Padois (IRSST)
(technical-chair@caa-aca.ca)

Exhibits and Sponsorship coordinator:

Julien Biboud (MÉCANUM)
(awc2023exhibitors@caa-aca.ca)

Semaine Canadienne de l'Acoustique

Montréal, Québec, 3-6 Octobre 2023

La Semaine Canadienne de l'acoustique aura lieu du 3 au 6 octobre 2023 au centre-ville de Montréal, au Québec. Vous êtes invités à assister à cette conférence de trois jours durant laquelle les derniers développements en matière d'acoustique et de vibration au Canada seront présentés. Chaque journée débutera par une conférence plénière qui sera suivie de sessions thématiques. Vous pourrez échanger lors de la réception de bienvenue et du banquet. Une réunion du comité des normes d'acoustique du bâtiment de l'ASTM sera également organisée ainsi qu'une visite technique et une exposition de produits et services liés à l'acoustique et à la vibration.

Palais des congrès de Montréal

Prenez quelques jours avant ou après la conférence pour profiter de la région! Le Québec est célèbre pour ses couleurs d'automne, lorsque les arbres prennent des teintes vives de rouge, d'orange et de jaune avant de perdre leurs feuilles. C'est un spectacle annuel qui attire des touristes du monde entier et qui reste impressionnant même pour ceux d'entre nous qui le voient chaque année ! Montréal garde aussi quelques évènements de marque à cette période de l'année comme l'OFF Festival de Jazz et le Festival du nouveau cinéma.

Lieu et hébergement

La conférence se déroulera au Plaza dans le centre-ville de Montréal (https://plazapmg.com/plaza-centre-ville/). Des chambres seront disponibles à l'hôtel Bonaventure, à 5 minutes à pied du centre de conférence, avec un tarif spécial pour les réservations faites sous le nom "AWC2023 conference". Prolonger votre séjour à l'hôtel au même tarif afin de profiter du centre-ville et de la région. Veuillez consulter le site web de la conférence pour plus d'informations sur l'inscription : https://awc.caa-aca.ca

Pont Jacques Cartier

Centre ville de Montréal

Sessions plénières et techniques

Des sessions plénières, techniques et des ateliers sont prévues tout au long de la conférence. Chaque journée débutera par une conférence plénière d'intérêt pour la communauté de l'acoustique. Des sessions techniques sont également prévues pour couvrir tous les domaines de l'acoustique :

AÉROACOUSTIQUE / ACOUSTIQUE DU BÂTIMENT ET ARCHITECTURALE / ACOUSTIQUE BIOMÉDICALE / ACOUSTIQUE MUSICALE/ ACOUSTIQUE PHYSIQUE / ACOUSTIQUE SOUS-MARINE / AUDIOLOGIE / BIOACOUSTIQUE / BRUIT ET CONTRÔLE DU BRUIT / CHOCS ET VIBRATIONS / INTELLIGENCE ARTIFICIELLE EN ACOUSTIQUE / LINGUISTIQUE / MATÉRIAUX ET MÉTAMATÉRIAUX ACOUSTIQUES / NORMES EN ACOUSTIQUE / PSYCHOACOUSTIQUE / TRAITEMENT DU SIGNAL / ULTRASONS

Si vous désirez organiser une session sur un sujet précis, veuillez communiquer avec le président technique le plus tôt possible.

Résumés

Les **résumés des articles doivent être soumis au plus tard le 15 juin 2023** sur le site Web de la conférence. **Les articles de deux pages, à soumettre le 15 juillet 2023**, seront publiés dans les actes de la conférence.

Exposition et parrainage

La conférence offre aux entreprises fournissant des produits et des services la possibilité de s'engager auprès de la communauté acoustique par le biais d'expositions et de parrainages.

L'exposition des produits et services facilite l'interaction entre les vendeurs et les personnes intéressées. Les entreprises et les organisations souhaitant participer à l'exposition doivent contacter le coordinateur de l'exposition et du parrainage pour obtenir de plus amples informations. Les exposants sont encouragés à réserver le plus tôt possible pour bénéficier des meilleures places.

La conférence offrira des possibilités de parrainage. En plus des niveaux diamant, or et argent, certaines sessions techniques, événements sociaux et pauses café pourront être sponsorisées. Les sponsors peuvent ajouter leur logo sur le site web de la conférence dans les 10 jours suivant leur parrainage. D'autres informations et avantages du parrainage peuvent être obtenus auprès du coordinateur des expositions et du parrainage ou sur le site web de la conférence.

Étudiant·e·s

Les étudiant·e·s sont vivement encouragé·e·s à participer à la conférence. Les étudiant·e·s présentant un article seront éligibles pour obtenir un des trois prix de $500 à décerner. Des bourses de participation seront également offertes aux étudiant·e·s dont les communications sont acceptées pour présentation (voir conditions sur le site de la conférence).

Inscription

Pour plus d'informations sur l'inscription, veuillez consulter le site Web de la conférence. https://awc.caa-aca.ca

Contacts.

Président de la conférence:

Olivier Doutres (ÉTS)
(conference@caa-aca.ca)

Président technique:

Thomas Padois (IRSST)
(technical-chair@caa-aca.ca)

Coordonnateur des expositions et du parrainage:

Julien Biboud (MÉCANUM)
(awc2023exhibitors@caa-aca.ca)

PRIZE ANNOUNCEMENT • ANNONCE DE PRIX

CANADIAN ACOUSTICAL ASSOCIATION
ASSOCIATION CANADIENNE D'ACOUSTIQUE

Prize

EDGAR AND MILLICENT SHAW POSTDOCTORAL PRIZE IN ACOUSTICS
ALEXANDER G. BELL GRADUATE STUDENT PRIZE IN SPEECH COMMUNICATION AND HEARING
ECKEL GRADUATE STUDENT PRIZE IN NOISE CONTROL
FESSENDEN GRADUATE STUDENT PRIZE IN UNDERWATER ACOUSTICS
RAYMOND HÉTU UNDERGRADUATE STUDENT PRIZE IN ACOUSTICS
THOMAS D. NORTHWOOD GRADUATE STUDENT PRIZE IN ARCHITECTURAL AND ROOM ACOUSTICS
ALBERT S. BREGMAN GRADUATE STUDENT PRIZE IN PSYCHOLOGICAL ACOUSTICS

Prix

PRIX POST-DOCTORAL EDGAR ET MILLICENT SHAW EN ACOUSTIQUE
PRIX ETUDIANT ALEXANDER G. BELL EN COMMUNICATION ORALE ET AUDITION (2E OU 3E CYCLE)
PRIX ETUDIANT ECKEL EN CONTROLE DU BRUIT (2E OU 3E CYCLE)
PRIX ETUDIANT FESSENDEN EN ACOUSTIQUE SOUS-MARINE (2E OU 3E CYCLE)
PRIX ETUDIANT RAYMOND HETU EN ACOUSTIQUE (1ER CYCLE)
PRIX ETUDIANT THOMAS D. NORTHWOOD EN ACOUSTIQUE ARCHITECTURALE ET ACOUSTIQUE DES SALLES (2E OU 3E CYCLE)
PRIX ETUDIANT ALBERT S. BREGMAN EN PSYCHOACOUSTIQUE (2E OU 3E CYCLE)

Deadline for Applications:
June 30th 2023

Date limite de soumission des demandes:
30 juin 2023

Consult CAA website for more information
Consultez le site Internet de l'ACA pour de plus amples renseignements
(http://www.caa-aca.ca)

CANADIAN ACOUSTICS ANNOUNCEMENTS - ANNONCES TÉLÉGRAPHIQUES DE L'ACOUSTIQUE CANADIENNE

Looking for a job in Acoustics?

There are many job offers listed on the website of the Canadian Acoustical Association!

You can see them online, under http://www.caa-aca.ca/jobs/

August 5th 2015

INTER-NOISE 2023 to be held August 20-23, 2023, in Makuhari Messe (Japan)

We are very pleased to inform you that the website of INTER-NOISE 2023 has been launched. Its link is https://internoise2023.org/.

The INTER-NOISE 2023 is held at Makuhari Messe (https://www.m-messe.co.jp/en/) from August 20-23, 2023, which is sponsored by International Institute of Noise Control Engineering (I-INCE) and is co-organized by Institute of Noise Control Engineering of Japan (INCE/J), Acoustical Society of Japan (ASJ).

August 12th 2022

AWC2023 to be held in Montreal (QC) October 3-6, 2023

The Acoustics Week in Canada will be held from October 3-6, 2023 in downtown Montreal, Quebec. For more information on registration, please visit the conference website: https://awc.caa-aca.ca

Dear Members and Friends of the Canadian Acoustical Association, The Acoustics Week in Canada will be held from October 3-6, 2023 in downtown Montreal, Quebec. You are invited to be part of this three-day conference featuring the latest developments in Canadian acoustics and vibration. The conference will be held at the Plaza in downtown Montreal . A block of rooms is available at the Bonaventure Hotel which is 5-minute walk from the conference centre. Here are some important dates to remember: Abstract submission deadline: June 15, 2023 Paper submission deadline: July 15, 2023 Registration starts: June 16, 2023 Registration deadline for proceeding papers: August 1st 2023 Late registration fees start: August 15, 2023 Plenary, technical, and workshop sessions are planned throughout the conference. Each day will begin with a keynote talk of broader interest and relevance to the acoustics community. Technical sessions are planned to cover all areas of acoustics including: ACOUSTIC METAMATERIAL /AEROACOUSTICS / ARCHITECTURAL AND BUILDING ACOUSTICS / BIO-ACOUSTICS AND BIOMEDICAL ACOUSTICS / EDUCATION IN ACOUSTICS / HEARING PROTECTION DEVICES / ARTIFICIAL INTELLIGENCE IN ACOUSTICS / MUSICAL ACOUSTICS / NOISE AND NOISE CONTROL / PHYSICAL ACOUSTICS / PSYCHO- AND PHYSIO-ACOUSTICS / SHOCK AND VIBRATION / SIGNAL PROCESSING / SPEECH SCIENCES AND HEARING SCIENCES / STANDARDS AND GUIDELINES IN ACOUSTICS / ULTRASONICS / UNDERWATER ACOUSTICS / For more information on registration, please visit the conference website: https://awc.caa-aca.ca Looking forward to seeing you there, Olivier Doutres (ÉTS, conference chair, conference@caa-aca.ca), Thomas Padois (IRSST, technical chair, technical-chair@caa-aca.ca) and Julien Biboud (Mécanum, exhibits and sponsorship coordinator, awc2023exhibitors@caa-aca.ca)

April 5th 2023

AWC2023 New abstract deadline: July 1st, 2023

La date limite a été prolongée jusqu'au 1er juillet pour les résumés de 300 mots : https://awc.caa-aca.ca/index.php/AWC/index/pages/view/AWC2023_AbstractInfo The deadline has been extended until July 1st for 250 words abstracts: https://awc.caa-aca.ca/index.php/AWC/index/pages/view/AWC2023_AbstractInfo

[VERSION FRANÇAISE CI-DESSOUS] The organization of the "Acoustics Week in Canada" (AWC23) is going well. We are pleased to announce that approximately 130 abstracts have already been submitted, and we would like to express our gratitude to all who have participated thus far. Here are some important reminders and updates: For those who have not yet submitted their abstracts, we are pleased to inform you that the deadline has been extended until July 1st for 300 words abstracts. You still have time to contribute and be a part of this exciting event, via https://awc.caa-aca.ca/index.php/AWC/index/pages/view/AWC2023_AbstractInfo Once your abstract has been accepted, please ensure that your two-page article is uploaded by July 15th for inclusion in the September proceedings issue of Canadian Acoustics. It is important to note that at least one author must be registered for the conference by August 1st for the article to be published, otherwise only the abstract will be included in the proceedings issue with Canadian Acoustics journal. Please be aware that late registration fees will come into effect starting August 15th. We hope that you have a wonderful summer vacation and look forward to your active participation in AWC23. Prof. Olivier Doutres [VERSION FRANÇAISE] L'organisation de la "Semaine canadienne de l'acoustique" (AWC23) avance bien. Nous sommes heureux de vous annoncer que près de 130 résumés ont déjà été soumis, et nous tenons à exprimer notre gratitude à tous ceux qui ont participé jusqu'à présent. Voici quelques rappels et mises à jour importants : Pour ceux qui n'ont pas encore soumis leur résumé, nous avons le plaisir de vous informer que la date limite a été prolongée jusqu'au 1er juillet pour les résumés de 300 mots. Vous avez encore le temps de contribuer et de participer à cet événement passionnant, via https://awc.caa-aca.ca/index.php/AWC/index/pages/view/AWC2023_AbstractInfo Une fois que votre résumé aura été accepté, veuillez vous assurer de téléverserr votre article de deux pages d'ici le 15 juillet pour qu'il soit inclus dans le numéro de septembre des actes du journal Acoustique canadienne. Il est important de noter qu'un auteur doit être inscrit à la conférence d'ici le 1er août pour que l'article soit publié; faute de quoi, seul le résumé sera inclus dans les actes de la conférence. Veuillez noter que des frais d'inscription tardive seront appliqués à partir du 15 août. Nous espérons que vous passerez de merveilleuses vacances d'été et nous nous réjouissons de votre participation active à l'AWC23. Prof. Olivier Doutres

June 19th 2023

À la recherche d'un emploi en acoustique ?

De nombreuses offre d'emploi sont affichées sur le site de l'Association canadienne d'acoustique !

Vous pouvez les consulter en ligne à l'adresse http://www.caa-aca.ca/jobs/

August 5th 2015

La semaine AWC2023 aura lieu à Montréal (QC) du 3 au 6 octobre 2023

La Semaine canadienne de l'acoustique aura lieu du 3 au 6 octobre 2023 au centre-ville de Montréal, au Québec. Pour plus d'informations sur l'inscription, veuillez consulter le site Web de la conférence. https://awc.caa-aca.ca

Chèr.e.s membres et ami.e.s de l'Association canadienne d'acoustique, La Semaine canadienne de l'acoustique aura lieu du 3 au 6 octobre 2023 au centre-ville de Montréal, au Québec. Vous êtes invités à assister à cette conférence de trois jours durant laquelle les derniers développements en matière d'acoustique et de vibration au Canada seront présentés. La conférence se déroulera au Plaza Centre-Ville de Montréal. Des chambres seront disponibles à l'hôtel Bonaventure, à 5 minutes à pied du centre de conférence. Voici quelques dates importantes de la conférence : Soumission résumés :15 juin 2023 Soumission article de 2 pages : 15 juillet 2023 Ouverture inscription : 16 juin 2023 Limite inscription pour publication article : 1 août 2023 Ouverture inscription tardive : 15 août 2023 Des sessions plénières, techniques et des ateliers sont prévus tout au long de la conférence. Chaque journée débutera par une conférence plénière d'intérêt pour la communauté de l'acoustique. Des sessions techniques sont également prévues pour couvrir tous les domaines de l'acoustique, à savoir . ACOUSTIQUE DU BÂTIMENT ET ARCHITECTURALE / ACOUSTIQUE BIOMÉDICALE / ACOUSTIQUE MUSICALE / ACOUSTIQUE PHYSIQUE / ACOUSTIQUE SOUS-MARINE / AÉROACOUSTIQUE / AUDIOLOGIE / BIOACOUSTIQUE / BRUIT ET CONTRÔLE DU BRUIT / CHOCS ET VIBRATIONS / ENSEIGNEMENT DE L'ACOUSTIQUE / INTELLIGENCE ARTIFICIELLE EN ACOUSTIQUE / LINGUISTIQUE / MÉTAMATÉRIAUX ACOUSTIQUES/ NORMES EN ACOUSTIQUE / PSYCHOACOUSTIQUE / PROTECTEURS AUDITIFS / TRAITEMENT DU SIGNAL / ULTRASONS / Pour plus d'informations sur l'inscription, veuillez consulter le site Web de la conférence. https://awc.caa-aca.ca Au plaisir de vous voir à la conférence, Olivier Doutres (ÉTS, président de la conférence, conference@caa-aca.ca), Thomas Padois (IRSST, président technique, technical-chair@caa-aca.ca) and Julien Biboud (Mécanum, coordonnateur des expositions et du parrainage, awc2023exhibitors@caa-aca.ca)

April 5th 2023

AWC2023 : Extension au 1er juillet pour les résumés

La date limite a été prolongée jusqu'au 1er juillet pour les résumés de 300 mots : https://awc.caa-aca.ca/index.php/AWC/index/pages/view/AWC2023_AbstractInfo The deadline has been extended until July 1st for 250 words abstracts: https://awc.caa-aca.ca/index.php/AWC/index/pages/view/AWC2023_AbstractInfo

[ENGLISH MESSAGE BELOW] L'organisation de la "Semaine canadienne de l'acoustique" (AWC23) avance bien. Nous sommes heureux de vous annoncer que près de 130 résumés ont déjà été soumis, et nous tenons à exprimer notre gratitude à tous ceux qui ont participé jusqu'à présent. Voici quelques rappels et mises à jour importants : Pour ceux qui n'ont pas encore soumis leur résumé, nous avons le plaisir de vous informer que la date limite a été prolongée jusqu'au 1er juillet pour les résumés de 300 mots. Vous avez encore le temps de contribuer et de participer à cet événement passionnant, via https://awc.caa-aca.ca/index.php/AWC/index/pages/view/AWC2023_AbstractInfo Une fois que votre résumé aura été accepté, veuillez vous assurer de téléverserr votre article de deux pages d'ici le 15 juillet pour qu'il soit inclus dans le numéro de septembre des actes du journal Acoustique canadienne. Il est important de noter qu'un auteur doit être inscrit à la conférence d'ici le 1er août pour que l'article soit publié; faute de quoi, seul le résumé sera inclus dans les actes de la conférence. Veuillez noter que des frais d'inscription tardive seront appliqués à partir du 15 août. Nous espérons que vous passerez de merveilleuses vacances d'été et nous nous réjouissons de votre participation active à l'AWC23. Prof. Olivier Doutres [ENGLISH VERSION] The organization of the "Acoustics Week in Canada" (AWC23) is going well. We are pleased to announce that approximately 130 abstracts have already been submitted, and we would like to express our gratitude to all who have participated thus far. Here are some important reminders and updates: For those who have not yet submitted their abstracts, we are pleased to inform you that the deadline has been extended until July 1st for 300 words abstracts. You still have time to contribute and be a part of this exciting event, via https://awc.caa-aca.ca/index.php/AWC/index/pages/view/AWC2023_AbstractInfo Once your abstract has been accepted, please ensure that your two-page article is uploaded by July 15th for inclusion in the September proceedings issue of Canadian Acoustics. It is important to note that at least one author must be registered for the conference by August 1st for the article to be published, otherwise only the abstract will be included in the proceedings issue with Canadian Acoustics journal. Please be aware that late registration fees will come into effect starting August 15th. We hope that you have a wonderful summer vacation and look forward to your active participation in AWC23. Prof. Olivier Doutres

June 19th 2023

Pourquoi publier dans Acoustique canadienne ?

Parce que, c'est...

- Une revue respectée, forte de 40 années de publications uniquement dédiée à l'acoustique au Canada
- Une publication trimestrielle en format papier et électronique, rejoignant une large communauté d'experts à travers le monde
- Une publication "accès libre" dont le contenu est disponible à tous, 12 mois après publication
- Une alternative intéressante pour une évaluation par les pairs, fournissant aux auteurs des commentaires pertinents, objectifs et constructifs

Application for Membership

CAA membership is open to all individuals who have an interest in acoustics. Annual dues total $120.00 for individual members and $50.00 for student members. This includes a subscription to ***Canadian Acoustics***, the journal of the Association, which is published 4 times/year, and voting privileges at the Annual General Meeting.

Subscriptions to *Canadian Acoustics* *or* Sustaining Subscriptions

Subscriptions to ***Canadian Acoustics*** are available to companies and institutions at a cost of $120.00 per year. Many organizations choose to become benefactors of the CAA by contributing as Sustaining Subscribers, paying $475.00 per year (no voting privileges at AGM). The list of Sustaining Subscribers is published in each issue of ***Canadian Acoustics*** and on the CAA website.

Please note that online payments will be accepted at http://jcaa.caa-aca.ca

Address for subscription / membership correspondence:

Name / Organization ____________________

Address ____________________

City/Province ____________ Postal Code ________ Country ____________

Phone ____________ Fax ____________ E-mail ____________

Address for mailing Canadian Acoustics, if different from above:

Name / Organization ____________________

Address ____________________

City/Province ____________ Postal Code ________ Country ____________

Areas of Interest: (Please mark 3 maximum)

1. Architectural Acoustics
2. Engineering Acoustics / Noise Control
3. Physical Acoustics / Ultrasound
4. Musical Acoustics / Electro-acoustics
5. Psychological / Physiological Acoustic
6. Shock and Vibration
7. Hearing Sciences
8. Speech Sciences
9. Underwater Acoustics
10. Signal Processing / Numerical Methods
11. Other

For student membership, please also provide:

____________ ____________ ____________________

(University) *(Faculty Member)* *(Signature of Faculty Member)* *(Date)*

I have enclosed the indicated payment for:
[ ] CAA Membership $ 120.00
[ ] CAA Student Membership $ 50.00

Corporate Subscriptions (4 issues/yr)
[ ] $120 including mailing in Canada
[ ] $128 including mailing to USA,
[ ] $135 including International mailing

[ ] Sustaining Subscription $475.00
(4 issues/yr)

Please note that the preferred method of payment is by credit card, online at http://jcaa.caa-aca.ca

For individuals or organizations wishing to pay by check, please register online at *http://jcaa.caa-aca.ca* and then mail your check to:

Executive Secretary, Canadian Acoustical:
Dr. Roberto Racca
c/o JASCO Applied Sciences
2305–4464 Markham Street
Victoria, BC V8Z 7X8 Canada

Formulaire d’adhésion

L'adhésion à l'ACA est ouverte à tous ceux qui s'intéressent à l'acoustique. La cotisation annuelle est de 120.00$ pour les membres individuels, et de 50.00$ pour les étudiants. Tous les membres reçoivent ***l'Acoustique Canadienne***, la revue de l'association.

Abonnement pour la revue *Acoustique Canadienne* et abonnement de soutien

Les abonnements pour la revue ***Acoustique Canadienne*** sont disponibles pour les compagnies et autres établissements au coût annuel de 120.00$. Des compagnies et établissements préfèrent souvent la cotisation de membre bienfaiteur, de 475.00$ par année, pour assister financièrement l'ACA. La liste des membres bienfaiteurs est publiée dans chaque issue de la revue ***Acoustique Canadienne***..

Notez que tous les paiements électroniques sont acceptés en ligne http://jcaa.caa-aca.ca

Pour correspondance administrative et financière:

Nom / Organisation ____________________

Adresse ____________________

Ville/Province ____________________ Code postal__________Pays ____________________

Téléphone ____________________ Téléc. ______________Courriel ____________________

Adresse postale pour la revue Acoustique Canadienne

Nom / Organisation ____________________

Adresse ____________________

Ville/Province ____________________ Code postal__________Pays ____________________

Cocher vos champs d'intérêt: (maximum 3)

1. Acoustique architecturale
2. Génie acoustique / Contrôle du bruit
3. Acoustique physique / Ultrasons
4. Acoustique musicale / Électro-acoustique
5. Physio / Psycho-acoustique
6. Chocs et vibrations
7. Audition
8. Parole
9. Acoustique sous-marine
10. Traitement des signaux /Méthodes numériques
11. Autre

Prière de remplir pour les étudiants et étudiantes:

______________ ____________________ ____________________ ______________

(Université) (Nom d'un membre du corps professoral) (Signature du membre du corps professoral) (Date)

Cocher la case appropriée:
[ ] Membre individuel 120.00 $
[ ] Membre étudiant(e) 50.00 $

Abonnement institutionnel
[ ] 120 $ à l'intérieur du Canada
[ ] 128 $ vers les États-Unis
[ ] 135 $ tout autre envoi international

[ ] Abonnement de soutien 475.00 $ (comprend l'abonnement à *L'acoustique Canadienne*)

Merci de noter que le moyen de paiement privilégie est le paiement par carte crédit en ligne à *http://jcaa.caa-aca.ca*

Pour les individus ou les organisations qui préféreraient payer par chèque, l’inscription se fait en ligne à *http://jcaa.caa-aca.ca* puis le chèque peut être envoyé à :

Secrétaire exécutif, Association canadienne d’acoustique :
Dr. Roberto Racca
c/o JASCO Applied Sciences
2305–4464 Markham Street
Victoria, BC V8Z 7X8 Canada

SUSTAINING SUBSCRIBERS - ABONNÉS DE SOUTIEN

The Canadian Acoustical Association gratefully acknowledges the financial assistance of the Sustaining Subscribers listed below. Their annual donations (of $475 or more) enable the journal to be distributed to all at a reasonable cost.

L'Association Canadienne d'Acoustique tient à témoigner sa reconnaissance à l'égard de ses Abonnés de Soutien en publiant ci-dessous leur nom et leur adresse. En amortissants les coûts de publication et de distribution, les dons annuels (de 475$ et plus) rendent le journal accessible à tous les membres.

Acoustec Inc.
Jean-Philippe Migneron - 418-496-6600
info@acoustec.qc.ca
acoustec.qc.ca

Acoustex Specialty Products
Mr. Brian Obratoski - 2893895564
Brian@acoustex.ca
www.acoustex.net

AcoustiGuard-Wilrep Ltd.
Mr. William T. Wilkinson - 888-625-8944
wtw@wilrep.com
acoustiguard.com

BKL Consultants Ltd.
Mark Bliss - 604-988-2508
bliss@bkl.ca
www.bkl.ca

dB Noise Reduction
Mehrzad Salkhordeh - 519-651-3330 x 220
mehrzad@dbnoisereduction.com
dbnoisereduction.com

HGC Engineering Ltd.
Mr. Bill Gastmeier -
bill@gastmeier.ca
hgcengineering.com

Hottinger Bruel & Kjaer inc.
Andrew Khoury - 514-695-8225
andrew.khoury@hbkworld.com
bksv.com

Jade Acoustics Inc.
Ms. Dalila Giusti - 905-660-2444
dalila@jadeacoustics.com
jadeacoustics.com

JASCO Applied Sciences (Canada) Ltd
Roberto Racca - +1.250.483.3300 ext.2001
roberto.racca@jasco.com
www.jasco.com

Pliteq Inc.
Wil Byrick - 416-449-0049
wbyrick@pliteq.com
www.pliteq.com

RWDI
Mr. Peter VanDelden - 519-823-1311
peter.vandelden@rwdi.com
rwdi.com